Roddy, D. J., Pepin, R. O., and Merrill, R. B., editors.
(1977) *Impact and Explosion Cratering*, Pergamon Press (New York), p. 343–404.
Printed in the United States of America

# The Ries impact crater

JEAN POHL

Institut für Allgemeine und Angewandte Geophysik, Universität München, Theresienstrasse 41, 8 München 2, Germany

DIETER STÖFFLER

Institut für Mineralogie, Universität Münster, Gievenbecker Weg 61, 44 Münster, Germany

HORST GALL

Bayerische Staatssammlung für Paläontologie und hist. Geologie, Richard-Wagner-Strasse 10, 8 München 2, Germany

KORD ERNSTSON

Institut für Geologie, Universität Würzburg, Pleicherwall 1, 87 Würzburg, Germany

**Abstract**—Presently available data on the Ries impact structure as far as they relate to the interpretation of the crater-forming process are summarized and discussed. The Ries projectile impacted a stratified target of horizontal layers of various sedimentary rocks (limestones, shales, sandstones), about 600–700 m thick, underlain by a basement of crystalline rocks. The main structural characteristics of the crater are: flat-floored central basin (crater depth ≈0.6–0.7 km) due to uplifted crystalline basement bordered by an inner ring of uplifted basement and sedimentary megablocks (radius 6 km), zone of megablocks from all stratigraphic units between 6 and 12–13 km radius. The perimeter of the crater is defined by an outer circular system of downfaulted target rocks at 12–13 km radius (tectonic rim). Continuous crater deposits occur in the megablock zone and in the "Vorries" which extends from the tectonic rim up to a radial distance of at least 40 km. A melt-bearing top unit of suevite breccia forms a continuous fallback layer in the central cavity and isolated fallout patches outside the inner ring up to a radius of 22 km. Distant ejecta may reach as far as 350 km. Ballistic ejection and secondary mass transport by the impact of landing ejecta is considered to be the main mechanism for the emplacement of the continuous deposits beyond the megablock zone. Inside this zone most of the displaced masses were transported by gliding and overthrusting mechanisms. The subsurface structure of the crater is modelled by density and seismic velocity models indicating brecciation and fracturing as deep as 6 km. The crater reveals a negative gravity anomaly of −18 mgal. The central cavity is characterized by strong, but irregular negative magnetic anomalies due to the suevite layer of up to 400 m thickness. Estimates of the total volume of excavated rocks ranges from 124 to 200 $km^3$. The total melt volume is on the order of 0.1–0.5 $km^3$. The depth of the transient crater cavity is estimated to be about 2 km. Modification of this cavity is achieved by central uplifting of the basement and subsidence of the marginal zone of the crater (megablock zone).

## 1. INTRODUCTION

THE RIES (Ries of Nördlingen or Ries Kessel) is a flat circular basin, 22–23 km in diameter, which is located between the Jurassic limestone plateaus of the Swabian and Franconian Alb, about 110 km NW of München, Bavaria (Fig. 1).

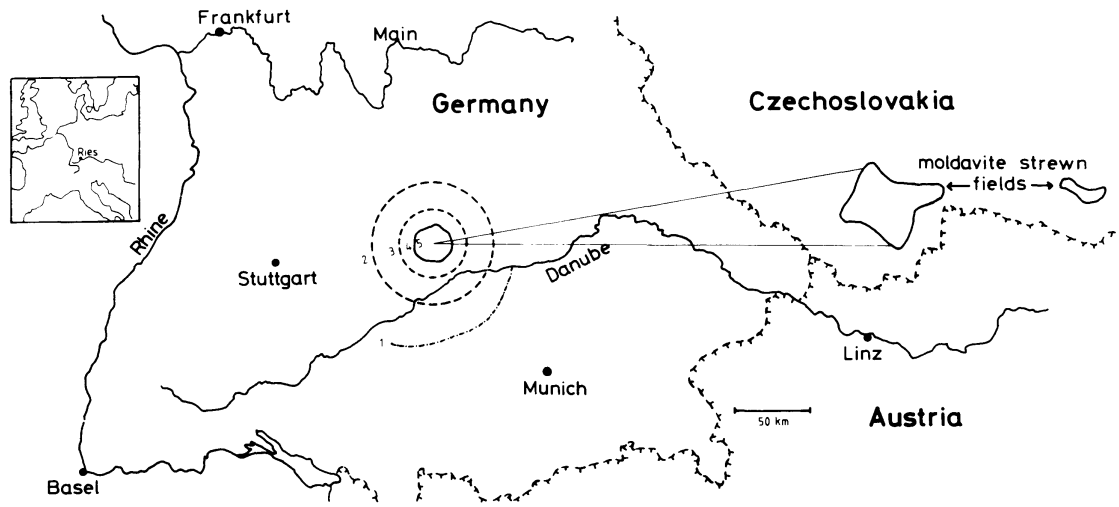


Fig. 1. Map of central Europe showing the location of the Ries and its ejecta; 1 = outer limit of distribution of Malmian Reuter blocks, 2 and 3 = maximum extent of Bunte breccia and suevite, respectively, 4 = tectonic rim of the crater, 5 = inner ring.

Geological investigations of the Ries area began as early as 1834 (v. Cotta) resulting in a variety of theories about its origin. The theory that the Ries was formed by meteorite impact was first proven by the discovery of coesite (Shoemaker and Chao, 1961) although it was already suggested by Werner in 1904. Most of the older literature is reviewed by Oberrhein. Geol. Verein (1926), Dorn (1948), Preuss (1964) and Dehm (1969). Research along an impact hypothesis was summarized and reviewed since 1961 by Preuss (1964), Engelhardt (1967a), Bayer. Geol. Landesamt (1969), Dennis (1971), Chao (1973), Engelhardt and Stöffler (1974), and Gall *et al.* (1975). The impact concept is unanimously accepted by now.

The Ries crater represents one of the best investigated, large, complex terrestrial impact structures with a well preserved "ejecta blanket." Therefore, the Ries may serve as an important reference point for the discussion of impact cratering mechanics, although the complex layered structure of the Ries target may differ from the average situation on planetary surfaces.

It is the objective of this paper to present a synopsis of field and laboratory data relevant to the mechanics of the crater-forming process. It is hoped to provide useful constraints for theoretical and experimental studies simulating impact events of the magnitude and conditions of the Ries.

## 2. Structure and Composition of the Target

### 2.1. *Pre-impact geology*

The Ries impact occurred in the upper Tortonian (upper Miocene; Table 1) 14.8 m.y. ago (Bolten and Müller, 1969; Gentner *et al.*, 1963) in a target that consisted of horizontally layered sediments of early Permian, Mesozoic, and

Tertiary age above a variety of crystalline basement rocks of pre-Permian age. The basement is part of a mountain belt formed during the Variscan orogeny and subsequently peneplained during the Permian and early Triassic.

The target consists of eight major stratigraphic units shown in a reconstructed pre-impact profile (Fig. 2). Overall thickness and lithologic facies of the sedimentary rocks are not quite constant for the entire target area. Thickness and distribution of the uppermost and the lower part of the sedimentary strata are highly irregular. The uppermost unit (0–50 m thick) consists of middle Oligocene (Müller, 1972) and upper Miocene sediments (sands, shales, fresh-water limestone, coal) formed as part of the Molasse sedimentation of the Alpine geosyncline (Table 1). These sediments covered a large part of the crater area. South of the crater, the upper Miocene occurs in a continuous layer underneath the Ries crater deposits (Fig. 3). Details of the remaining stratigraphic units can be seen from Fig. 2. The occurrence of Buntsandstein is still questionable; if at all, it could be present W to NW of the target. The Permian (sandstones and rhyolite) fills elongated troughs in the crystalline basement striking generally WSW.

The most distinct unconformity in the Ries stratigraphy is formed by the surface of the crystalline basement which had a relief of at least 100 m in the target area at the time of the impact (Section 4). The stratigraphy and structure of the basement are very complicated and not well known. A reconstruction was attempted by Graup (1975, Fig. 4). The most important feature is that most of the

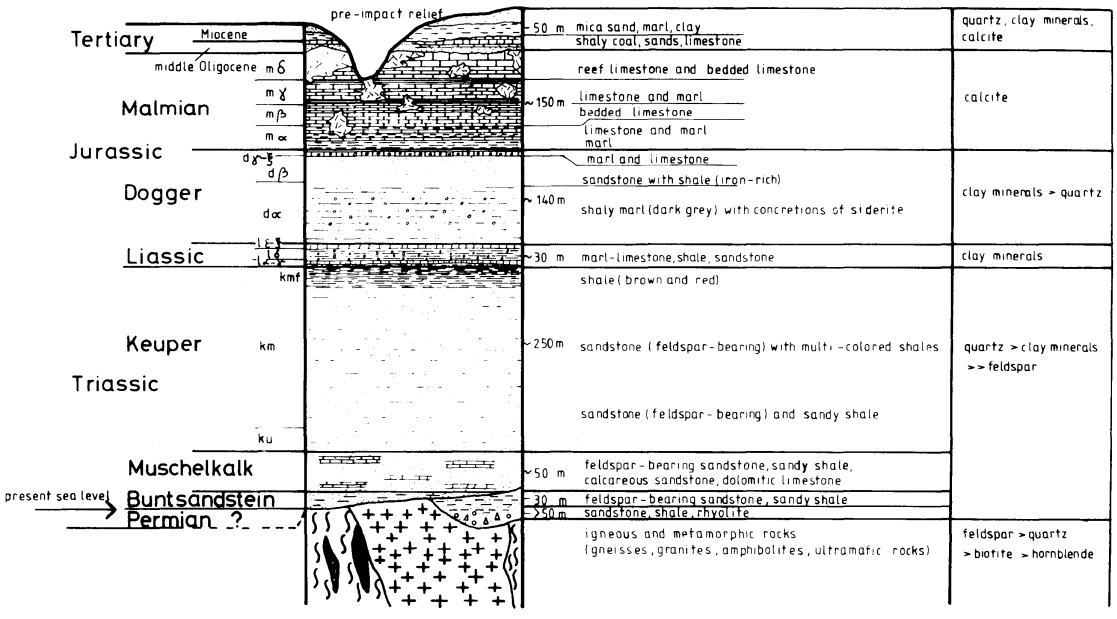


Fig. 2. Geological and mineralogical profile of the central area of the Ries crater before impact. From the area W of the crater to the area E of the crater Triassic, Liassic and Dogger decrease from 350 to 250 m, 46 to 16 m, and 160 to 125 m. Malmian decreases to about 110–120 m.

1977iecp.symp..343P

Table 1. Tertiary sedimentation in the Ries crater area*

| | | | Crater | Vorries† | Sedimentation | | Erosion state |
|---|---|---|---|---|---|---|---|
| | Pliocene | | ↕ | ↕ | Post-impact Obere Süsswassermolasse | Fluviatile, limnic, max 150 m | Relicts |
| | | Sarmatian | ↕ | | Post-impact lake sedimentation | Lacustrine, limnic-brackish, max 500 m | Partly eroded |
| | | | | | Impact | | |
| Upper Tertiary | | Tortonian | ↕ | ↕ S | Pre-impact Obere Süsswassermolasse OSM | Fluviatile-lacustrine, limnic max 80 m | Strongly eroded |
| | Miocene | Helvetian | | ↕ S | Obere Meeresmolasse OMM | Marine, max 60 m | Partly eroded |
| | | Burdigalian | | | | | |
| | | Aquitanian | | ↕ SW | Untere Süsswasser-molasse USM | Lacustrine, limnic, max 20 m | Strongly eroded |
| | Oligocene | | ↕ | ↕ SE | Marginal facies of Untere Meeresmolasse UMM | Fluviatile-lacustrine, limnic-brackish, max 75 m | Strongly eroded |
| Lower Tertiary | Eocene | | | | | | |
| | Paleocene | | | | | | |

*See also Fig. 2.2.
†S, SE, SW indicate the sedimentation area relative to the crater.

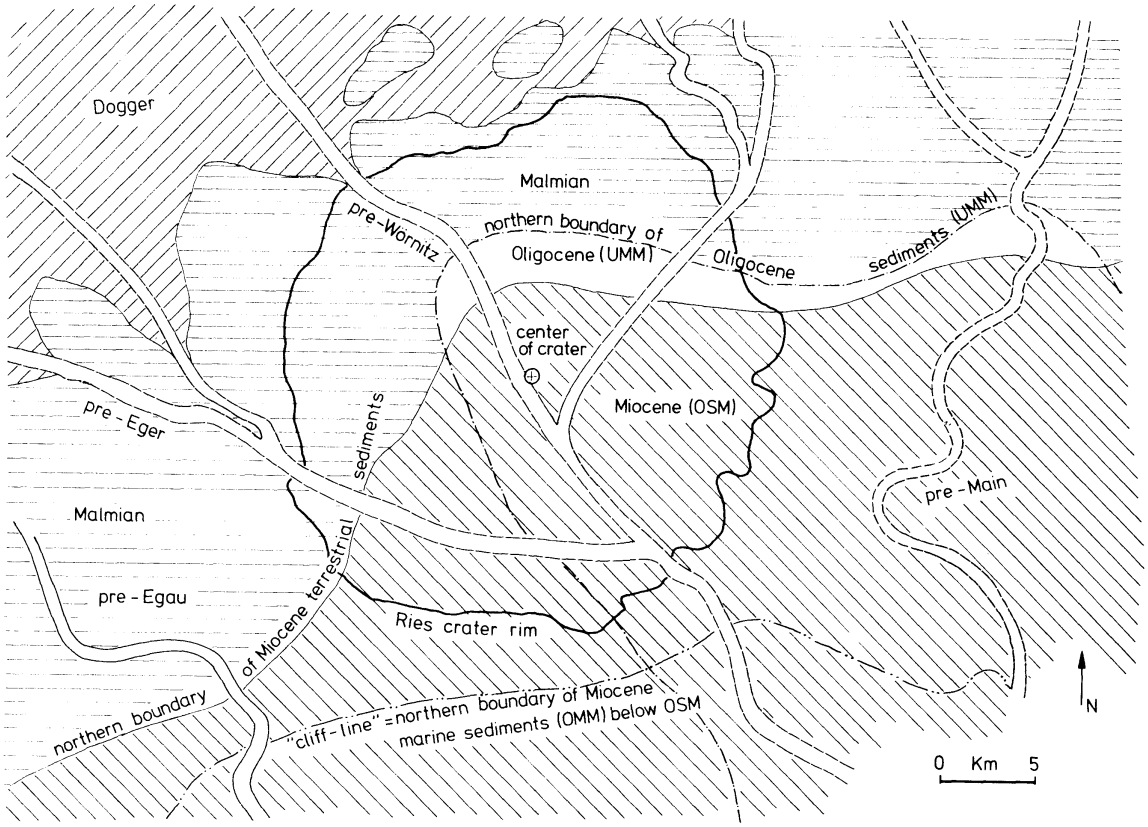


Fig. 3. Probable geological map of the Ries area before impact. Maximum extent of Tertiary sediments is indicated. UMM = Untere Meeresmolasse, OMM = Obere Meeresmolasse, and OSM = Obere Süsswassermolasse.

surface is formed by a granitic intrusion which cuts through older gneisses, amphibolites and ultrabasic rocks with steeply (?) inclined foliation planes (see also Bayer. Geol. Landesamt, 1974, 1977).

Details of the mineralogical and chemical composition of the target rocks will be discussed along with the properties of the impact formations (see section 3.2).

## 2.2. *Pre-impact morphology*

The Upper Malmian limestone strata were exposed as a land surface for most of the Cretaceous and Tertiary. This land surface was then covered by an incomplete sequence of Oligocene and Miocene sediments as indicated in Figs. 2, 3 and Table 1. In the Tortonian, shortly before the impact occurred, the Ries area became a region of relatively strong erosion which was drained into the Molasse basin by a number of predominantly NW-SE running rivers (Gall *et al.*, 1975, 1977; Fig. 3). The western rivers penetrated as deep as Dogger (100–150 m of relief) and the "pre-Main" river reached the lowermost Malmian (150–200 m of relief) (Bader and Schmidt-Kaler, 1977). This erosion cut the Malmian limestone plateau into a system of isolated mesas, most distinctly developed in

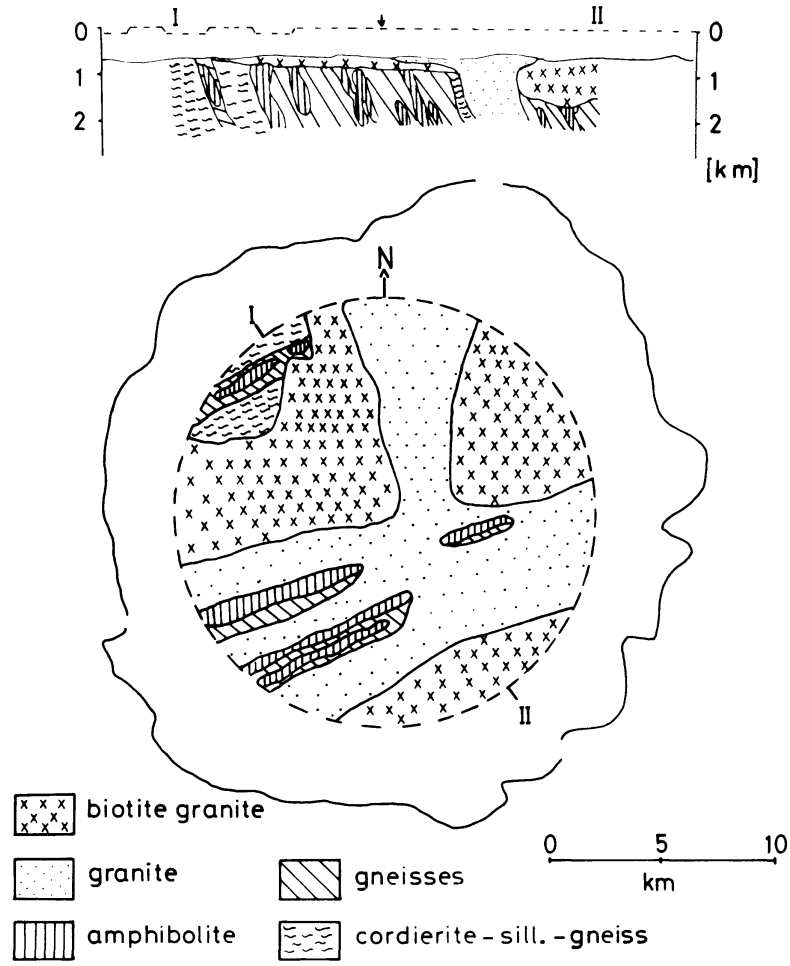


Fig. 4. Geological map and vertical cross section of the crystalline basement of the Ries crater area reconstructed by Graup (1975); modified after Graup (1977); irregular circular line = tectonic rim of the crater; I–II indicates the position of the cross section.

the northern part of the Ries (Fig. 3; Gall *et al.*, 1975, 1977). The marked escarpment of the Malmian limestone presently extending across the Ries crater from WSW to ENE at its S-rim probably was not as pronounced prior to impact as it is now, because the sedimentary strata were not yet tilted to the SE. In contrast to previous assumptions Gall *et al.* (1977) believe that most of the crater area was covered by the Malmian limestone plateau which was more thoroughly dissected into mesas in the northern part (Fig. 3). Thus the target surface displayed a maximum relief of about 150 m near to the point of impact. It is not known whether the impact occurred onto the Upper Malmian limestone (probably covered by 20–50 m of Tertiary sands, marls or shales) or onto the slope or bottom of a valley cut into Dogger sandstones.

## 3. Surface Formations of the Crater

### 3.1. *Present morphology and surface geology*

The present Ries is an almost circular, flat basin, 22–23 km in diameter, typically 410–430 above sea level (Fig. 5). It can be subdivided into a flat *central basin*, about 410–420 m in altitude and 11–12 km in diameter formed by post-impact Tertiary lake sediments. This plain is bordered in the W, SW, and E by a ring-shaped chain of isolated hills standing about 50 m above the basin. The zone between this *inner ring* and the *morphological rim* of the basin (22–23 km diameter) is formed in part by additional plains of post-impact lake sediments and in part by a hummocky relief extending into the rim area. The hummocks marginal to the plains reach elevations of 450–500 m in the northern part and 550–600 m in the southern part of the Ries.

The autochthonous rocks of the northern rim zone consist of Keuper, Liassic, and Dogger whereas the southern rim zone is formed by Malmian limestones. The hummocks of the inner ring and those extending to a radius of 12–13 km are mainly displaced megablocks up to 1 km in size of the sedimentary rock strata (Keuper, Liassic, Dogger, Malmian) and of the crystalline basement, sometimes covered by post-impact lacustrine limestone. Blocks of crystalline rocks uplifted from the basement by 450–550 m prevail in the inner ring. For reasons discussed below it is believed that at a radius of 12–13 km some concentric fault system separates displaced and down-faulted megablocks from the autochthonous, undisturbed strata marking what is called the *tectonic rim* of the crater (Figs. 6, 7; Gall *et al.*, 1977). The concentric zone between the inner

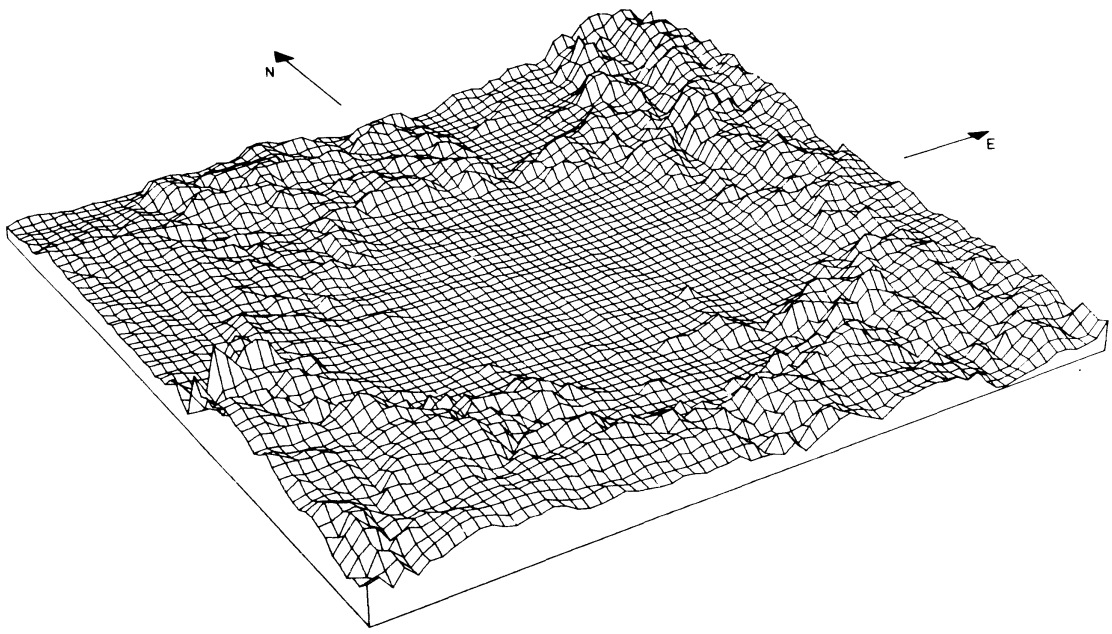


Fig. 5. Morphology of the present Ries Basin; grid distance 0.5 km, vertical exaggeration 12.5-fold, horizontal coordinate lines 400 m above sea level.

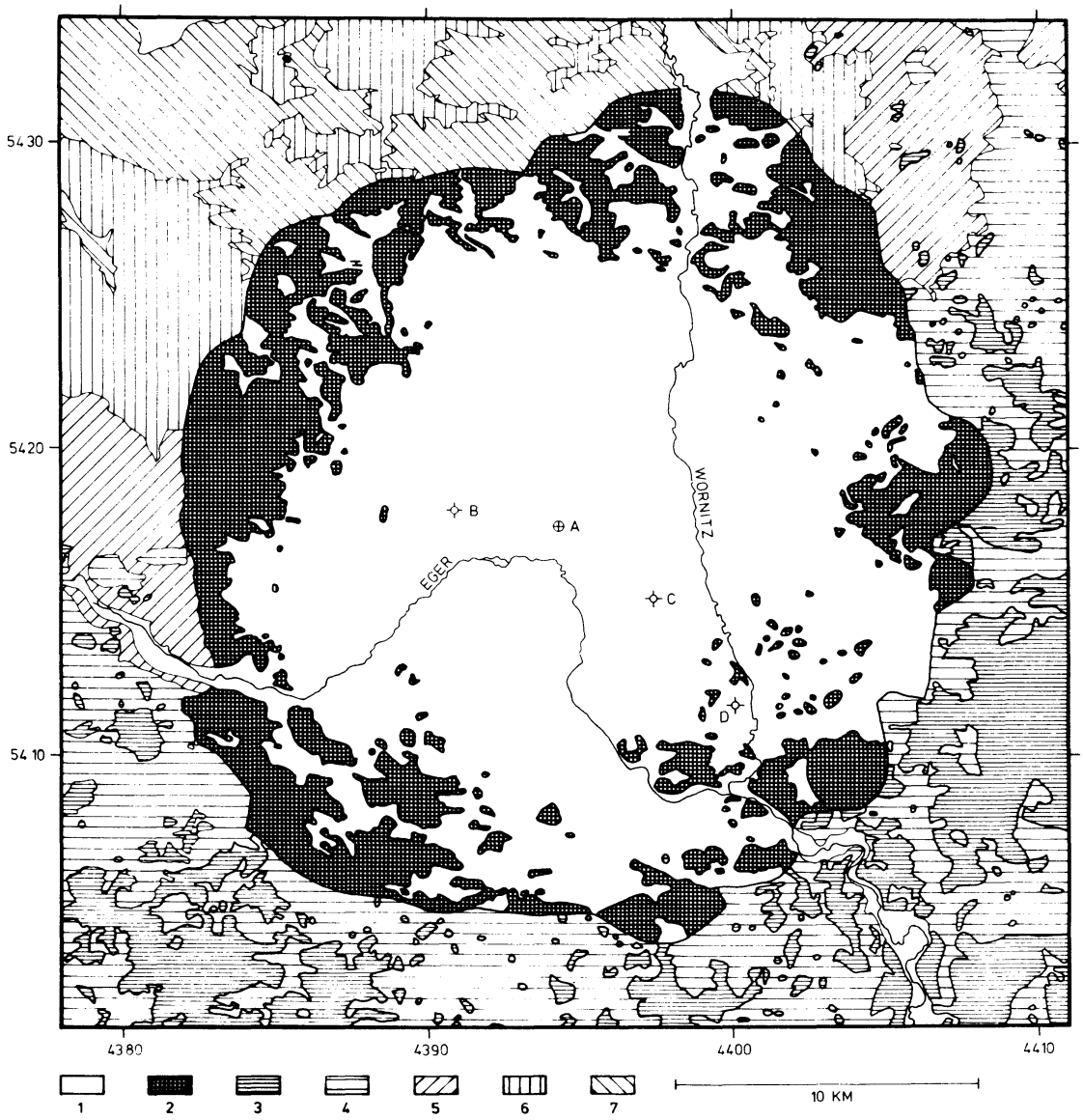


Fig. 6. Geological map of the Ries crater; A = center of crater, B = drillhole Nördlingen 1973, C = drillhole Deiningen, D = drillhole Wörnitzostheim; 1 = post-impact Tertiary and Quaternary sediments, 2 = megablock zone (out-cropping), 3 = "Vorries" continuous deposits, 4 = Malmian, 5 = Dogger, 6 = Liassic, 7 = Keuper; 2 and 3 are displaced rocks, 4–7 are autochthonous rocks; this simplified map is based on the Geological Map 1 : 100,000 (Schmidt-Kaler *et al.*, 1970), on detailed geological maps 1 : 25,000 and on a preliminary draft for the geological map 1 : 50,000 (Gall and Müller, 1977).

ring and the tectonic rim will be called *megablock zone.* In the area outside the tectonic rim which is called the *Vorries zone*, displaced rock masses form a more or less continuous blanket in the SW, S, and SE and have been geologically mapped to a radial distance of up to 42 km from the center of the crater (Fig. 7; Gall *et al.*, 1975). This formation will be referred to as continuous Vorries deposits. Beyond the edge of the continuous Vorries deposits we define a *zone*

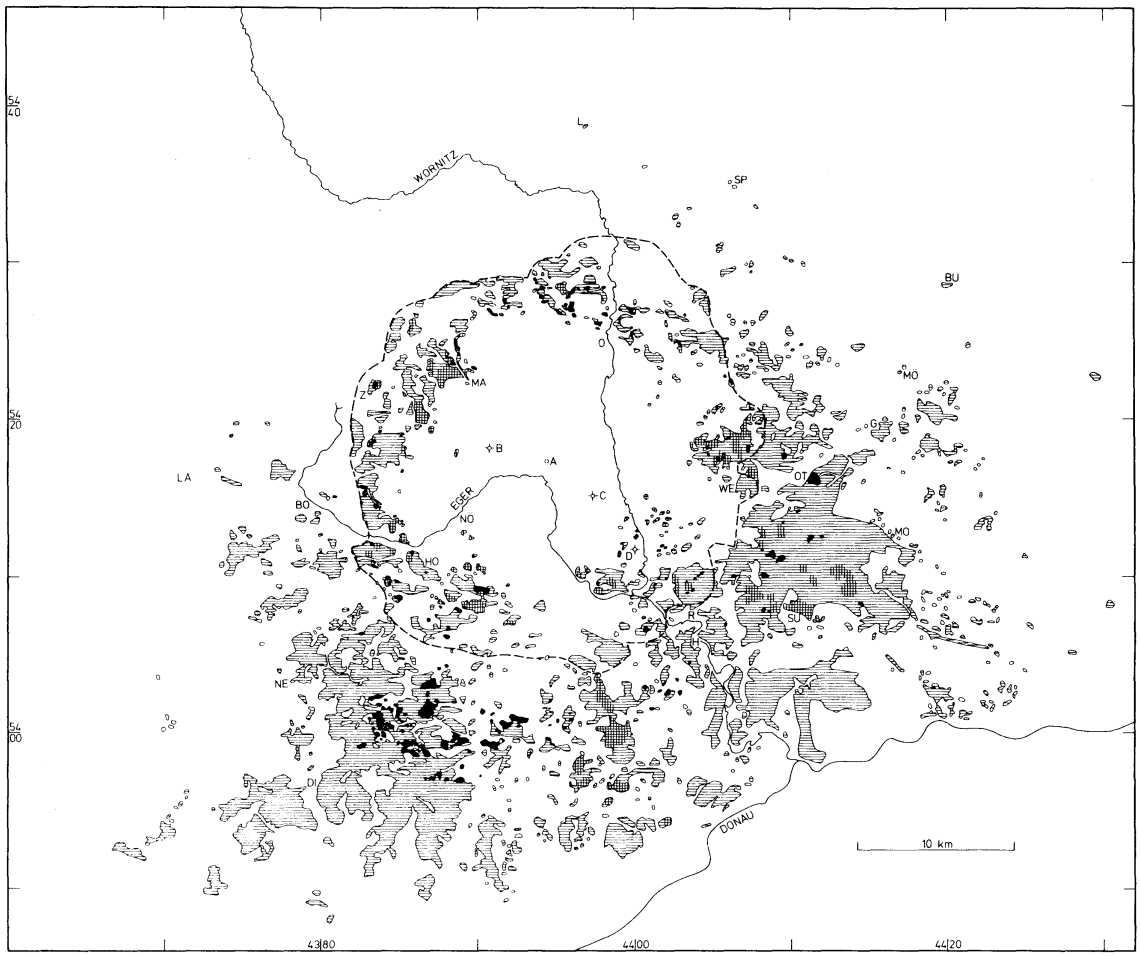


Fig. 7. Geological map of displaced rock masses at the Ries crater; horizontal hatching = Bunte breccia and megablocks; black = suevite; cross hatching = crystalline basement rocks; A = crater center; B = drilling Nördlingen 1973; C = drilling Deiningen; D = Wörnitzostheim; dashed line = tectonic rim of the crater; Bu = Bubenheim; Di = Dischingen; G = Gundelsheim; H = Harburg; Ho = Holheim; K = Kirchheim; La = Lauchheim; L = Lentersheim; Ma = Maihingen; Mö = Möhren; Mo = Monheim; Ne = Neresheim; Nö = Nördlingen; Ö = Öttingen; Ot = Otting; P = Polsingen; R = Ronheim; Sp = Spielberg; Su = Sulzdorf; U = Ursheim; We = Wemding; Z = Zipplingen; modified from Schmidt-Kaler *et al.* (1970).

*of distant ejecta* in which three types of rocks occur which are presumably related to the Ries event; the Reuter blocks and the Molasse bentonites south of the Danube, and the moldavite tektites of Czechoslovakia (see section 3.2.5).

The present morphology of the Vorries deposits is very smooth and relatively continuous in the E and SE where it is covered in some places by post-impact upper Miocene and Pliocene fluviatile sediments (Table 1). It is more hummocky and discontinuous in the S and SW. Only isolated remnants of ejecta were found in the W and NE (Fig. 7; Gall *et al.*, 1975). No displaced rock masses occur beyond the northwestern tectonic rim of the crater (Fig. 7), where the radial distribution of the megablocks ends abruptly. Due to the partial cover by

post-Ries Tertiary sediments, deep soil layers and intense vegetation, the geological mapping of the displaced rock masses—mostly done before the impact theory of the Ries was accepted—does not represent an accurate inventory of the present distribution of rock formations produced by the cratering event. Nevertheless, a distinct asymmetry of the distribution of displaced rocks is obvious (Fig. 7). Gall *et al.* (1975) have shown that most of the non-concentric, irregular features of the distribution of displaced rocks are caused by post-impact erosion which affected various parts of the Ries area with very different intensities: For a long period of time after the impact, the Ries area was covered by post-Tortonian sediments which filled the central crater cavity, and covered the impact formations, thereby protecting the entire structure from erosional destruction. It was not until the Upper Pliocene and Pleistocene, when the northern area was tectonically uplifted to tilt the previously flat target strata to the SE, that the post-Tortonian cover, appreciable parts of the impact formations in the W, N and NE, as well as the complete crater deposits outside the tectonic rim in the NW were removed. The main reason for this differential surface denudation is, that the Malmian limestone plateau to the S was mainly drained by a subsurface karst system. Inside the tectonic rim of the crater (radius of about 12–13 km), part of the post-impact lake sediments (possibly up to 100 m) were also eroded, but the displaced rocks of the megablock zone remained less affected (Gall *et al.*, 1976; Dehm *et al.*, 1977) (for a summary of the post-impact Tertiary stratigraphy see Table 1).

In conclusion, abundant evidence argues in favour of a more or less concentric distribution of a primary, continuous blanket of displaced rocks around the Ries Basin ranging up to a radial distance of at least 40 km from the point of impact. According to the morphology and surface geology, the crater and its impact formations can be subdivided into major concentric zones and structural elements: central basin, inner ring, zone of megablocks, tectonic rim of the crater, Vorries continuous deposits, and zone of distant ejecta (Figs. 1, 5–7).

### 3.2. *Classification and composition of impact formations*

The main criteria used in classifying the impact formations of the Ries are the geological setting, the stratigraphic provenance, the petrographic composition, and the stage of shock metamorphism. In addition, for polymict breccia formations, textural properties have to be considered.

The impact formations fall into two major groups which may be called *allochthonous* or *displaced rocks* and *autochthonous* or *in situ rocks*. According to the geological setting the displaced rocks may be subdivided into *outer impact formations* or *outer crater deposits* deposited in the inner ring structure and outside the inner ring (radius 5–6 km) and *inner impact formations* or *inner crater deposits* occurring within the central crater cavity inside the inner ring. According to criteria of petrographic composition and grain size we classify the displaced Ries rocks into 6 major units (Table 2; compare also Hüttner, 1969; Engelhardt *et al.*, 1969; Engelhardt and Stöffler, 1974; Gall *et al.*, 1975): (1)

Table 2. Impact formations of the Ries crater (stages of shock metamorphism according to Stöffler, 1971a).

| Impact formation | Particle size (m) | Stratigraphic provenance | Shock metamorphism | Geological setting | Texture |
|---|---|---|---|---|---|
| Impact melt | As inclusions < 0.2–0.5 m | Crystalline rocks | Stage IV 550–1000 kbar | As inclusions in suevite or as larger coherent bodies | Polymict (mixed with rock and mineral clasts) |
| Suevite | < 0.2–0.5 m | Crystalline rocks ≫ sedimentary rocks | Stages 0–IV < ~ 1000 kbar | Central crater cavity, megablock zone, and Vorries zone | Polymict |
| Dike breccias | < 0.2–0.5 m | Crystalline rocks ≫ sedimentary rocks | Stages 0–II < ~ 350 kbar | Crater basement megablocks, surface megablocks | Polymict |
| Crystalline breccia | < 0.5–1 m | Crystalline rocks | Stages 0–II < ~ 350 kbar | As irregular bodies within or on top of Bunte breccia, central crater cavity | Polymict |
| Bunte breccia | < 25 m | Sedimentary rocks ≫ crystalline rocks | Stages 0–II < ~ 350 kbar | Megablock zone and Vorries zone | Polymict |
| Megablocks | ~ 25–1000 m | All stratigraphic units | Stages 0–I < ~ 50–100 kbar | Crater basement, inner ring, megablock zone and Vorries | Monomict |
| Brecciated and fractured autochthonous rocks | — | All stratigraphic units | Stage 0 < ~ 50 kbar | At the tectonic rim, undisplaced crater basement | Monomict |

megablocks, (2) Bunte breccia, (3) crystalline breccia, (4) dike breccia, (5) suevite, and (6) impact melt rock.

For the outer impact formations it may be convenient in some cases to consider (1)–(4) throughout the megablock zone and the Vorries as one unit which represents the *bulk continuous deposits* (in German: Bunte Trümmermassen, Hüttner, 1969) as opposed to the suevite and impact melt which overlay the bulk deposits with a distinct discontinuity (Fig. 7).

3.2.1. *Megablocks and Bunte breccia.* Displaced fragments of all stratigraphic units of the Ries target rocks which are larger than 25 m in size and can be mapped geologically will be called *megablocks* (German: Schollen; they were called "klippes" by Dennis, 1971). Megablocks are composed of a coherent, though brecciated or fractured mass of one or more rock types which still show their primary stratigraphic relation (Figs. 8, and 9). They reach dimensions of more than 1 km and are predominant in the megablock zone (Fig. 6). Smaller blocks, however, were observed in the Vorries up to radial distances of more than 35 km. Analysis of the drill core Nördlingen 1973 (Bayer. Geol. Landesamt, 1974, 1977) indicates that megablocks of crystalline rocks also occur at the base of the suevite breccia layer in the central crater cavity (Engelhardt and Graup, 1977; Stöffler, 1977). The lateral dimensions of these blocks are not known (see section 4.6).

With decreasing block size a continuous transition into finer-grained breccia called *Bunte breccia* is observed in the outer impact formations (Hüttner, 1969). An intimate mixture of megablocks and Bunte breccia is most typical for the Vorries whereas in the megablock zone Bunte breccia (block size $<25$ m) is less abundant compared to megablocks.

Bunte breccia is a polymict breccia of clastic material derived from all stratigraphic units of the target (Figs. 10, 11). The clast size ranges from a few microns upward (Hüttner, 1969). The following *compositional characteristics* of the finer-grained variety of Bunte breccia were found (Schneider, 1971 and own analyses) from localities within a radius of about 12–18 km. Among the rock clasts Malmian limestone predominates over Dogger, Liassic, Keuper, and basement rocks. Crystalline basement rocks usually range from 3–10% of the total volume of rock clasts (Fig. 12). The main mineral clasts are quartz, alkali feldspar, plagioclase, and mica (decreasing abundance) (Fig. 13). The fine-grained matrix consists mainly of calcite and subordinate amounts of kaolinite, mixed layer illite-montmorillonite, illite, and montmorillonite. In Bunte breccia from the outer zone of the Vorries deposits, the matrix is dominated by local Tertiary sand and clay (Hörz, 1976; Schneider, 1971) and rock clasts from lower stratigraphic levels of the target are less abundant.

The *macroscopic texture* of Bunte breccia is very complicated and varies from place to place (Hüttner, 1969). There is no indication of sorting. In certain parts the breccia appears more fine-grained ($<20$ cm), in others many large blocks (1–25 m) are mixed with smaller amounts of the fine-grained variety. A most important observation is that many rock clasts in the Bunte breccia are

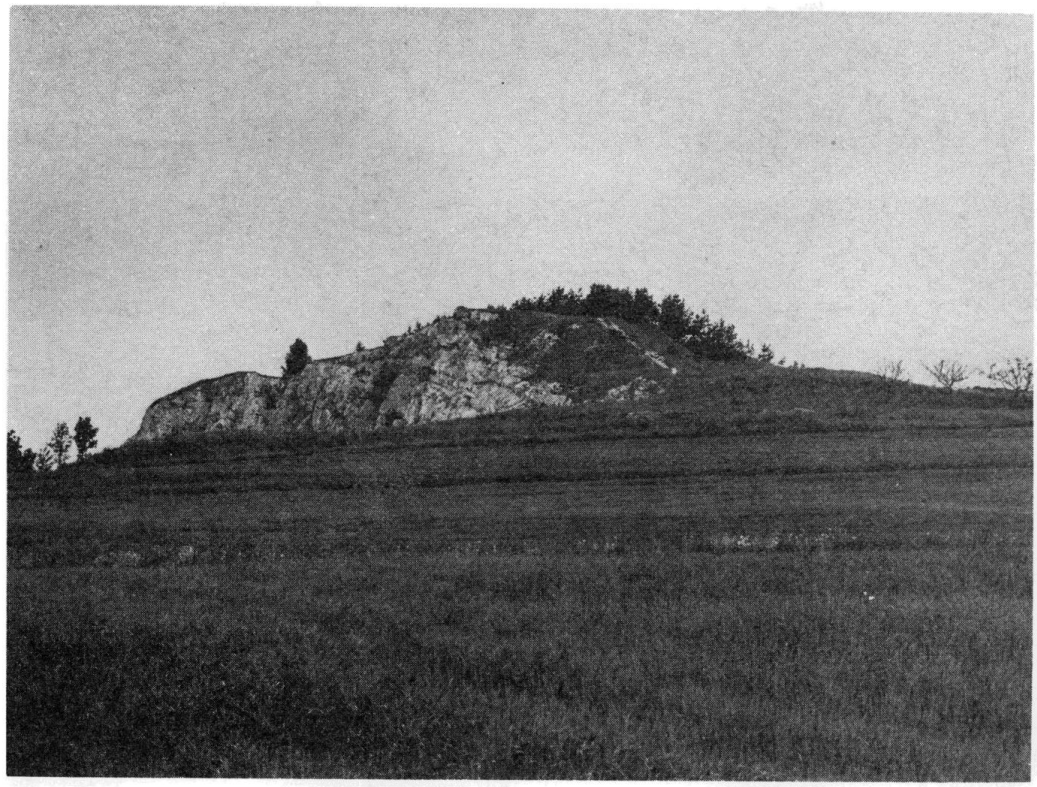

Fig. 8. Megablock of Malmian limestone near Ebermergen, in the south-eastern continuous deposits, 18.5 km from the point of impact (dimensions of block ≈ 300 m).

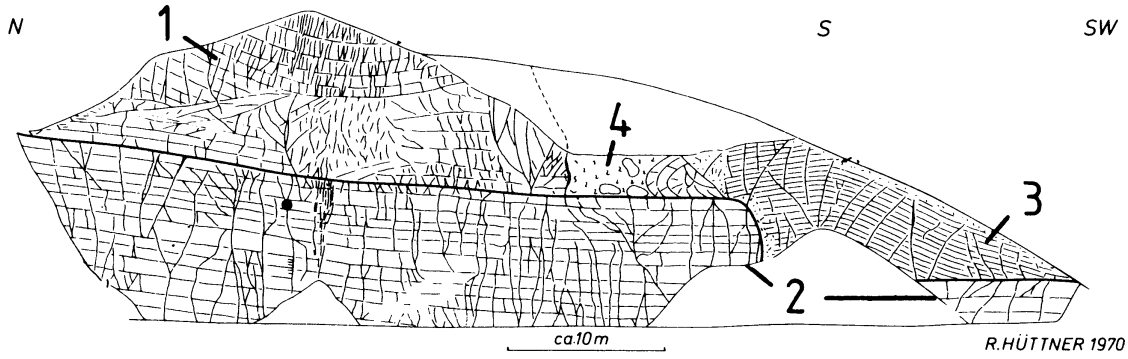


Fig. 9. Displaced Malmian megablocks (1 = Malmian $\delta$, 3 = Malmian $\beta$) and Bunte breccia (4) overriding the original target surface (heavy solid line; 2 = Malmian $\delta$); quarry Schneider near Ursheim; from Hüttner in Schmidt-Kaler *et al.* (1970).

monomict or sometimes polymict breccias, indicating several phases of deformation during the process of excavation, transport and deposition. Soft rock clasts (clay, shale, marl) sometimes display a strong deformation (folding, bending, elongation in one direction) and flow-like parallel alignments, especially near the target surface (Wagner, 1964; Hüttner, 1969).

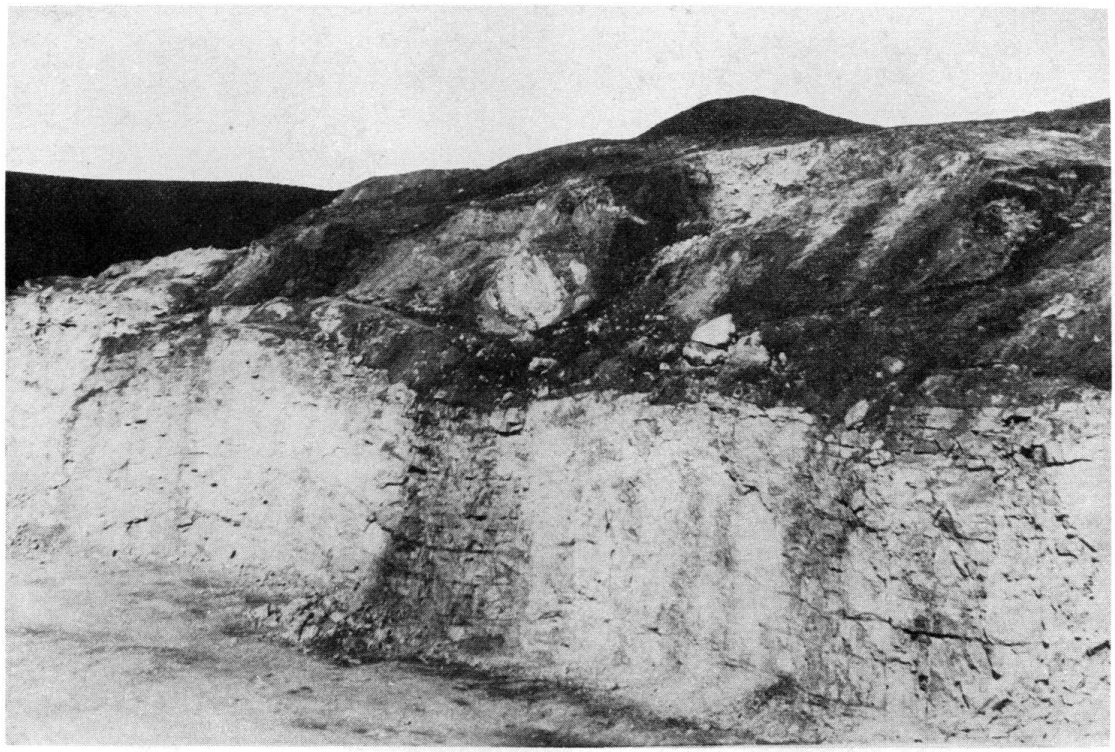

Fig. 10. Bunte breccia on top of limestone (Malmian δ) which forms the polished and striated target surface; photograph courtesy of J. Kavasch; lateral dimension about 100 m; quarry Bschor near Ronheim.

3.2.2. *Crystalline breccia and dike breccias.* Occasionally irregular bodies of polymict *crystalline breccias* of some tens of meters in size, which consist only of a mixture of crystalline rock fragments of different lithology and degree of shock metamorphism (stages 0, I, II) occur in the inner ring, the megablock zone and in the Vorries (Hüttner, 1969; Stöffler, 1969; Abadian, 1972). The stratigraphic relations of these crystalline breccias to the surrounding Bunte breccia and megablocks are not always clear. In some outcrops they are obviously on top of Bunte breccia. In cases where the lateral extension of these breccias is less than 25 m they may be considered per definitionem as part of Bunte breccia. The abundance and distribution of crystalline breccia is not well known and the present data is restricted to a few outcrops such as Leopold-Meyers-Keller at Nördlingen. Some quantitative modal data are plotted in Fig. 18 (Abadian, 1972).

*Dike breccias* show some similarities to crystalline breccia in terms of their petrographic composition. They occur as dikes of irregular shape and various thickness in the decimeter to meter range penetrating displaced megablocks of various lithology, most frequently crystalline rocks. The dikes contain fragmental material of variable lithological and stratigraphic provenance. Results of petrographic analyses (Stöffler, 1969; Abadian, 1972; Abadian *et al.*, 1973) suggest that two types of dikes can be distinguished: I. Dikes filled with a mixed breccia of fragmental material which is predominantly derived from rocks

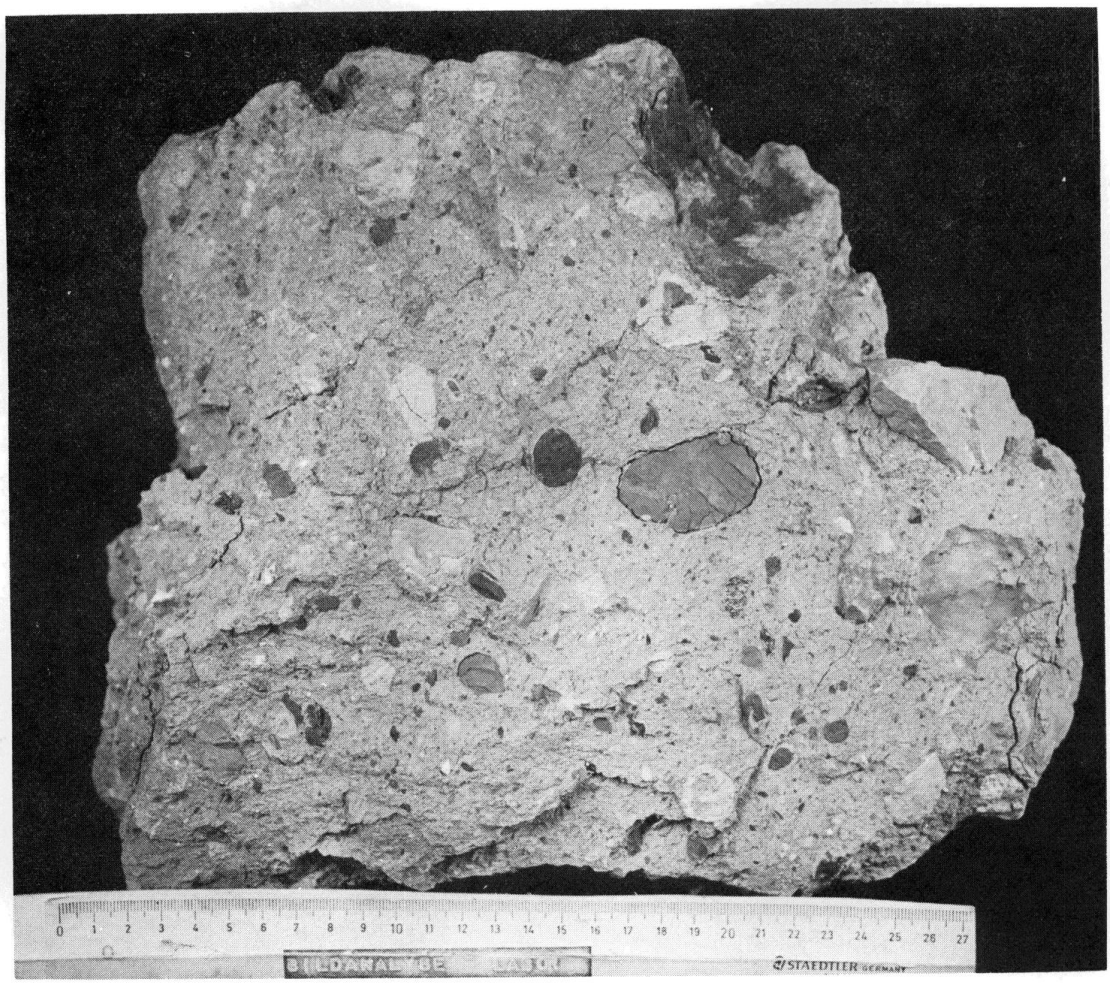

Fig. 11. Bunte breccia fragments of Malmian limestone, Liassic shale, Keuper shale and sandstone, crystalline rocks and Tertiary shale; quarry Bschor, Ronheim; scale = cm.

different in composition and stratigraphic provenance from the adjacent country rock. II. Dikes filled with brecciated material which is partly or predominantly derived from the adjacent country rock by some frictional process.

Type I dikes were observed only in megablocks near to the surface (Fig. 14). In most cases they consist of a mixture of moderately shocked crystalline rock fragments (see section 3.4.1). Abadian *et al.* (1973) interpreted the type I-dikes as open fractures which were filled by ejected material after the deposition of the megablocks.

Type II dikes are represented by two kinds of dikes which occur in megablocks of the surface deposits (Abadian *et al.*, 1973) and in displaced blocks of the crater basement as revealed by the drillhole Nördlingen 1973 (Stöffler *et al.*, 1977). Type II dikes of the surface megablocks consist almost exclusively of rock fragments derived from the adjacent rock by a frictional process (Abadian *et al.*, 1973). The dikes discovered in the crystalline crater basement by drilling

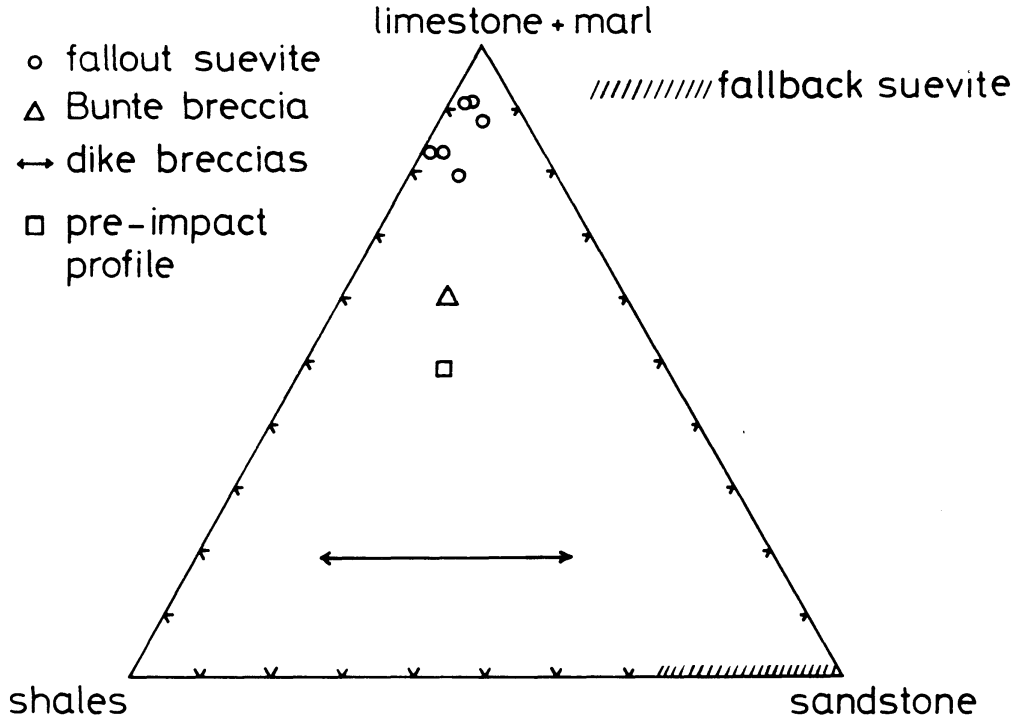


Fig. 12. Proportions of limestone + marl, shale and sandstone in the coarse (~1–10 cm) fragment population of Ries impact breccias and in the pre-impact profile of the sedimentary rock strata. Bunte breccia from Otting, fallback suevite from the drill core Nördlingen 1973 (from Stöffler *et al.*, 1977).

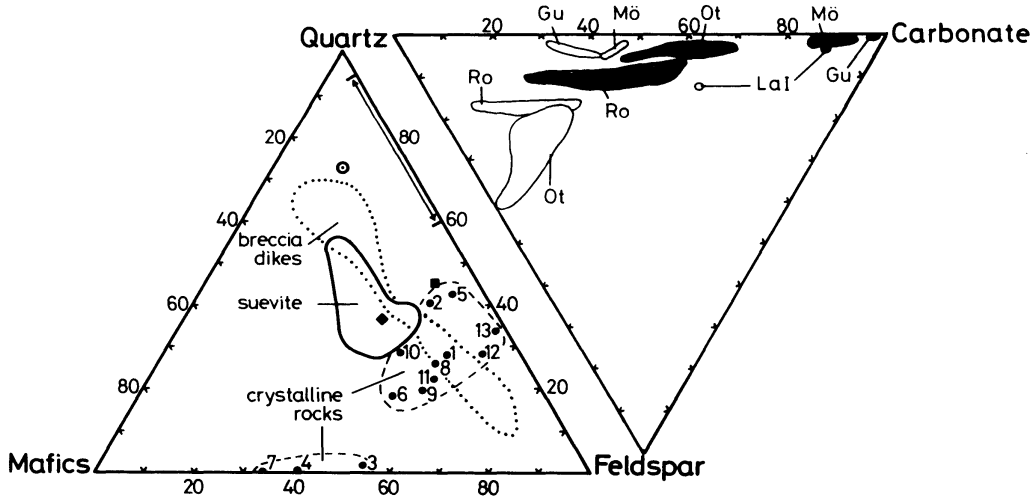


Fig. 13. Relative abundances of quartz, feldspar (alkali feldspar + plagioclase), carbonate and mafic mineral fragments (biotite + amphibole + chlorite) in suevites, dike breccias and Bunte Breccia and in various types of crystalline basement rocks of the Ries. 1, 2, 4, 5, 6, = various gneisses; 3 = amphibolite; 7 = hornblende diorite; 8–11 = granodioritic rocks; 12, 13 = granites (data for 1–13 from Graup, 1975) ⊙ Bunte Breccia of Otting; ◆ suevite of Otting; ■ suevite of Zipplingen; arrow = quartz: feldspar ratio of 10 occurrences of Bunte Breccia (Schneider, 1971); solid line and dotted line = fields of suevite and dike breccia samples, respectively, drill core Nördlingen 1973 (data of Stöffler *et al.*, 1977). Bunte Breccia samples in right triangle given for the grain size ranges. 0.063–0.125 mm (white areas) and 1–2 mm (gray areas) at the localities of Gundelsheim (Gu), Lauchheim (La I), Möhren (Mö), Otting (Ot), and Ronheim (Ro) (data from Schneider, 1971).

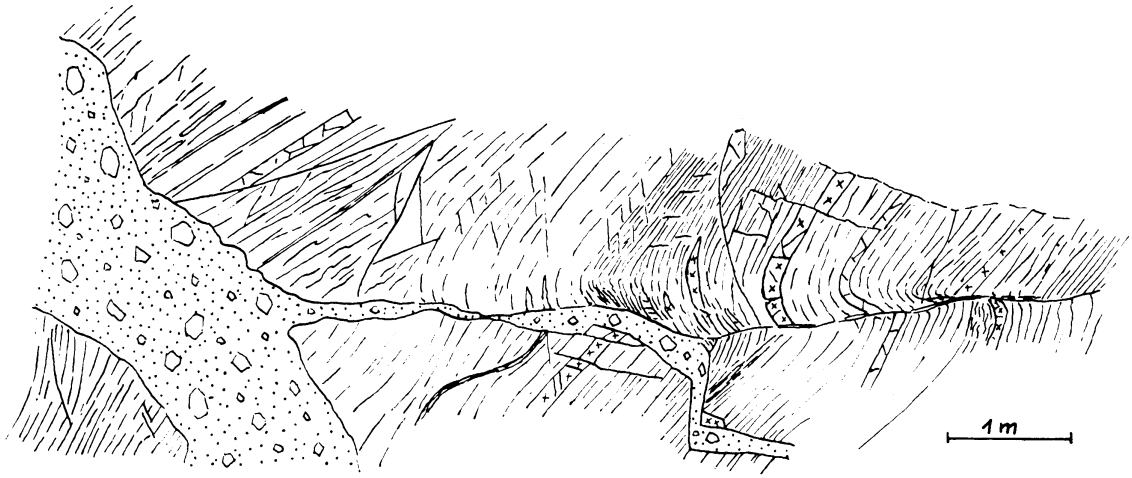


Fig. 14. Dike breccia in gneiss at Klostermühle, Maihingen after G. Wagner, published by Hüttner (1969); parallel and subparallel lines in gneiss indicate the primary schistosity and foliation.

contain not only fragmental country rocks but also a variable proportion of rock fragments of the sedimentary strata and other, higher shocked regions of the crystalline basement (Figs. 12, 13, 18). About 70 dikes several centimeters to about one meter in thickness were found in the drill core Nördlingen 1973 between about 600 and 1200 m depth (Figs. 21, 29). Shocked quartz fragments and a relatively high abundance of sedimentary rock fragments are restricted to the upper section of these dikes (above about 1170 m, Stöffler *et al.*, 1977). These dikes are interpreted as being formed by an injection process which took place during the early stage of crater excavation (Stöffler, 1977).

3.2.3. *Suevite.* Suevite is a polymict breccia of clastic material derived predominantly from the crystalline basement. The particle sizes of the rock and mineral clasts range from a few microns up to about 20 cm, in rare cases up to half a meter (Figs. 16, 17). The particle size distribution is typical for impactoclastic material because of a strong deficiency of fine-grained material (see Stöffler *et al.*, 1976). Most characteristic is that the rock and mineral clasts belong to all stages of shock metamorphism, including partially and completely molten rock material. The crystalline rock fragments display a great variety of different rock types such as granites, gneisses, and amphibolites. Only about 0.2–5% of the rock clast population are sedimentary rocks. The fine-grained detrital matrix mainly composed of quartz, feldspar biotite, and amphibole fragments shows no effects of welding or severe recrystallization. Montmorillonite, which is an abundant matrix constituent, probably results from a secondary alteration of fine-grained clastic or glassy (?) material.

Based on texture, composition and structural position, two types of suevite formations can be distinguished:

(a) *Fallout suevite*, deposited outside the inner ring, forms isolated patches (Fig. 7) on top of megablocks or Bunte breccia (Fig. 16).

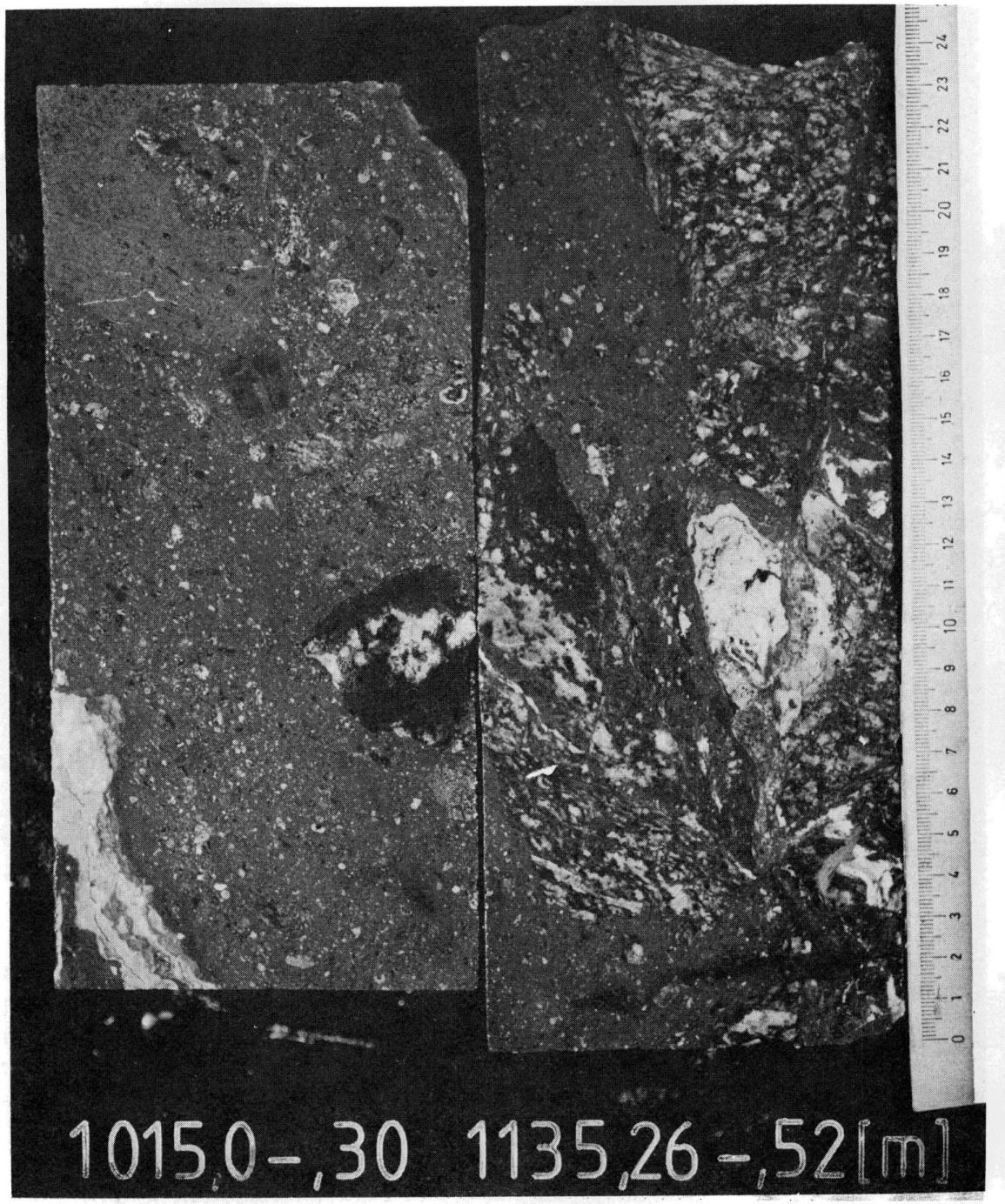


Fig. 15. Sections of dike breccias from the drill core of Nördlingen 1973. The vein-like intrusion into the biotite gneiss country rock is best visible in the right photograph. Lower left corner: brecciated fluorite dikelet. Scale = cm.

Fallout suevite has been studied thoroughly in the past 15 years (Shoemaker and Chao, 1961; Hörz, 1965; Pohl, 1965; Stöffler, 1966, 1971b; Förstner, 1967; Chao, 1967, 1968, 1973; Engelhardt *et al.*, 1969; Pohl and Angenheister, 1969). The most typical in the *modal composition* of the fallout suevite is the abundance of dark-brown to black glass bodies, mostly some mm to a few dm in size, which often have a characteristic bomb- or pancake-like shape (Hörz, 1965). The average glass content is about 15 vol.%. The chemical and petrographic composition of these glasses will be discussed in section 3.2.4. The fallout suevite differs from its fallback counterpart in the abundance and type of sedimentary rock inclusions (Ackermann, 1958; Engelhardt *et al.*, 1969). 80 to 90% of these inclusions (Fig. 12) which comprise only 0.05–1.2% of the total rock, are Malmian limestones. The modal composition, the macroscopic texture and the color vary between the widely distributed occurrences of suevite to some degree whereas the chemical composition of the glass bombs is rather constant compared to the large compositional variation of the lithic clasts (see section 3.2.4).

(b) *Fallback suevite* forms the top layer of the impact formations within the central crater cavity as revealed by the drillings of Deiningen (Förstner, 1967) and Nördlingen 1973 (Bayer. Geol. Landesamt, 1974, 1977). In the drill core Nördlingen 1973 a complete section of the suevite layer was obtained (Figs. 21, 29). This suevite profile can be subdivided into 3 major units: suevitic sandstones and conglomerates from 314 to 331.5 m, melt-rich suevite from 331.5 to about 525 m, melt-poor suevite from 525 to 602 m as intercalations within the brecciated crystalline basement.

Small, brownish, elongated to isometric bodies of extremely vesiculated and recrystallized melt particles, less than a millimeter to some centimeters in size, are the most contrasting feature of the *modal composition* and *texture* as compared to the fallout suevite (Fig. 17). In addition, the fallback suevite contains many less sedimentary rock inclusions among which only sandstone and shale, but no limestone was found. The melt particles are also less abundant compared to the fallout suevite (about 3–5 vol.% on the average for the entire suevite layer).

Some relevant properties of the *mineral and lithic clast population* in both types of suevite are presented in Figs. 12, 13, and 18 (see also Stöffler *et al.*, 1977). The most important conclusions which can be drawn from these data for the origin of fallout and fallback suevite are: (1) the lithic clast population of both suevites (Fig. 18) is dominated by gneisses and differs distinctly from the petrographic composition of the crystalline megablocks, 79% of which are granites; (2) the abundance of melt and sedimentary rock inclusions is markedly higher in the fallout suevite than in the fallback suevite; and (3) the mineral clast population of both types of suevite deviates from a mere mixture of comminuted basement rocks because of excess quartz, possibly derived from comminuted sandstone (Fig. 13).

3.2.4. *Impact melt.* Shock produced melt of the Ries target rocks is found in two types of impact formations: (1) as inclusions in suevite (Fig. 17, see section 3.2.3), and (2) as isolated bodies of impact melt rocks.

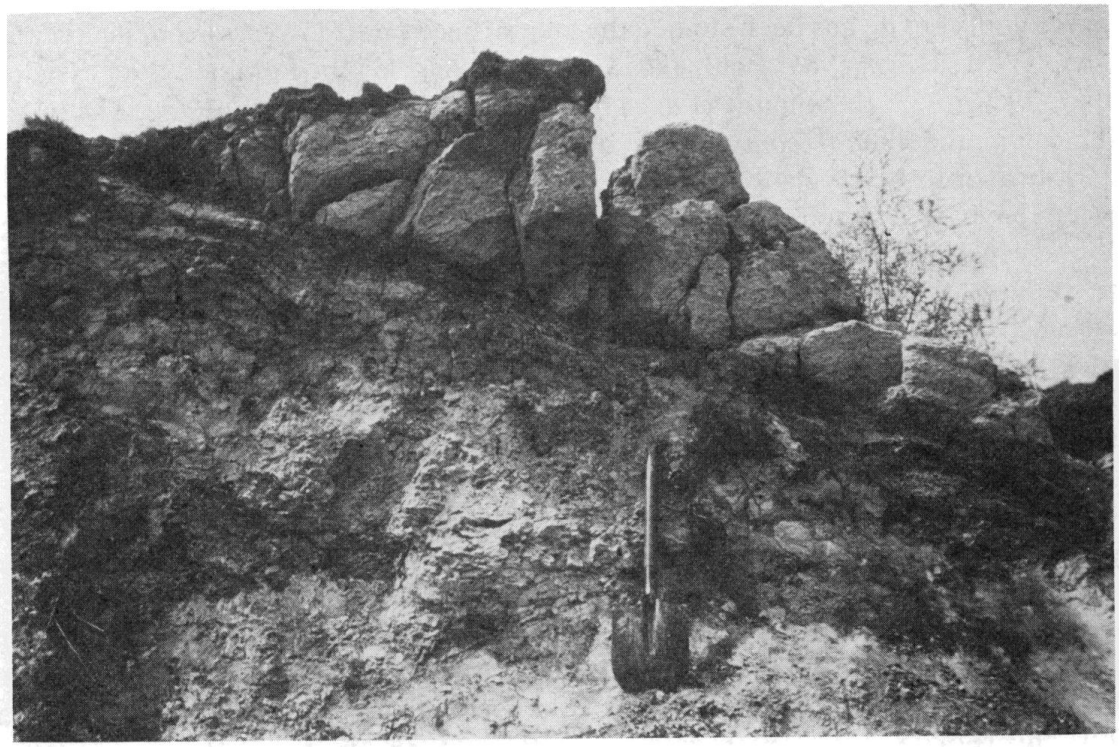

Fig. 16. Suevite on top of Bunte breccia, quarry of Aumühle, northern part of megablock zone.

Only two occurrences of *impact melt rock*, with lateral extents of 10–50 m were found near Polsingen and Amerbach in the megablock zone, about 1.5–3 km inside the tectonic rim of the crater. They overlay megablocks or Bunte breccia. The reddish melt rock consists of a vesicular, fine-grained recrystallized glass matrix with fluidal texture in which many angular fragments of crystalline rocks in different stages of shock metamorphism are embedded. The matrix glass is completely crystallized to a fine-grained aggregate of feldspar, pyroxene, hematite, and cristobalite.

The *glass bombs of the fallout suevite* most intensely investigated by Hörz (1965), Engelhardt (1976b, 1972), El Goresy (1968) and Stähle (1972) are mixtures of fluidal, vesiculated and schlieren-rich glass with fragmental inclusions of comminuted basement rocks in all stages of shock metamorphism. Quartz fragments (6–23%), 5–30% which display shock effects, are most abundant; less frequent are crystalline rock fragments (1–7%), plagioclase (0.1–0.3%), $SiO_2$-glass (1–3%) and accessories (Zircon, apatite, biotite comprising 0–0.7%) according to Engelhardt (1972). The decomposition products of some accessories indicate very high temperatures of the melt of at least 1950°C (El Goresy, 1968; Stähle, 1972). Ni-iron spherules are extremely rare in these glasses but Fe-sulfide spherules are more abundant (El Goresy, 1968; Chao, 1963; Stähle, 1972).

In contrast to the glass bombs of the fallout suevite, the *melt inclusions of the fallback suevite* (see section 3.2.3) have a pumice-like vesiculated texture and are completely recrystallized to montmorillonite and analcite (Förstner, 1967;

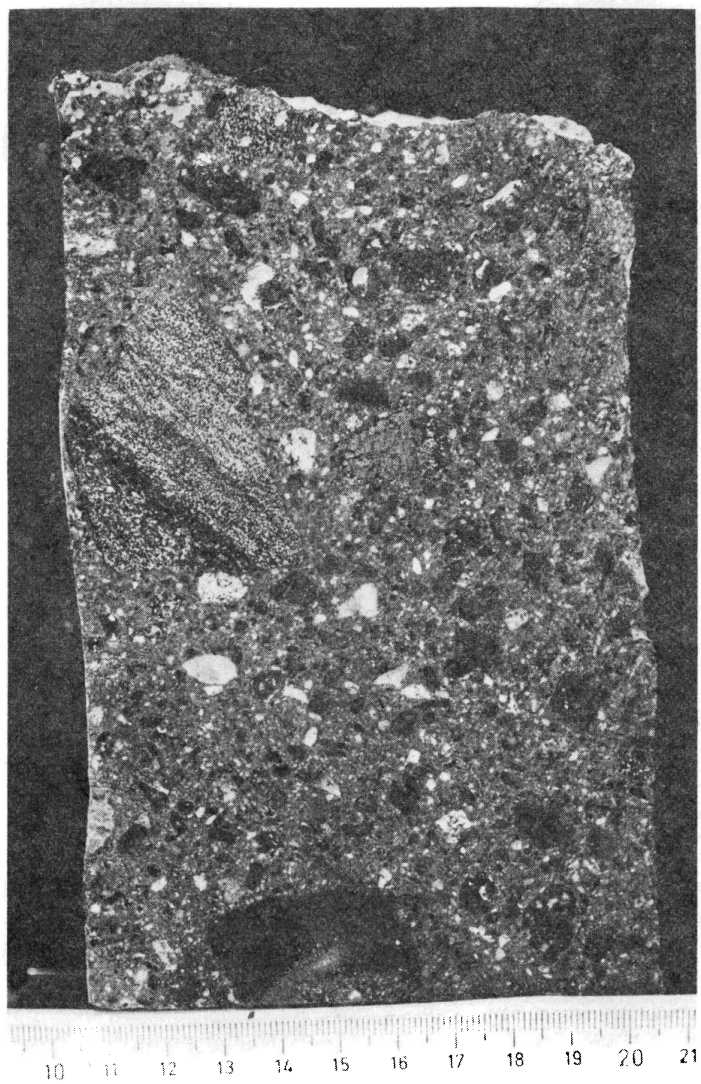


Fig. 17. Suevite from the drill core of Nördlingen (depth 417.5 m), dark inclusions are melt products, other fragments are crystalline rocks of lower shock metamorphism; scale = cm.

Stähle and Ottemann, 1977; Stöffler *et al.*, 1977). They contain many less fragmental inclusions than the glass bombs or are even free of them.

The chemical composition of the various occurrences of glassy impact melt is remarkably constant as far as the fallout suevite is concerned (Table 3, Fig. 19). The melt of the glass bombs probably originates from shock-fused crystalline basement rocks (Fig. 19), most probably from gneiss (Engelhardt, 1977) although the scatter of 88 analyses of different localities (Table 3; Stähle, 1972) is still large enough to allow for other crystalline source rocks or mixtures of source rocks. However, most of the melt volume in the Ries is contained in the fallback suevite or in a possible, yet unknown central impact melt layer. The composition of the melt in the fallback suevite is not known because its chemistry is severely

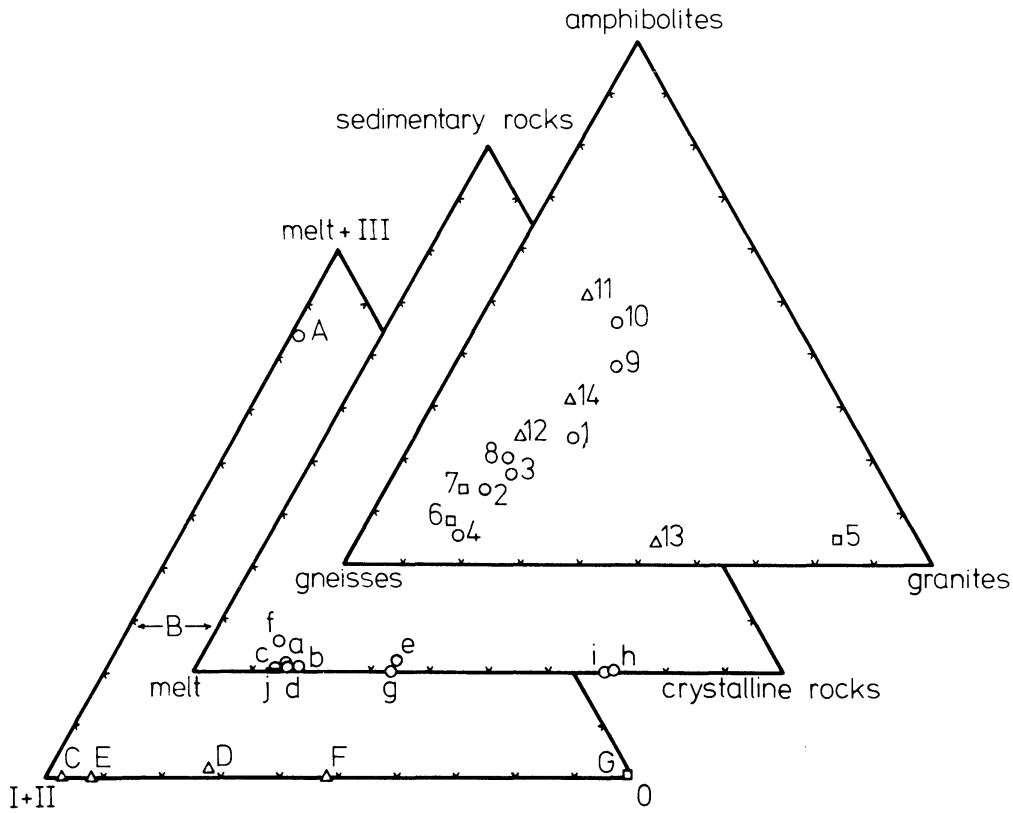


Fig. 18. Population plots of lithologies of coarse particles in polymict Ries breccias and of autochthonous and allochthonous crystalline basement rocks (circles = suevite, triangles = crystalline breccias, squares = crystalline basement megablocks).

*Right plot*: 1 = five fallout suevite occurrences (fragments of shock stages O and I); 2 = same as 1 but only fragments of shock stage II (Stöffler, unpublished data and data of Engelhardt *et al.*, 1969), 4 = suevite of Zipplingen (fragments of the 4–32 mm size class, Stöffler, unpublished data), 5 = large blocks and megablocks of crystalline rocks of the Ries ejecta blanket (Graup, 1975); 6 = crystalline basement below 602 m of the drill core of Nördlingen 1973, calculated from the core description of Bauberger *et al.*, 1974; 7 = same as 6 but including hornblende gneisses within amphibolites; 8 = suevite of the drill core of Nördlingen 1973 (fragments of the 8–28 mm size class, from Stöffler *et al.*, 1977); 9 = suevite of the drill core Nördlingen 1973 (fragments 60 mm, Bauberger *et al.*, 1974); 10 = same as 9 but including hornblende gneisses within amphibolites; 11, 12, 13, 14 = polymict crystalline breccias of Nördlingen, Maihingen, Appetshofen and Lierheim (data from Abadian, 1972).

*Middle plot*: a–g = fallout suevite occurrences (a–f = data of Ackermann, 1958); a, b = Aufhausen, c = Mauren, d = Aumühle; e = Bollstadt; f = Otting; g = Zipplingen (Stöffler *et al.*, 1977); h = fallback suevite, drill core Nördlingen 1973 (Stöffler *et al.*, 1977); i, j = fallback and fallout suevite of the drill cores of Deiningen and Wörnitzostheim, respectively (approximate values of Förstner, 1967).

*Left plot*: A = average of 5 fallout suevite occurrences (Engelhardt *et al.*, 1969); B = average of the drill core fallback suevite of Nördlingen 1973 (ratio stage 0 : I : II not exactly known, Stöffler *et al.*, 1977); C, D, E, F = polymict crystalline breccias (see 11, 12, 13, 14); G = large blocks and megablocks of crystalline rocks from the ejecta blanket (Graup, 1975).

1977iecp.symp..343P



Table 3. Chemical analyses of crystalline basement rocks, suevite, and glass bombs.

| | 1 | 2 | 3 | 4 | 5 | 6 | 7 | 8 | 9 | 10 | 11 | 12 |
|---|---|---|---|---|---|---|---|---|---|---|---|---|
| $SiO_2$ | 53.39 | 57.50 | 65.62 | 59.09 | 72.13 | 58.31 | 57.12 | 62.63 | 64.01 | 62.66 | 64.03 | 1.33 |
| $TiO_2$ | 0.70 | 0.88 | 0.43 | 0.98 | 0.13 | 0.98 | 0.86 | 0.33 | 0.78 | 0.78 | 0.79 | 0.096 |
| $Al_2O_3$ | 17.47 | 17.90 | 15.83 | 17.85 | 15.37 | 14.97 | 13.53 | 10.06 | 16.85 | 15.48 | 15.25 | 0.39 |
| $Fe_2O_3$ | 4.46 | 1.70 | 1.07 | 1.81 | 0.34 | 1.46 | 1.81 | 4.29 | 3.40 | 1.53 | 5.22 | 0.43 |
| FeO | 5.29 | 4.70 | 2.88 | 5.01 | 0.81 | 4.18 | 5.24 | 3.28 | 1.44 | 2.55 | | |
| MnO | 0.24 | 0.10 | 0.08 | 0.16 | 0.03 | — | — | — | — | — | 0.077 | 0.017 |
| MgO | 4.86 | 3.32 | 1.66 | 3.20 | 0.38 | 4.17 | 5.64 | 2.70 | 1.23 | 1.82 | 3.04 | 0.31 |
| CaO | 7.70 | 4.28 | 3.40 | 4.87 | 0.80 | 3.51 | 6.52 | 4.87 | 2.97 | 2.82 | 3.96 | 0.52 |
| $Na_2O$ | 3.55 | 3.91 | 2.90 | 3.35 | 3.45 | 4.52 | 3.26 | 3.62 | 4.01 | 4.70 | 3.02 | 0.46 |
| $K_2O$ | 1.21 | 2.43 | 4.09 | 2.35 | 5.66 | 3.23 | 1.85 | 3.24 | 3.63 | 5.74 | 4.01 | 0.82 |
| $P_2O_5$ | 0.20 | 0.18 | 0.57 | 0.29 | 0.24 | 0.31 | 0.26 | 0.33 | 0.40 | 0.33 | 0.21 | 0.059 |
| $H_2O$ | 1.39 | 2.93 | 1.41 | 1.91 | 0.60 | 3.35 | 2.19 | 3.82 | 1.05 | 1.35 | — | — |
| $CO_2$ | 0.39 | 0.82 | 1.21 | 0.12 | 0.29 | 0.60 | 1.34 | — | 0.54 | 0.93 | — | — |
| S | — | — | — | — | — | 0.71 | 0.48 | 0.28 | — | — | — | — |
| Σ | 100.85 | 100.65 | 100.85 | 100.99 | 100.23 | 100.38 | 100.23 | 99.55 | 100.31 | 100.69 | 99.61 | — |

1–5 = crystalline basement rocks from the drill core Nördlingen 1973 (from Graup, 1977), amphibolite (depth 625.3 m, 1), hornblende-biotite-plagioclase gneiss (711.9 m, 2), migmatic gneiss (926.5 and 1201.5 m, 3 and 4), granite (540.5 m, 5).

6–8 = drill core Nördlingen 1973 (from Stähle and Ottemann, 1977), suevite (depth 400.0 m, 6), melt-poor suevite (597.0 m, 7), dike breccia (737.1 m, 8).

9 = suevite (depth 61.1 m) from the drill core Wörnitzostheim (from Förstner, 1967).

10 = suevite (depth 340 m) of the drill core Deiningen (from Förstner, 1967).

11 = 88 microprobe analyses of 51 matrix glasses from glass bombs of fallout suevite occurrences (Amerdingen, Aufhausen, Aumühle, Bollstadt, Fünfstetten, Grossorheim, Mauren, Otting, and Zipplingen (from Stähle, 1972).

12 = standard deviation $\sigma$ of 88 analyses of No. 11.

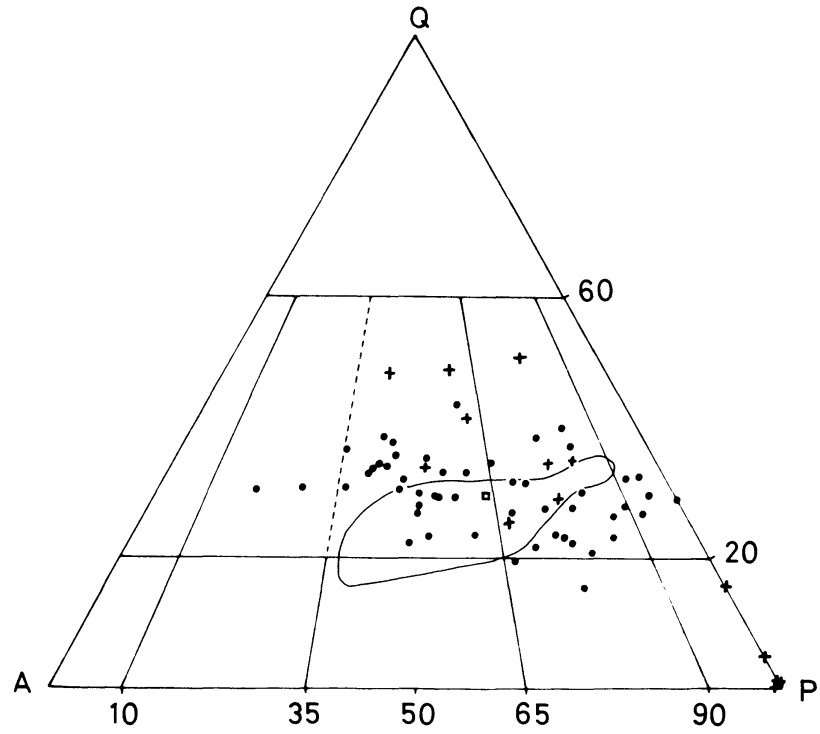


Fig. 19. Modal composition of crystalline basement rocks after Graup (1975) as compared to the normative composition of 52 samples of matrix glass (solid line; 88 microprobe analyses) from the fallout suevite of Amerdingen, Aufhausen, Aumühle, Bollstadt, Fünfstetten, Großsorheim, Mauren, Otting, and Zipplingen (data from Stähle, 1972); calculated according to the plutonic norm of Rittmann (1973); A = alkali feldspar, P = plagioclase, Q = quartz.

altered now. It is possible that the extremely vesiculated melt particles are derived in part from fused sedimentary rocks or from a more or less homogenized mixture of sedimentary and crystalline rocks and that they originate from a part of the melt zone which is different from that of the fallout glass bombs (for details see Stöffler, 1977).

Neither the Ries melt nor other Ries impact formations is markedly enriched in siderophile elements (Ir, Os, Re, Au, Pd) so that any contamination by the impacting body is uncertain (Morgan, 1976), although the Ni-content of the glass-bombs is slightly higher than that of the crystalline basement rocks (Hörz, 1965; Stähle, 1972).

3.2.5. *Distant ejecta.* There are three possible types of distant ejecta which might be related to the Ries impact event: (1) single rock fragments of Malmian limestone (Malmian δ and younger), generally less than 20 cm in size, were found south of the Danube at radial distances up to 70 km within fine-grained Molasse sediments of Ries age and at the boundary of Tertiary and Quaternary (Fig. 1; Reuter, 1926; Scheuenpflug, 1973; Engelhardt, 1975; Gall *et al.*, 1975). Part of these so called *Reuter blocks* are Ries ejecta (Gall and Müller, 1975; Gall *et al.*, 1975). (2) Thin layers of *bentonite* occur in the same area where the Reuter

blocks are found. The bentonites are tuff-like layers consisting mainly of fine glass particles recrystallized to montmorillonite. The Ries origin of these sediments is still controversial (Harr, 1976). (3) The *moldavite tektites* of the Czechoslovakian strewn field (Fig. 1) are commonly considered as Ries ejecta (Gentner *et al.*, 1963).

The strongest argument in favour of the Ries origin of the bentonites and moldavites is the common age of 14.7 m.y. which is the age of the Ries event (Gentner and Wagner, 1969). If the bentonites and moldavites originate from the Ries, they might represent fused silica-rich Tertiary sediments from the top of the target which were ejected with extremely high velocities at the very beginning of the impacting process (see Gault *et al.*, 1968; O'Keefe and Weiskirchner, 1970).

### 3.3. *Structure, stratigraphy and thickness of the outer impact formations*

Regional variations of the composition, thickness and structure of the Ries outer impact formations have been reviewed recently by Gall *et al.* (1975). The regional variation in the distribution of the fallback material inside the central crater cavity could be evaluated only by indirect geophysical observations and by extrapolation from drill core data. It will be discussed in section 4. Essential characteristics of the outer impact formations deposited outside the inner ring are schematically represented in Fig. 20. They will be discussed here following vertical and horizontal sections.

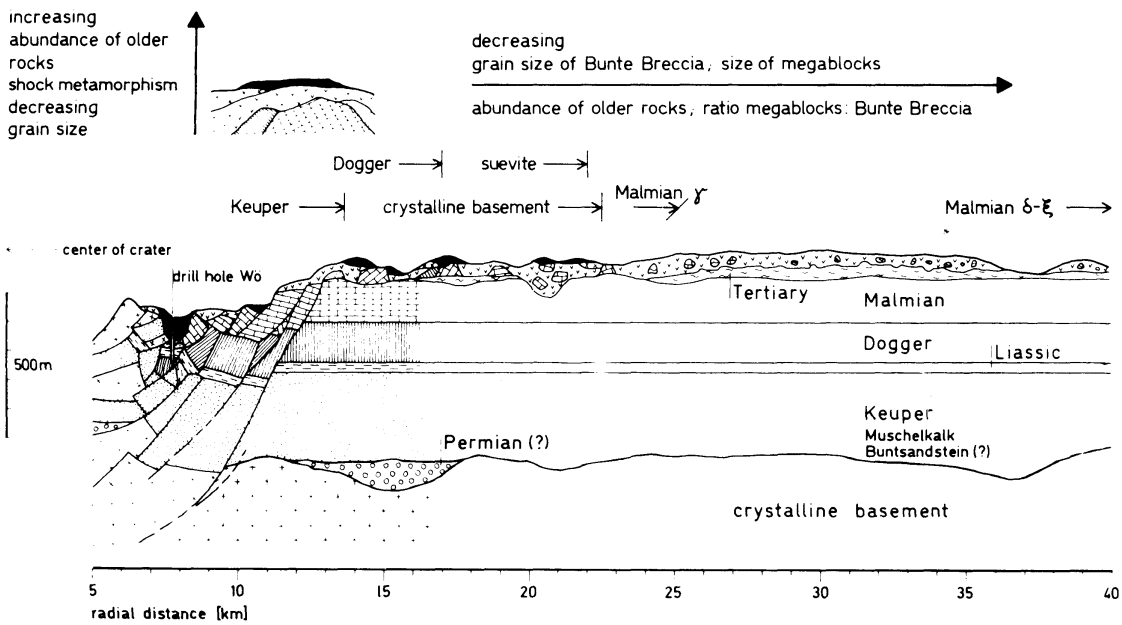


Fig. 20. Schematic profile of the megablock zone and southern "Vorries" continuous deposits; Wö = Wörnitzostheim; small arrows indicate the maximum radial extent of megablocks from different stratigraphic levels and of the suevite.

Within the *megablock zone* complete vertical sections of the displaced rock masses are not exposed and the information obtained from the surface geology has to be supplemented by geophysical and drilling data (e.g., drill holes of Wallerstein 1948, Nördlingen 1950, 1955, and Wörnitzostheim 1965; Fig. 21). Near the inner ring, the section of displaced rocks consists predominantly of megablocks, which have been uplifted mainly from the crystalline basement and the lowest section of the sedimentary strata (Triassic), occasionally covered by a layer of suevite of limited lateral extension. The drill core of Wörnitzostheim gives one of the few good examples of an inverted stratigraphy in the megablock zone, near the inner ring, with suevite, granite, and an inverted block of Keuper, Liassic and Dogger sediments going from top to bottom (Fig. 21, Gall *et al.*, 1976; Dressler and Graup, 1974). Quite commonly the primary stratigraphic relations of megablocks (e.g., megablock of Keuper, Liassic, and Dogger strata near Harburg described by Müller, 1969) is disturbed by shear faulting. Approaching the tectonic rim of the crater (Fig. 20) the number of megablocks of higher stratigraphic levels (Dogger and lower Malmian) increases and their structural position is less disturbed. Displacement by slumping dominates over tilting and overturning (Hüttner, 1969; Gall *et al.*, 1977). It is typical that fine-grained Bunte breccia is subordinate in the megablock zone, i.e., block sizes below about 10 m are rare. On the average, the particle size seems to decrease towards the top of the displaced masses. Other typical structural features are the polished and striated surfaces (Schliff-Fläche) on top of displaced Malmian

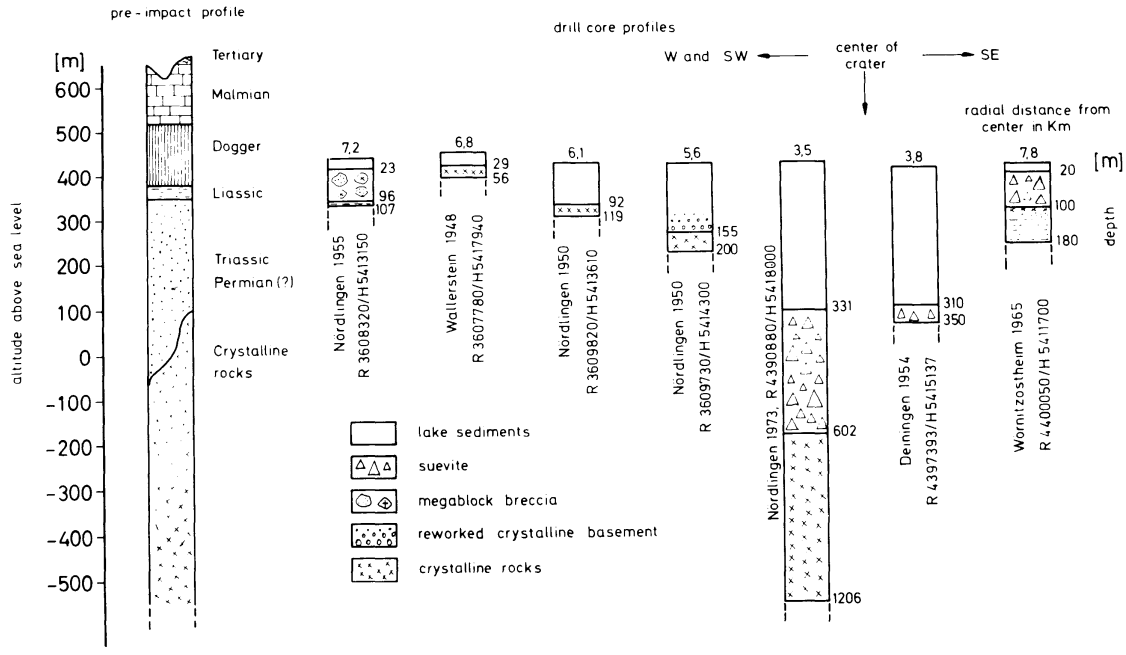


Fig. 21. Comparison of drill core profiles within the Ries crater with the pre-impact stratigraphy (left). Figures on top of the drill cores indicate the radial distance from the center of crater; R and H values refer to the grid system of the topographic maps 1 : 25,000 of the states of Baden-Württemberg and Bayern (Bavaria).

megablocks obviously produced by the violent gliding of masses of Bunte breccia after or during the displacement of the blocks (e.g., Holheim, Siegling quarry; Ronheim, Bschor quarry, Fig. 10). Polished and striated surfaces on top of autochthonous Malmian extend far beyond the tectonic boundary of the crater, e.g., exposures at Gundelsheim or Möhren, up to 24 km from the point of impact.

A remarkable observation in vertical sections of the continuous deposits of the megablocks and the *Vorries zone* is the lack of any regular, layered stratigraphy (Fig. 20). Although the gross principle of inverted stratigraphy appears to hold as far as it can be checked in field outcrops and drill holes, the sequence of inverted rocks is generally incomplete and irregular. The contacts between various stratigraphic units are often steeply inclined. Near the tectonic rim of the crater all main stratigraphic units may be found at the top of the continuous deposits if a cross section circumferential to the rim is considered. However, suevite, if present, is always found on top of other displaced rocks, mostly on Bunte breccia but also on large blocks of all stratigraphic levels (see sketch inset in Fig. 20). The contact to the underlaying polymict breccias (Bunte breccia) which usually have a very strong relief, is extremely sharp. Laminated structures were observed at this contact. Schneider (1971) found that in finer grained Bunte breccia (mostly analyzed in short profiles of the top section) the abundance of rock fragments of lower stratigraphic levels increases from the bottom to the top. This holds also for the abundance of shocked minerals (quartz), whereas the grain size decreases in the same direction.

A genetically important observation was made by field geologists as early as 1905 (v. Ammon) and recently discussed in detail by Hüttner (1958, 1969), Gall (1969), and Hörz *et al.* (1975): at some radial distance from the crater, Bunte breccia contains an appreciable amount of local material excavated from the ground surface and incorporated into the breccia probably by secondary cratering of landing ejecta (Fig. 22). This effect is most conspicuous in places where the pre-impact surface is formed by soft Tertiary sediments (clay, sand). The local material which was horizontally transported in some cases over a distance 1.5–3 km (Hüttner, 1969) comprises 20–80% of the breccia (Hüttner, 1969; Hörz, 1976). Schneider (1971) confirmed this observation by a detailed petrographic analysis of Bunte breccia from several localities.

As discussed by Hüttner (1969), Schneider (1971), and Gall *et al.* (1975) the following radial variations of various properties of the continuous deposits of the Ries appear relevant for the interpretation of the crater-forming process:

(a) The size or volume of megablocks decreases as a function of range, most conspicuously observed with Malmian limestone blocks (Fig. 23).
(b) The abundance of megablocks (>25 m) from the uppermost strata of the target increases as a function of range (Figs. 20, 24); the largest radial range of ejected blocks decreases with their primary depth in the target (Fig. 20). The radial extent of blocks from the crystalline basement and also the suevite does not follow this rule; they extend to a larger radial distance than Keuper or even Dogger megablocks. Their pattern of

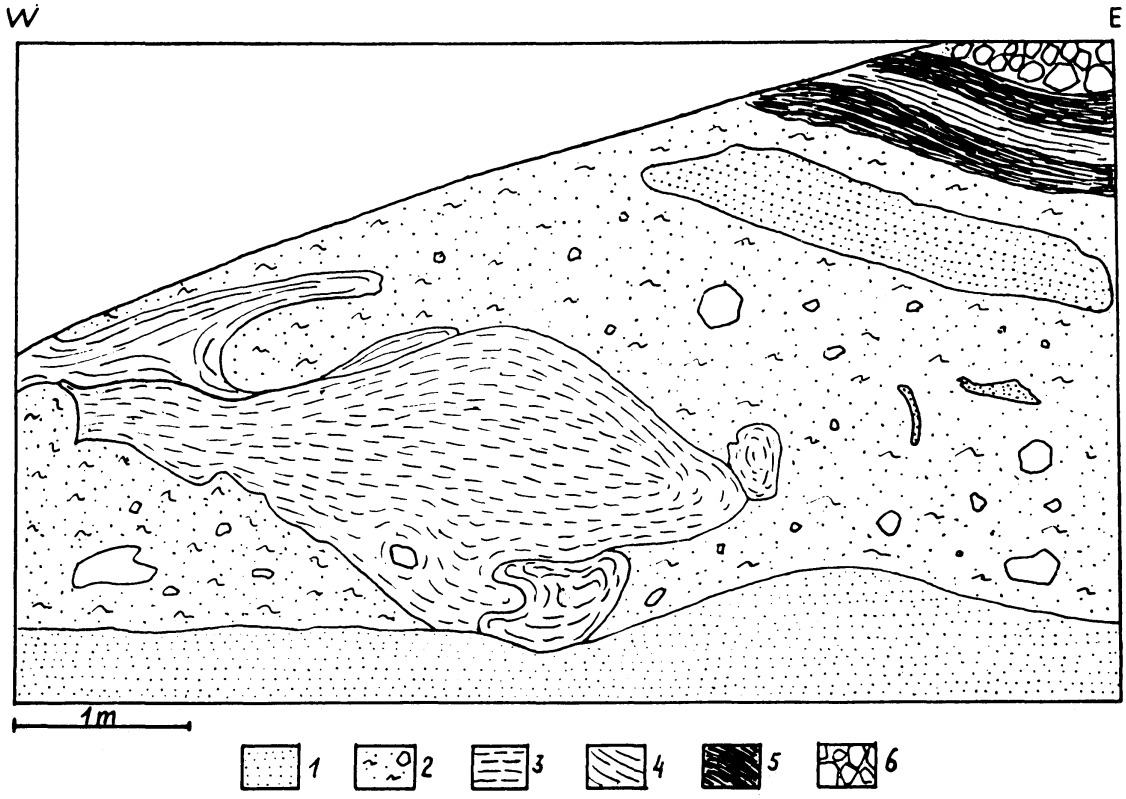


Fig. 22. Bunte breccia on top of Molasse sediments (Tertiary sandstone) with inclusions of large blocks of local Molasse sediments; quarry of Guldesmühle near Dischingen; 1 = Miocene (OMM = Obere Meeresmolasse) sand; 2 = matrix mainly derived from 1; 3 = Miocene (OSM = Obere Süsswassermolasse) marl; 4 = weathering products; 5 = Tertiary clay (?); 6 = blocks of Malmian limestone; from Hüttner (1969).

distribution is less concentric to the crater (Fig. 7, note possible ray-like extension of crystalline blocks).

(c) The ratio of fine-grained Bunte breccia to megablocks increases as a function of range.

(d) In areas of the megablock and Vorries zone where the effect of post-impact erosion is known or negligible, it is found that the thickness of the continuous deposits (Bunte breccia and megablocks taken as one unit) does not show a regular decrease as a function of range. This is probably due to the relief of the pre-impact surface and to mass transport and redistribution by secondary cratering (Oberbeck, 1975; Hörz, 1976). Local depressions of the target contain very thick deposits. In the pre-existing, former Main River valley thicknesses of up to 200 m were found at a distance of about 20 km from the crater center (Birzer, 1969; Bader and Schmidt-Kaler, 1977). On the average the thickness varies between 100 and a few meters.

(e) Suevite reaches a thickness of 84 m in the drill hole of Wörnitzostheim (Figs. 20, 21; Förstner, 1967; Pohl and Angenheister, 1969) in the

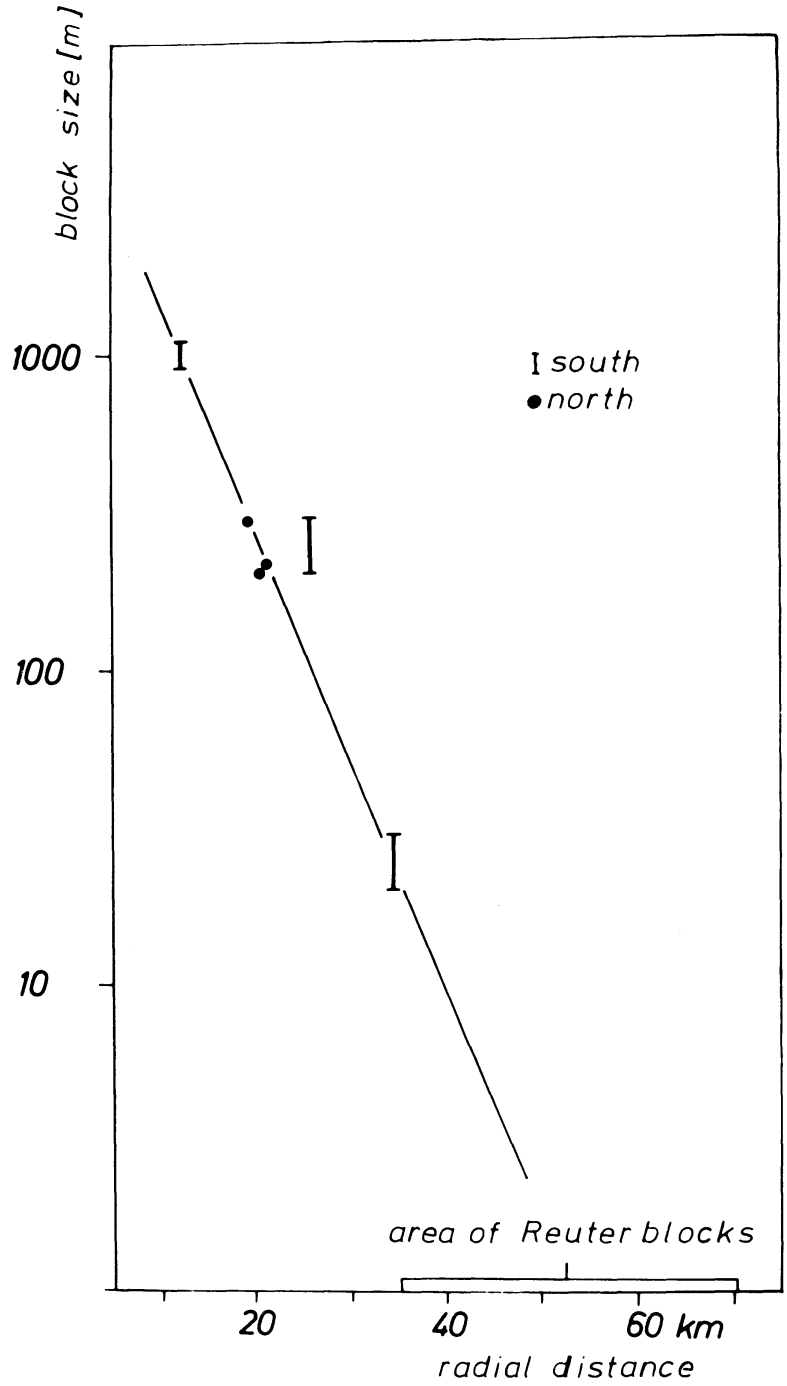


Fig. 23. Size of Malmian megablocks in the Ries outer impact formations as a function of range (after Gall *et al.*, 1975).

megablock zone. In the Vorries the thickness of suevite ranges between 25 and 5 m. Since the upper quenched zone of suevite (see section 3.4) is still preserved in many suevite outcrops (Engelhardt *et al.*, 1969) the intensity of erosion was very weak in some occurrences. Therefore 25 m is considered a maximum primary thickness in the Vorries.

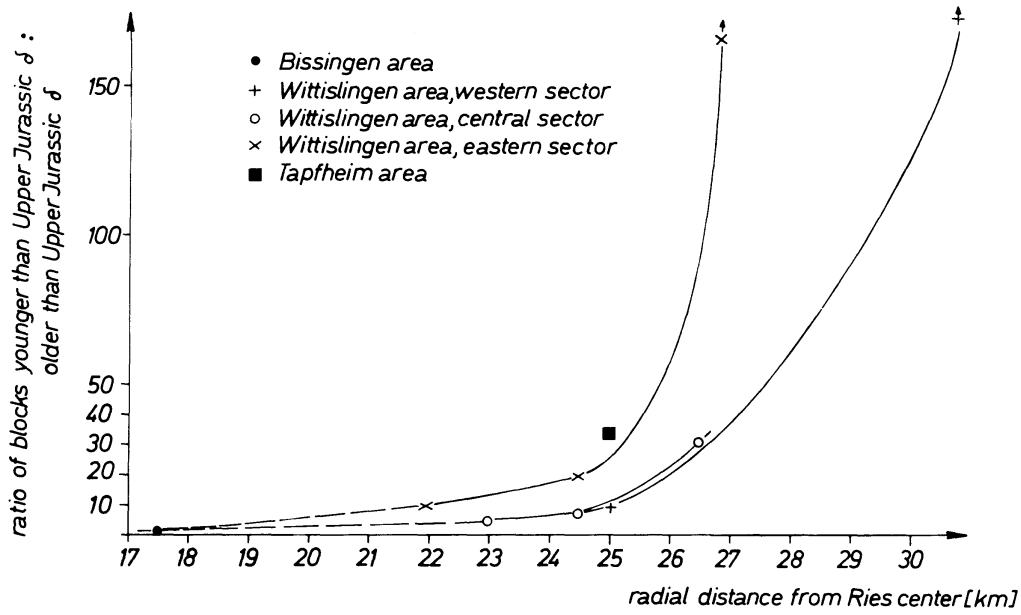


Fig. 24. Stratigraphic provenance of Malmian megablocks as a function of range at various radial sections of the Vorries continuous deposits (after Gall *et al.*, 1975).

(f) The volume fraction of local ground material increases as a function of range, reaching some 80% of the total volume of Bunte breccia at its outer margin (Hüttner, 1969; Schneider, 1971; Gall, 1974; Hörz, 1976).

### 3.4. *Shock metamorphism and thermal history of various impact formations*

In the following section the shock metamorphic properties of the polymict breccias, the megablocks of the outer crater deposits, and of the crater basement will be discussed. The degree of shock of any discrete rock fragment—whether it is a small clast in a polymict breccia or a megablock—will be defined according to the classification of progressive shock metamorphism proposed by Stöffler (1971a). Since the post-shock heat of a rock fragment is primarily a function of the shock peak pressure the thermal history of a particular breccia will be closely related to the relative proportions of rock and mineral clasts of different shock stage incorporated in that breccia. This will be discussed in the last section of this chapter.

A brief summary of the shock metamorphic properties of the main types of the Ries impact formations is given in Table 2.

#### 3.4.1. *Shock metamorphism of suevite and bulk continuous deposits*

*Impact melt* representing the highest stage of shock metamorphism is found in most terrestrial craters (e.g., Dence, 1971; Grieve *et al.*, 1977) as coherent sheets of melt rocks in the central area of the crater and as discrete smaller particles in suevite breccias. In the Ries only two smaller bodies of coherent melt in the eastern megablock zone are known. Geophysical data do not exclude the

possibility that a coherent layer of impact melt rock could be discovered in the central crater basin by drilling. *Suevite* contains the remaining fraction of melt along with rock and mineral clasts of all stages of shock metamorphism. Petrographic and chemical properties of the melt inclusions have been discussed in section 3.2.3. Quantitative data with respect to the distribution of shock stages in the total clast population are given in Fig. 18 (see also Engelhardt *et al.*, 1969; Stöffler *et al.*, 1977). The fraction of melt and rock clasts of shock stage III is distinctly higher in the fallout suevite than in the fallback suevite of the drill hole Nördlingen 1973. The abundance of clasts of stage 0 (planar deformation structure lacking) is remarkably low in the fallout suevite. Quenched high pressure polymorphs like coesite and stishovite are present in this type of suevite (Shoemaker and Chao, 1961; Stöffler, 1971b). In the fallback suevite of the drill hole Nördlingen 1973 (Fig. 21) a vertical variation in the abundance of shock effects was found (Stöffler *et al.*, 1977): the volume fraction of melt inclusions and of shocked quartz fragments decreases continuously with depth in the lower part of the suevite section, below about 380 and 450 m respectively (Fig. 25) indicating a complex mixing and deposition history of the fallback suevite. Unequivocal shock effects as defined by stages I–IV in the sedimentary rock clasts have not been observed in the fallout suevite although they cannot be excluded with certainty in the fallback suevite. Microscopically observable shock effects in the mineral and rock fragments of the *Bunte breccia* are restricted to quartz and crystalline rocks. Planar elements in quartz fragments and shock stages 0, I, II in crystalline rock clasts (e.g., Schneider, 1971) indicate that this material is derived from zones of the crater basement which were affected by peak shock pressures below about 400 kbar. Occasionally these rock clasts display shatter cones. Shock effects in the sedimentary rock fragments (e.g., sandstones, shales) are consistently lacking. Since sedimentary rocks comprise more than 90–95% of the volume of Bunte breccia it must be concluded that the bulk of the rock material in the Bunte breccia was affected by shock pressures much less than 50 kbar. The clast population of the *crystalline* breccias and *dike breccias* belongs to shock stages 0, I and II (Fig. 18); stage III is extremely rare (Abadian, 1972). Coesite and stishovite are common constituents of these rocks (Stöffler, 1971b). The rocks penetrated by dikes are usually very weakly shocked (stage 0). This holds also for all *megablocks* in the megablock and Vorries zone. The mode of brecciation and fracturing of these blocks, however, is quite characteristic. It is basically different in competent and incompetent rocks. Limestone, expecially massive reef limestone, and crystalline rocks failed by brittle fracturing; marl, shale, and clay display severe plastic deformation but unusual brittle fracturing is also frequently observed (Hüttner, 1969). Different types of deformation can be distinguished in limestone and crystalline rocks (Wagner, 1964; Hüttner, 1969): (a) extremely intense *fracturing*: the fractures are irregularly oriented and have an extreme but variable spacing in the millimeter to centimeter range, in contrast to the preexisting tectonic fracture systems, which are spaced in the order of decimeter to meter. (b) *brecciation*: highly angular rock fragments produced by brittle fracturing

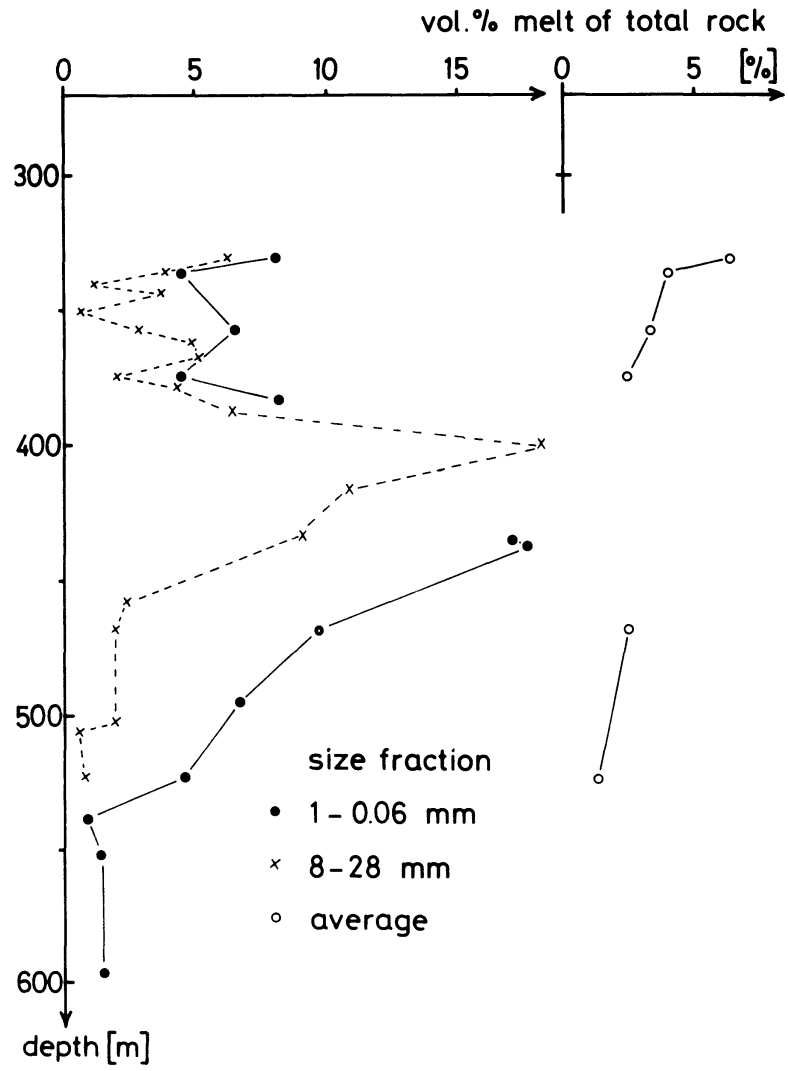


Fig. 25. Abundance of melt products in the suevite of the drill core Nördlingen 1973 as a function of depth (modified after Stöffler, 1977), average calculated on the basis of the grain size distribution.

moved and rotated such that larger fragments (up to some centimeters) are embedded in a more fine-grained matrix (Figs. 26, 27). This may be called a monomict breccia ("Gries").

Within one megablock, regions of both types of deformation may alternate within the range of a decimeter to several meters (Fig. 28), producing complicated megatextures of fractured rocks within monomict breccias or vice versa. Only weak shock effects have been observed in the minerals of the crystalline megablocks (stage 0). Kink bands in biotite are most typical; planar deformation structures in quartz indicating peak pressures of more than 90 kbar, are mostly absent (Stöffler, 1969; Graup, 1975). In brecciated limestone a change of the thermo-luminescence was observed (Engelhardt, 1975).

3.4.2 *Shock metamorphism of the crater basement.* The crystalline rocks at the base of the suevite layer in the drill core Nördlingen 1973 (see Figs. 21, 29), which can be interpreted as displaced megablocks, reveal shock effects in quartz, feldspar, biotite, hornblende, and other constituents (Engelhardt and Graup, 1977). These authors derived an attenuation of the peak pressure from about 160 kbar at a depth of 505 m to about 90 kbar at 670 m on the basis of shock effects in quartz. In this depth range a high intensity of shatter coning was found (Bayer. Geol. Landesamt, 1977) which decreases below about 600 m. The attenuation of the peak shock pressures in the whole profile is discontinuous (Fig. 29). At 1206 m the peak pressure may have been less than 10 kbar (kinking in biotite).

3.4.3 *Thermal history.* Thermal annealing of breccias or of their substrates after deposition is restricted to suevite. All other impact formations lack any mineralogical or other effects which could be assigned unequivocally to post-shock heat. This means that the bulk continuous deposits of the megablock and Vorries zone never experienced any shock-induced increase of temperature. In contrast, suevite was deposited as a relatively hot impact formation on top of all other types of displaced rock masses (Fig. 16). The top and bottom zones of the *fallout suevite* were thermally quenched upon deposition of the suevite, leaving a central hot zone in which shock-produced glasses recrystallized to a fine-grained aggregate of plagioclase and clinopyroxene (Engelhardt *et al.*, 1969). Vertical vents indicate outgassing of the hot suevite and hydrothermal formation of secondary minerals after deposition, mainly montmorillonite, quartz and zeolites. The highly vesiculated glasses of the fallback suevite are completely recrystallized to montmorillonite and analcite (Förstner, 1967; Stähle and Ottemann, 1977; Stöffler *et al.*, 1977). The vesicles are filled with euhedral zeolite minerals (erionite, clinoptilolite, harmotome, phillipsite). The zeolite assemblage varies in composition as a function of depth (Stöffler *et al.*, 1977). These minerals indicate a maximum range of post-depositional temperatures of 250–750°C. More accurate temperature estimates are based on the remanent magnetization (Pohl, 1977) and on fission track measurements (Wagner, 1977) from which temperatures of at least 600°C are inferred. Depending on the thickness of the hot suevite layers cooling will take a rather long time. Calculations made for the 200 m thick suevite layer found in the drill core Nördlingen 1973, assuming an infinite horizontal extension, show that cooling from 600 to 100°C takes about 2000 years (Pohl, 1977). Simultaneously the layers below the hot suevite blanket are heated to a certain extent. The high post-depositional heat of suevite resulted in a strong *remanent magnetization* (Angenheister and Pohl, 1964; Pohl and Angenheister, 1969; Pohl, 1974, 1977). The intensity of magnetization is often several orders of magnitude higher than the mean magnetization of unshocked basement rocks from which the suevite was derived. Data from various suevite localities are summarized in Table 4 and Fig. 29. All measured samples have a reversed natural remanent magnetization with a constant direction. The intensity of remanent magnetization varies between a few gammas and several hundred gammas.

The remanence is carried mainly by magnetite which is present in all con-

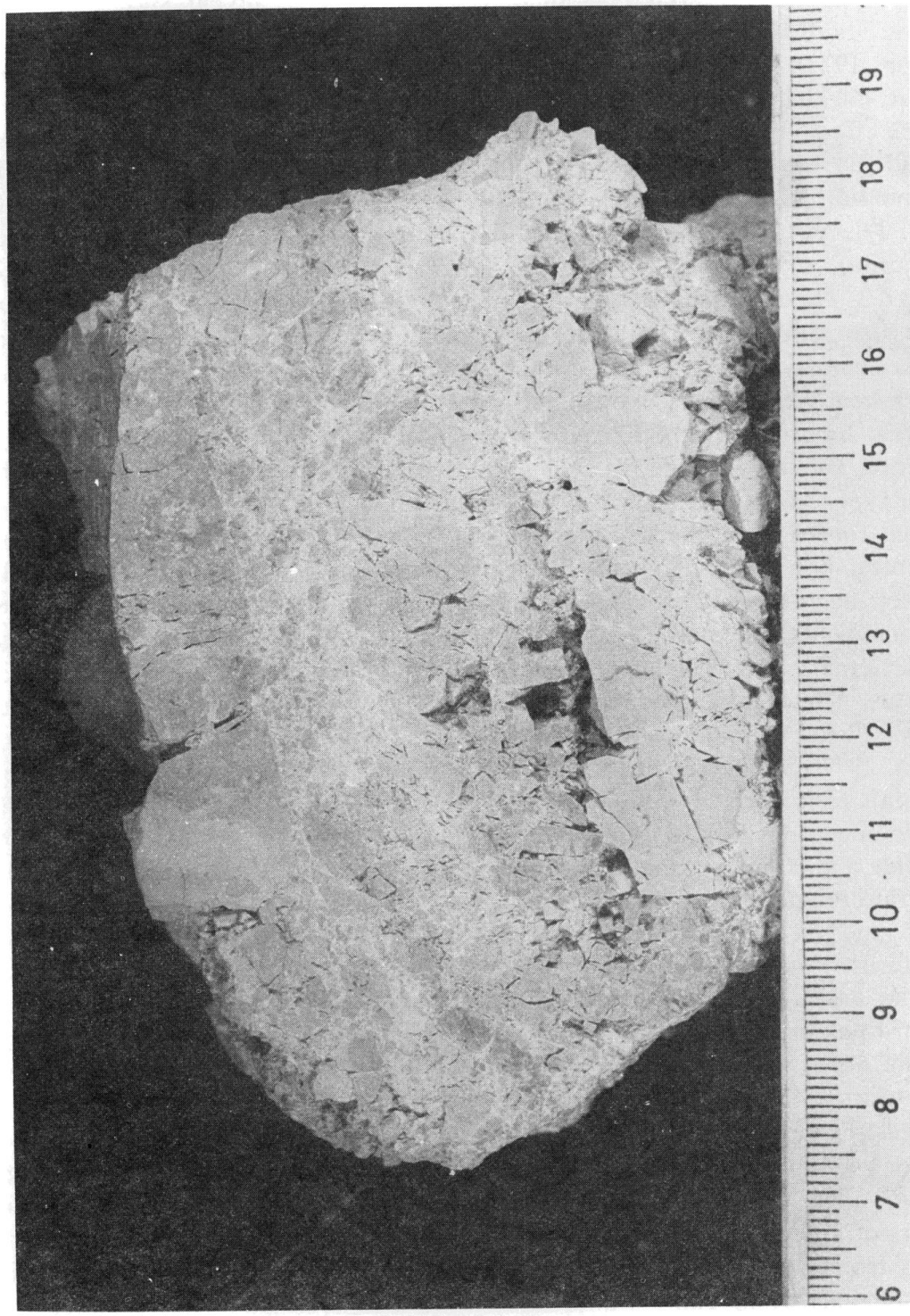


Fig. 26. Brecciated Malmian limestone ("Gries"), Dirgenheim, southern continuous deposits; scale = cm.

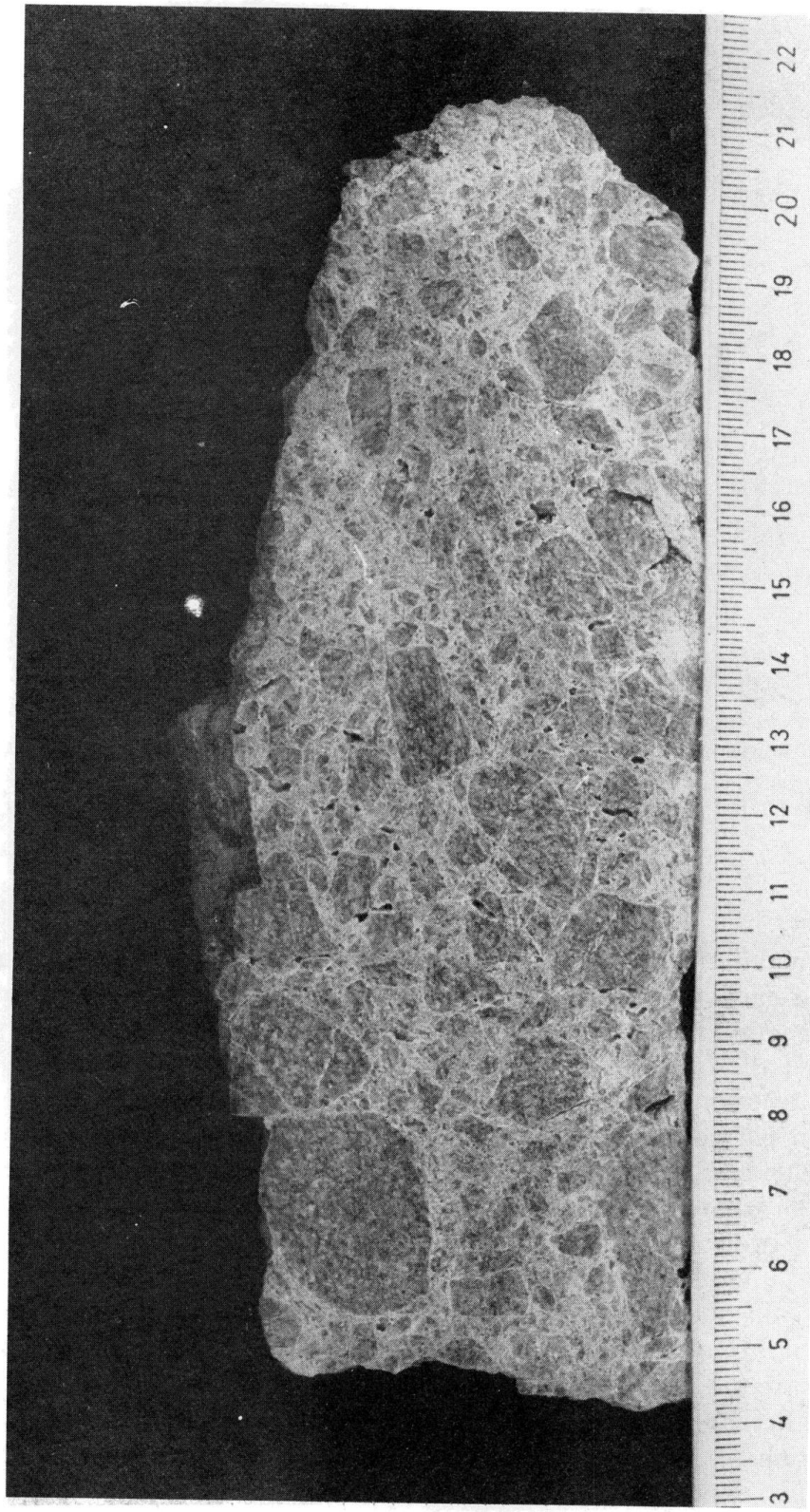


Fig. 27. Brecciated granite ("Gries"); W of Schmähingen, southern megablock zone; scale = cm.

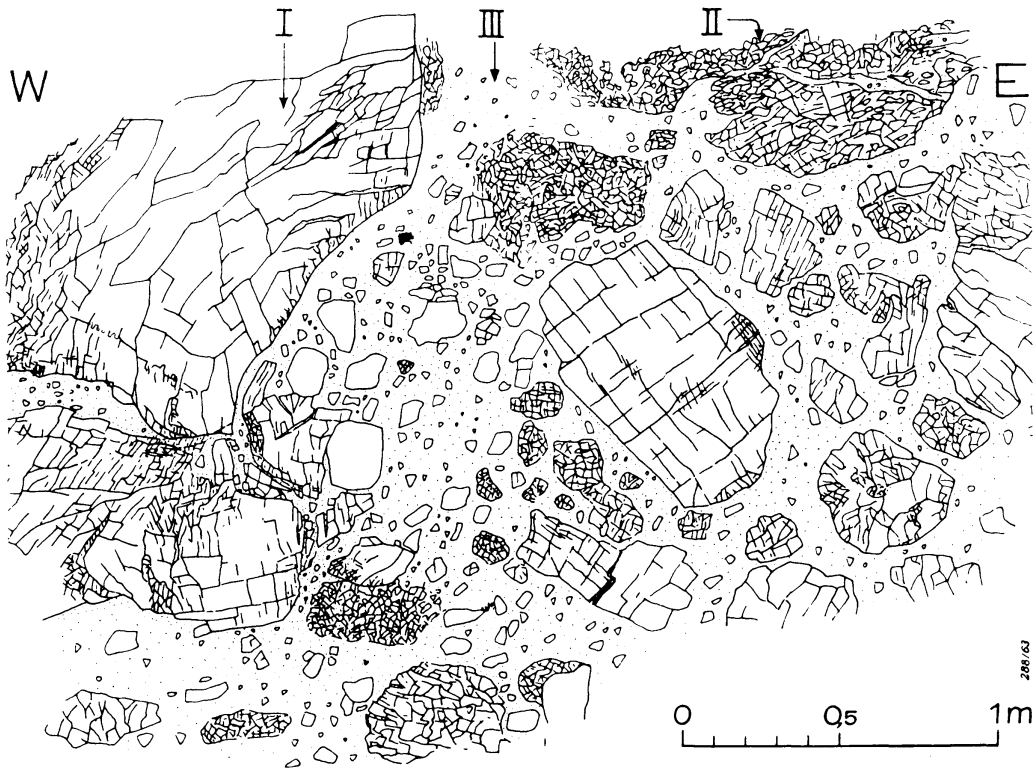


Fig. 28. Malmian megablock near Eglingen, southern continuous deposits, with three different types of deformation (from Wagner, 1964), 21 km from the point of impact; I = fracturing but primary joints and bedding planes preserved, II = intense fracturing, III = brecciation.

stituents of suevite: Rock fragments, glass and matrix. There is no predominance for particular carriers. Maghemite, as a second magnetic phase which carries an important fraction of the NRM, has been identified in the lower part (c. 450–525 m) of the high-temperature suevite and in the low-temperature suevite (525–650 m) from the drill core Nördlingen 1973.

The main part of the natural remanent magnetization which is carried by magnetite with high temperatures is best explained as a thermoremanent magnetization. Therefore the mean temperatures of suevite at the time of deposition were on the order of 600°C, in agreement with temperature estimates from mineralogical investigations (Hörz, 1965; El Goresy, 1968; Stöffler *et al.*, 1977) and from fission track dating (Wagner, 1977). The increase of magnetization of the suevite in comparison with the magnetization of the constituent rocks is mainly due to the generation of magnetite by shock metamorphism and/or subsequent thermal metamorphism, especially in the high-temperature suevite. The production of large quantities of magnetite by these processes from Fe-bearing mafic minerals and melts has been described by many authors (references in Pohl, 1971; Stähle, 1972). It is characteristic for suevitic impact breccias on earth.

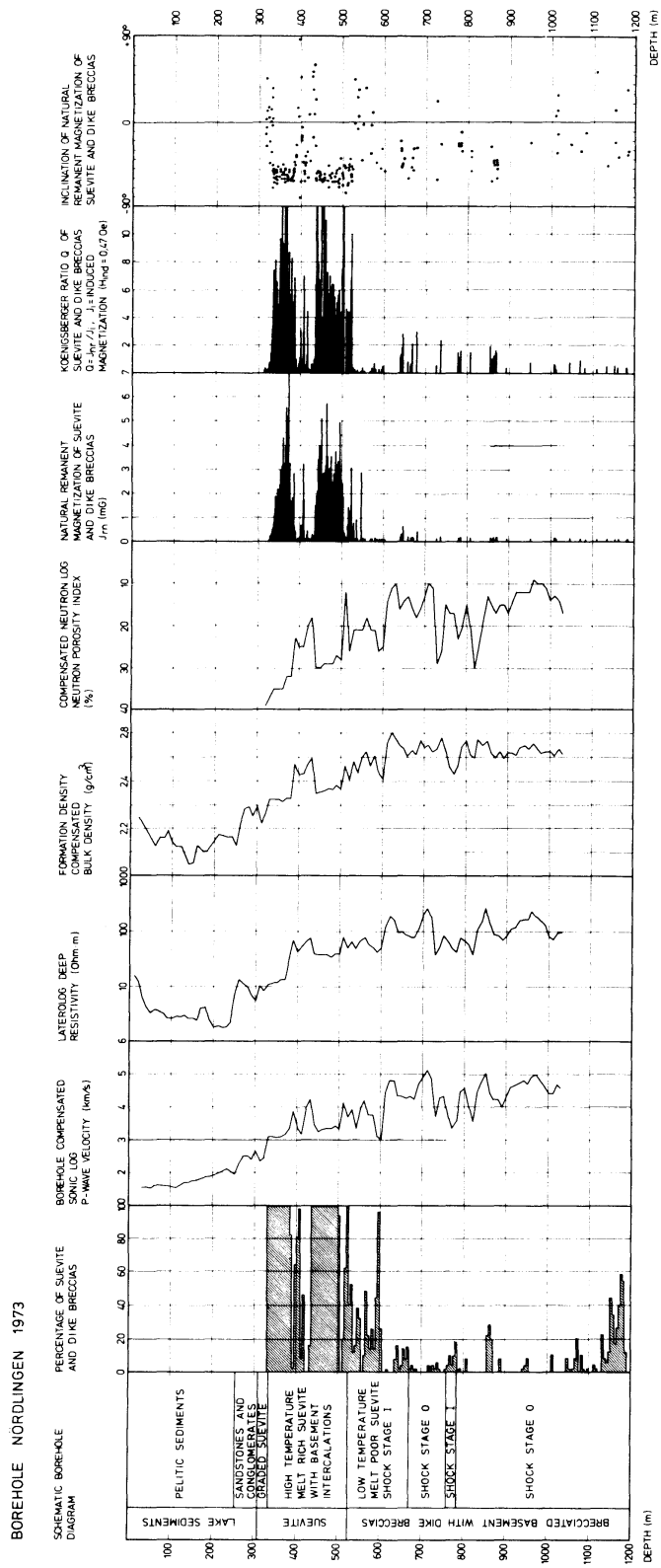


Fig. 29. Drillhole Nördlingen 1973. Schematic drill core profile and geophysical measurements. In the schematic drill core profile the indicated shock stage refers to the basement rocks, not to the suevite and dike breccias. Magnetic properties measured on basement rocks are not shown except for basement intercalations in suevite between 331.5 and 525 m. Positive inclinations between 331.5 and 525 m are due to these intercalations. Positive inclinations in suevitic breccias below 525 m are due to unstable components of the natural remanent magnetization.

1977iecp.symp..343P



Table 4. Natural remanent magnetization of suevite (high-temperature suevite).

| | | Natural remanent magnetization $J_{nr}$(mG) | | Susceptibility ($10^{-6}$ cgs) | | Koenigsberger ratio $Q = J_{nr}/J_i$ ($J_i$ induced in 0.47 Oe) | | Declination (°) | Inclination (°) |
|---|---|---|---|---|---|---|---|---|---|
| | | mean | max<br>min | mean | max<br>min | mean | max<br>min | mean | mean |
| Fall-out suevite | Surface outcrops 12 sites* | 0.59 | 1.37<br>0.04 | 260 | 510<br>30 | 6.4 | 30<br>1.3 | 194 | −57 |
| | Drillhole Wörnitzostheim Depth 20–100 m | 3.00 | 14.30<br>0.10 | 560 | 2000<br>64 | 11.3 | 30<br>1.5 | — | −59 |
| Fall-back suevite | Drillhole Deiningen I† Depth 332–350 m | 0.04 | 0.11<br>0.006 | 60 | 156<br>30 | 1.5 | 11<br>0.6 | — | −61 |
| | Drillhole Nördlingen 1973 Depth 331.5–390 and 435–525 m | 2.30 | 6.95<br>0.05 | 800 | 2600<br>80 | 5.9 | 20<br>0.9 | — | −56 |

*max and min are mean values of sites, Dec. and Inc. of surface outcrops after af-cleaning.
†Only the upper 20 m of the suevite were drilled.

## 4. Subsurface Structure of the Crater

The subsurface structure of the crater has been investigated by geophysical methods complemented by several drillholes. The following sections will review the measurements. An interpretive summary of the present knowledge of the crater structure is given at the end of the chapter.

### 4.1 *Drillholes*

Of the major drill sites which provided information on the subsurface structure of the crater, two are located inside the central crater (Nördlingen 1973, Deiningen 1953), four are in the area of the inner ring (Wallerstein, 1948, Nördlingen 1950, 1955) and one in the megablock zone (Wörnitzostheim 1965). The location of the main drillholes is shown in Figs. 6 and 32 and a summary of the drilled profiles is given in Fig. 21. The most important is the deep drillhole Nördlingen 1973 (Bayer. Geol. Landesamt, 1974, 1977). Figure 29 shows a schematic core diagram and measurements of physical parameters. Some results of the encountered impact formations, which are considered to be typical for the central crater cavity, have already been discussed in section 3. Further results will be mentioned in the following sections.

### 4.2 *Geoelectric measurements*

Geoelectric methods (DC-depth sounding with Schlumberger and dipole electrode configurations) have been used in the Ries crater to investigate the low resistivity upper layers down to a depth of 600–800 m (Ernstson, 1974; Engelhard and Hansel, 1976; Blohm, Friedrich, and Homilius, 1977). An electrical resistivity profile in the central crater obtained from the drill hole Nördlingen 1973 is shown in Fig. 29.

From the geoelectric measurements the thickness of the post-impact Tertiary lake sediments in the Ries crater, the location of the boundary of the central crater and the inner ring and some details of the complex structure of the inner ring were obtained. Figure 30 shows the thickness of the lake sediments near the area of the inner ring (Ernstson, 1974). From the circular form of this central basin bordered almost completely by the structure of the inner ring the center of the crater can be fixed with great accuracy. Figure 30 also gives an approximate idea of the morphology of the central part of the Ries crater shortly after the deposition of the fall-back ejecta. Not shown is the lake sediment's maximum thickness in the central crater, which may reach 400 m according to geoelectric and seismic data. The relief of the surface of the fall-back suevite material all over the central crater probably was not much greater than about 100–200 m. Geoelectric methods also yielded an indication about the highly varying thickness of the suevite layer and thus information concerning the relief of the brecciated crystalline rock masses below the suevite. Specifically it could be shown near the center that the basement rocks form a ring-like uplift with a diameter of 4–5 km, consistent with seismic, magnetic and gravity data. The maximum relief of this uplift is about 300 m (Fig. 40).

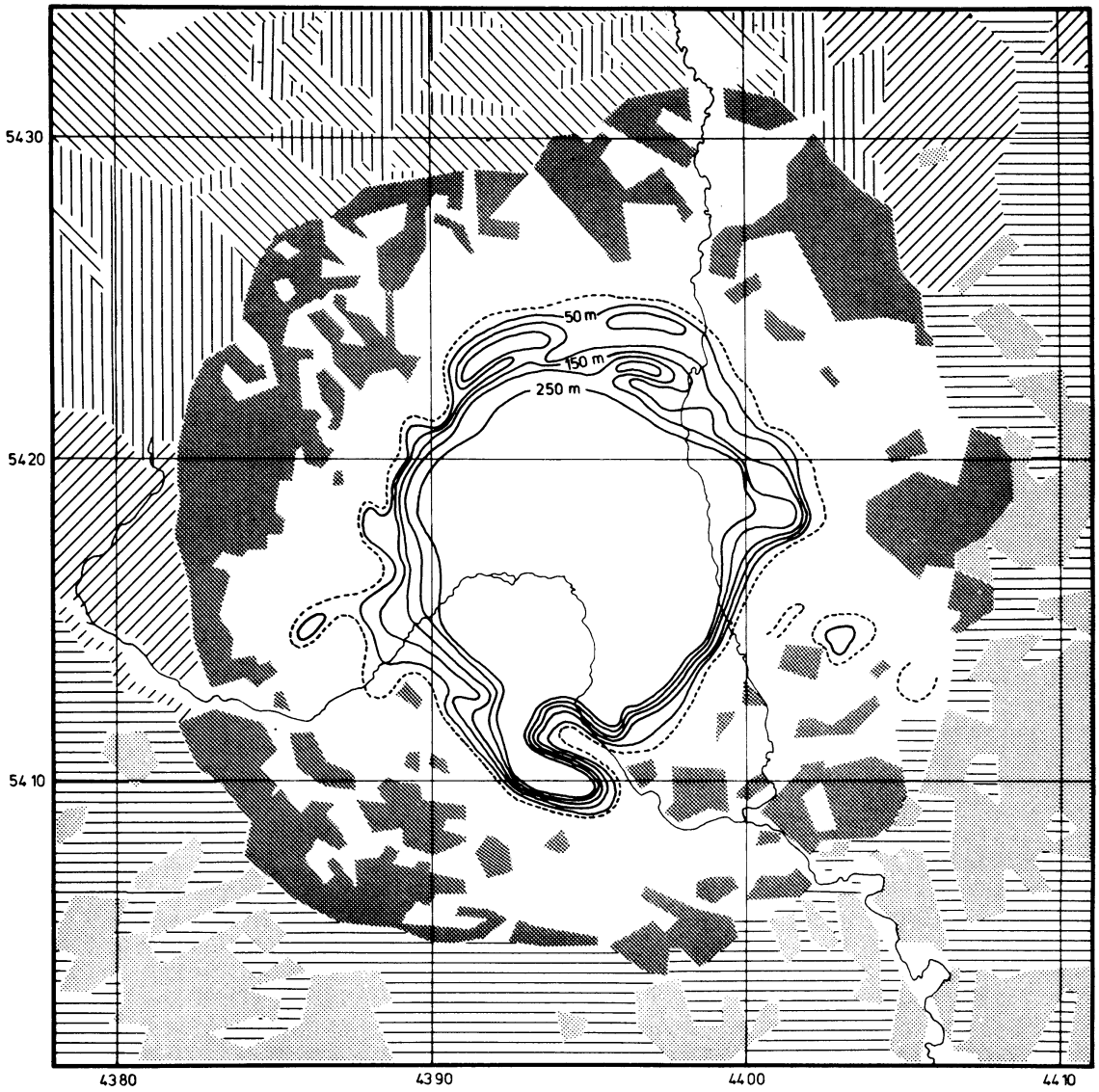


Fig. 30. Thickness of lake sediments (after Ernstson 1974). Maximum thickness is not shown. Schematic geology according to Fig. 6.

### 4.3 *Seismic measurements*

Early refraction seismic work by Reich and Horrix (1955) with refraction lines 3–4 km long established many of the main features of the crater: central crater cavity, inner ring, and megablock zone. The most detailed information on the near surface structure is provided by an EW reflection profile from the center of the crater to about 6 km W of the tectonic crater rim (Angenheister and Pohl, 1969, Fig. 32). A redrawing of the seismic record section is shown in Fig. 31. Good reflections were obtained from the bottom of the lake sediments in the central crater and from a mesozoic layer and the surface of the basement outside the crater. The crater boundary in the basement is indicated by the disap-

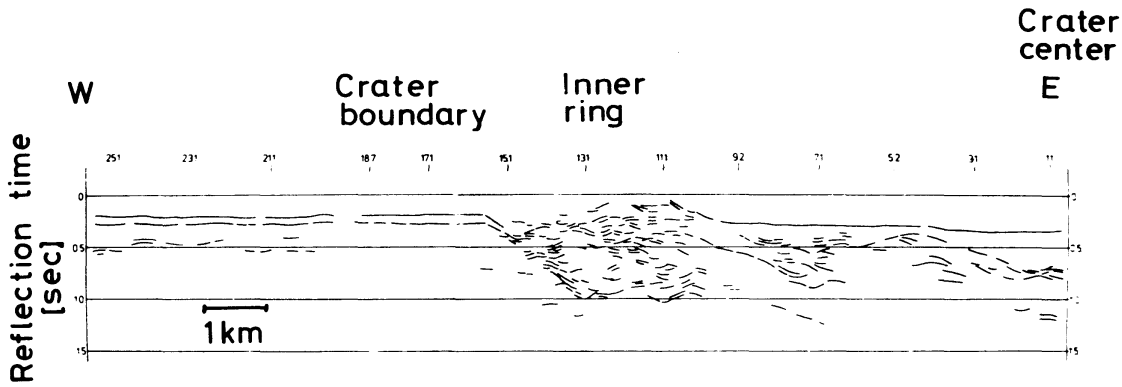


Fig. 31. Seismic reflection profile (RR in Fig. 32). Simplified diagram showing important events on the record section. Datum plane is 400 m above sea level (Angenheister and Pohl, 1969).

pearance of reflections from the undisturbed basement. It is located about 2.5 km inside the tectonic rim of the crater (Fig. 32). Towards the center the basement is fractured and has subsided, in part together with sedimentary layers, c. 100–200 m (Fig. 32), possibly as a series of down-faulted blocks which no longer form a continuous reflecting horizon. Still closer to the inner ring megablock crater deposits, with thicknesses up to several hundred meters, may also contribute to the scattering of the seismic signals and the "chaotic" aspect of the reflected signals. The inner ring is mainly characterized by a steep contact to the lake sediments (Fig. 40).

Velocity-depth soundings with symmetrical arrangement of shot points and receivers with respect to the sounding point were made at the center and outside of the crater in order to determine the depth of the brecciation zone (Pohl and Will, 1974). It could be shown that at depths of about 3 km the *P*-wave velocities are still considerably lower than in the undisturbed basement outside the crater. The velocity-depth distribution shown in Fig. 34 down to 2.5 km is taken from these measurements. The velocity distribution obtained from the surface measurements was confirmed for the upper 1000 m by the velocity measurements in the drill hole Nördlingen 1973 (Fig. 29).

Using the data obtained from the above described measurements, a new interpretation of two 40 km long refraction profiles (6, Harburg, and 7, Holheim, Fig. 32) was recently suggested (Ernstson and Pohl, 1977) utilising a ray-tracing program for two-dimensional velocity distributions. The underground structure is modelled by velocity isolines (Fig. 33). Results show a 20–25 km large bowl-shaped zone with reduced velocities. At the center lowered velocities can still be identified at depths of about 6 km, which is in agreement with the interpretation of gravity measurements described in section 4.4. The velocity distributions inside and outside the crater obtained from these models and their differences are shown in Fig. 34. Also shown is the density difference for density model II of Fig. 37. The agreement between the density and the velocity models can be explained by the correlation of the velocities and the densities measured

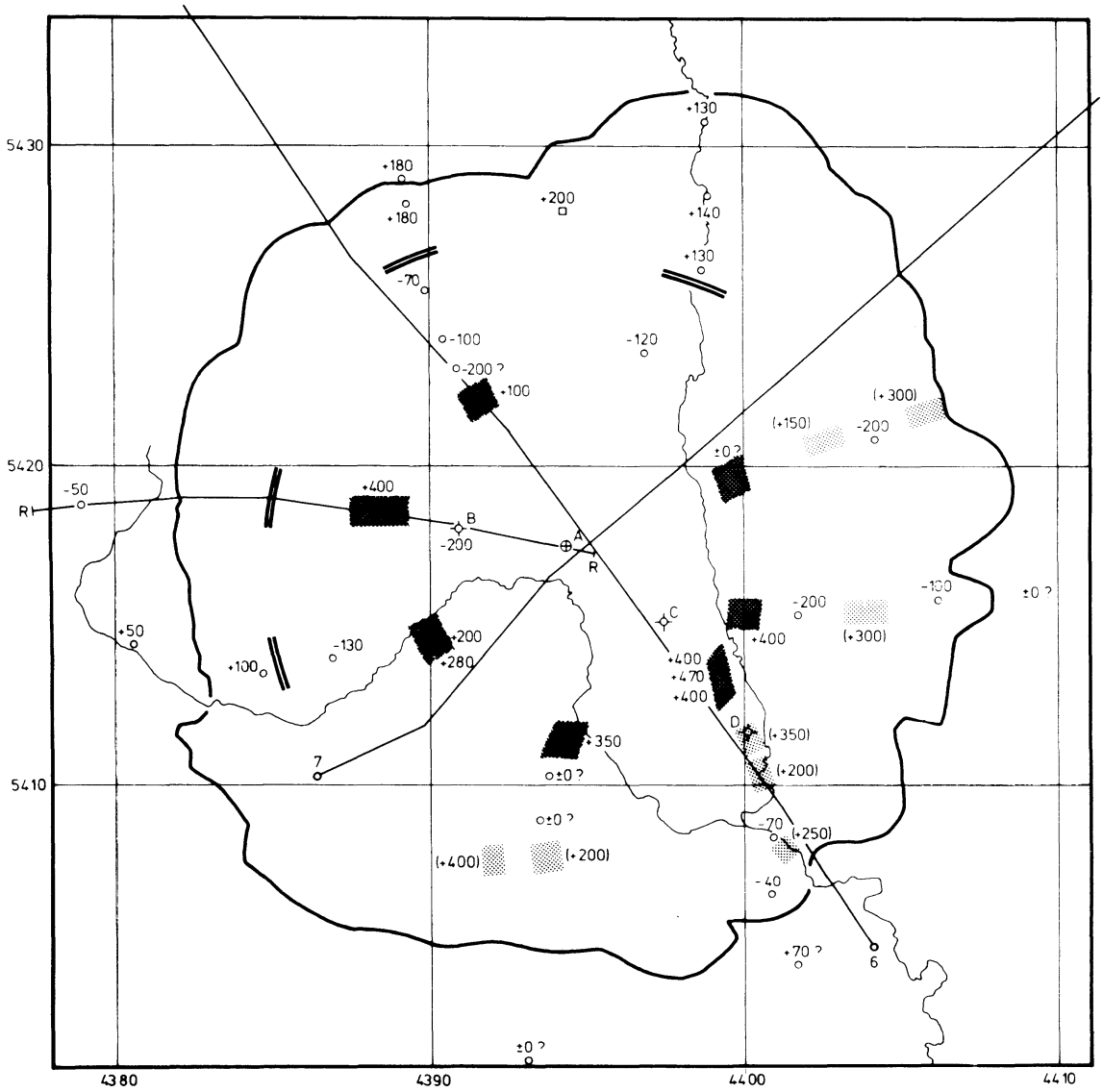


Fig. 32. Compilation of available elevation above sea level (in m) data of the crystalline basement and of subsurface crystalline basement and Malmian limestone (?) megablocks in the area of the inner ring and the megablock zone. Dark cross-hatching indicates location and depth of crystalline basement blocks in the area of the inner ring. Light cross-hatching indicates blocks with high seismic velocity in the marginal zone of the crater between the inner ring and the tectonic rim, probably Malmian limestone, possibly basement blocks. Heavy double line indicates approximate location of the crater boundary within the crystalline basement (○ seismic data, □ geoelectric data). Also shown is the location of the reflection profile (RR, see Fig. 31) and of two refraction profiles (6 and 7, see Fig. 33).

in the brecciated basement rocks in the drill hole Nördlingen 1973 (Ernstson and Pohl, 1974).

### 4.4 *Gravity measurements*

Figure 35 shows the Bouguer anomaly map published by Jung and Schaaf

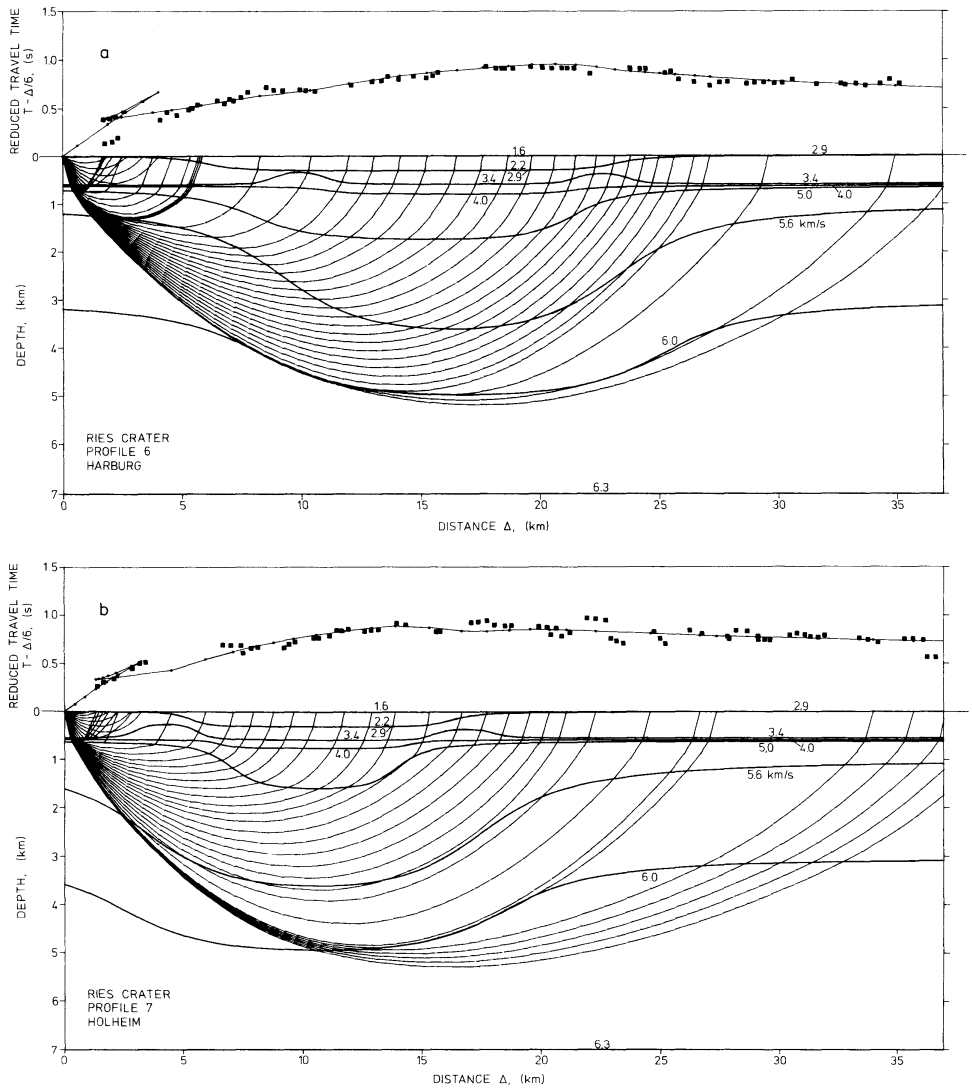


Fig. 33. Velocity distribution in the Ries crater calculated for refraction profiles 6 (Harburg) and 7 (Holheim) (see Fig. 32). Top: Full squares indicate measured travel times. Calculated travel times for models shown below are indicated by a continuous line. Bottom: Velocity distribution shown by velocity isolines in km/s (thick lines). Thinner lines are seismic ray paths. Vertical exaggeration 2×.

(1967). The datum plane is 400 m above sea level. For the determination of the anomaly due to the crater structure, various regional fields have been constructed by Kahle (1969). A residual anomaly which is thought to be due solely to the impact structure is shown in Fig. 36 (Kahle, 1969). The anomaly has a maximum negative value of about −18 mgal and its location is concentric to other structures within crater. On radial profiles the inner ring is marked by a relative maximum at a radial distance of c. 5–6 km from the center. A second kink at a radial of about 10 km can be associated with the crater boundary in the crystalline basement (see section 4.3). The residual anomaly has been used to calculate the total mass deficiency below the datum plane by Jung and Schaaf

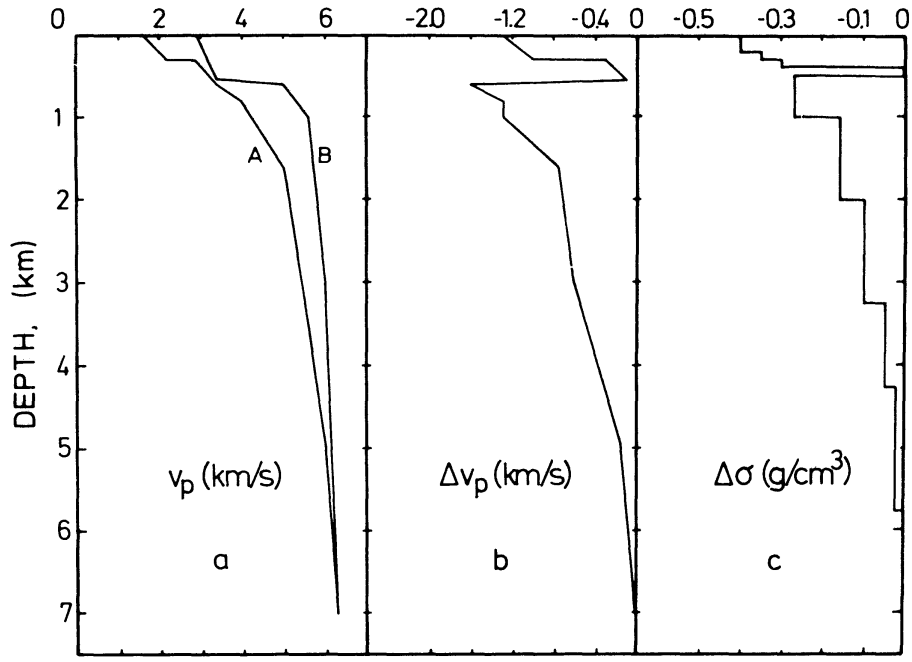


Fig. 34. (a) Velocity-depth-distribution (p-wave velocity) at the center of the crater (A) and outside (B) the crater, according to models shown in Fig. 33, (b): velocity differences $\Delta v_p = v_{pA} - v_{pB}$ at the center of the crater, (c) density differences $\Delta\sigma$ at the center of the crater between crater rocks and off-crater rocks according to the density model II (Fig. 37).

(1967), Kahle (1969), and Ernstson and Pohl (1977). The integration gives mass deficiencies between about 70,000 and 100,000 Mt, depending on the assumptions made for the zero level of the anomaly at great distances.

Model calculations for the density distribution in the crater made before 1974 (Jung *et al.*, 1969) suffered from a lack of reliable density data. Since that time the drill hole Nördlingen 1973 and several other drillholes outside the crater provided better data on the density distribution for the upper 1000 m (Table 5 and Fig. 29). This enabled new and refined model calculations (Ernstson and Pohl, 1977). Some results for density bodies with circular symmetry are shown in Fig. 37. Details of the near-surface structure have been omitted. The density difference between the undisturbed rocks outside the crater and the brecciated crater filling as a function of depth is given in Fig. 34. The models indicate the existence of a bowl-shaped zone of reduced density with a depth of at least 5–6 km at the center of the crater, in agreement with results of seismic modelling discussed in section 4.3.

### 4.5 *Magnetic field measurements*

Magnetic surveys have been made by Reich and Horrix (1955), Angenheister and Pohl (1969) and by Bundesanstalt für Geowissenschaften und Rohstoffe (1971). Figure 38 shows an airborne total intensity map (Bundesanstalt für

Geowissenschaften und Rohstoffe, 1971) and Fig. 39 a ground magnetic total intensity map (Pohl and Angenheister, 1969). The central part of the crater is characterized by negative anomalies ($-300\,\gamma$ on the ground magnetic map) which are due to the thick layer of reversely magnetized high-temperature fall-back suevite below the lake sediments (see also Figs. 29, 40 and Table 4). The presence of larger coherent impact melt bodies is not excluded by this interpretation.

Some negative anomalies of smaller extent in the megablock zone are due to local fallout suevite patches below shallow lake sediments as was shown, e.g., by the drillhole Wörnitzostheim (Fig. 21). Similar anomalies are measured above outcropping fallout suevite in the Vorries.

The large positive anomalies in the SW of the crater and outside the crater are not related to the impact structure. They are caused by basic or ultrabasic paleozoic rocks within the basement. Amphibolites with high magnetic susceptibility (Pohl, 1974) which are found in the ejecta and in the drillhole Nördlingen 1973 are probably part of these rocks.

### 4.6. *Subsurface structure*

From the geophysical and drillhole data, the following picture of the structure of the crater can be drawn. In agreement with the surface morphology and geology (section 3.1) the crater is divided (Fig. 40) into a central crater cavity surrounded by the rampart-like structure of the inner ring (diameter c. 12 km) and the marginal megablock zone between the inner ring and the tectonic rim (diameter 25–26 km). The *central crater* is filled with post-impact lake sediments with a thickness up to about 400 m. The lake sediments can be divided into an upper series of pelitic sediments (thickness 200–350 m) deposited under quiet water conditions and a lower series of sandstones and conglomerates deposited under turbulent conditions shortly after the impact (thickness 50–100 m?).

Below the lake sediments a graded suevite layer about 15 m thick was found in the drillhole Nördlingen which may represent a preserved part of the latest fallback material in the crater. This layer in turn is underlain by a high-temperature suevite fallback breccia with a highly variable thickness ranging from 0 to more than 400 m. The large basement blocks found within the suevite of the drillhole Nördlingen (Fig. 29) and the variation of petrographic characteristics (see sections 3.2.3, 3.2.4, and 5.3.2) indicate a multiphase process for the deposition of the fallback suevite. The petrographic character of the suevite may also show important lateral variations within the central crater.

The basis of the suevite layer consists of brecciated basement rocks probably all over the central crater. In the drillhole Nördlingen the brecciated basement consists of several thick rocks units (megablocks) showing, alternatively, shock metamorphism stage I and stage 0 (Fig. 29, Engelhardt and Graup, 1977). The upper unit (525–670 m) (mainly amphibolite and some granite) is characterized by the presence of numerous glass-poor, low-temperature suevitic dikes, by shatter cones and by traces of meteoritic material (El Goresy and Chao, 1976). The

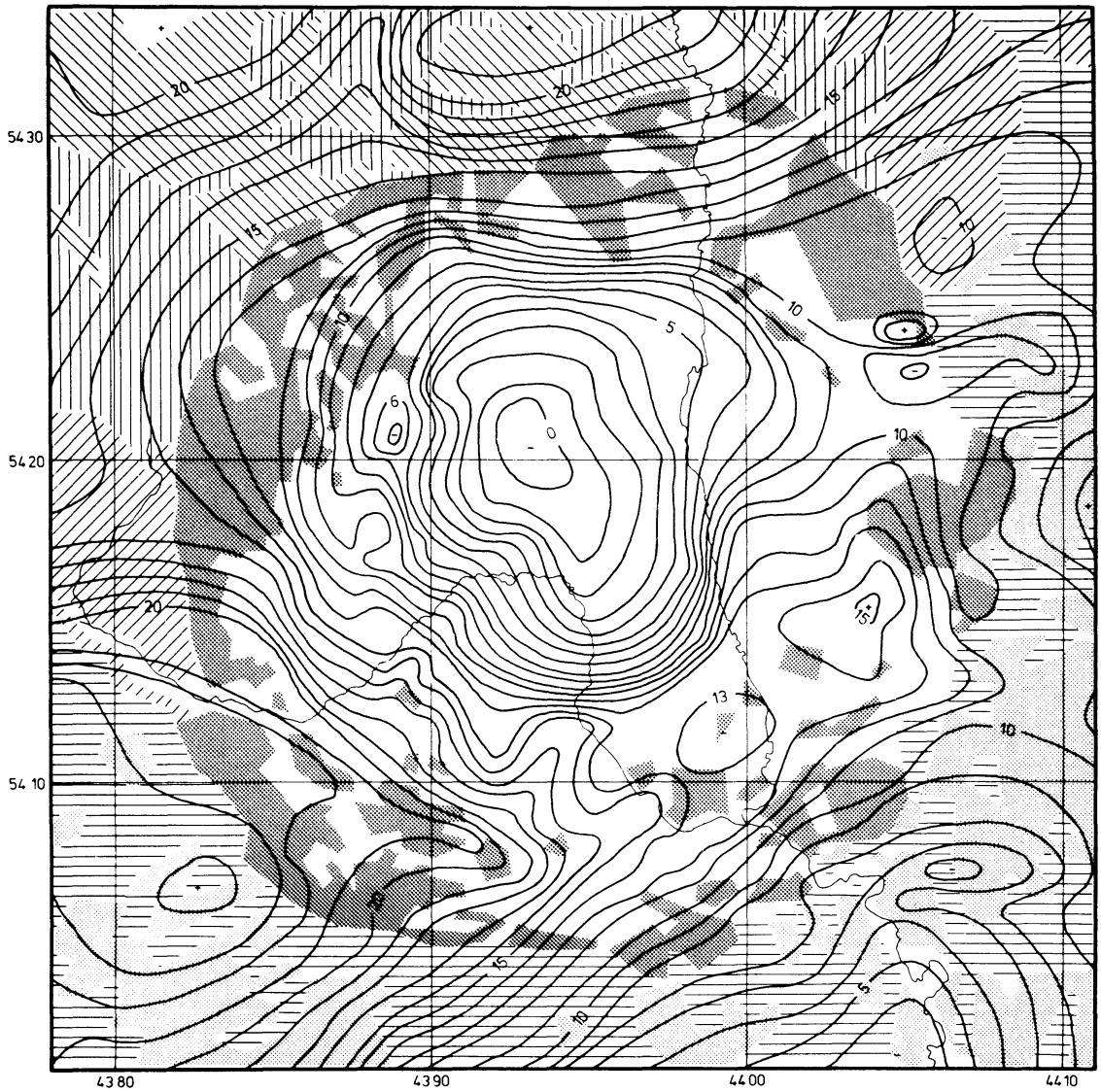


Fig. 35. Bouguer gravity anomaly in the Ries crater area (after Jung and Schaaf, 1967) in mgal. Schematic geology according to Fig. 6.

lower units contain also numerous breccia dikes as discussed in section 3.2.2. Part of these dikes contain sedimentary material.

The morphology of the surface of the basement in the central crater shows an important relief (Fig. 40). Towards the center the basement rocks form a series of peaks in a ring-like arrangement with a diameter of 4 to 5 km. The points of some of the peaks are probably at higher elevation than the precrater basement surface.

For depths greater than 1200 m both the reduced velocity and density indicate brecciation and fracturing down to about 6 km depth at the center of the crater. Fracturing and brecciation may extend still deeper, because microcracks are partly closed at this depth ($p \approx 2$ kbar) and cementation and healing have

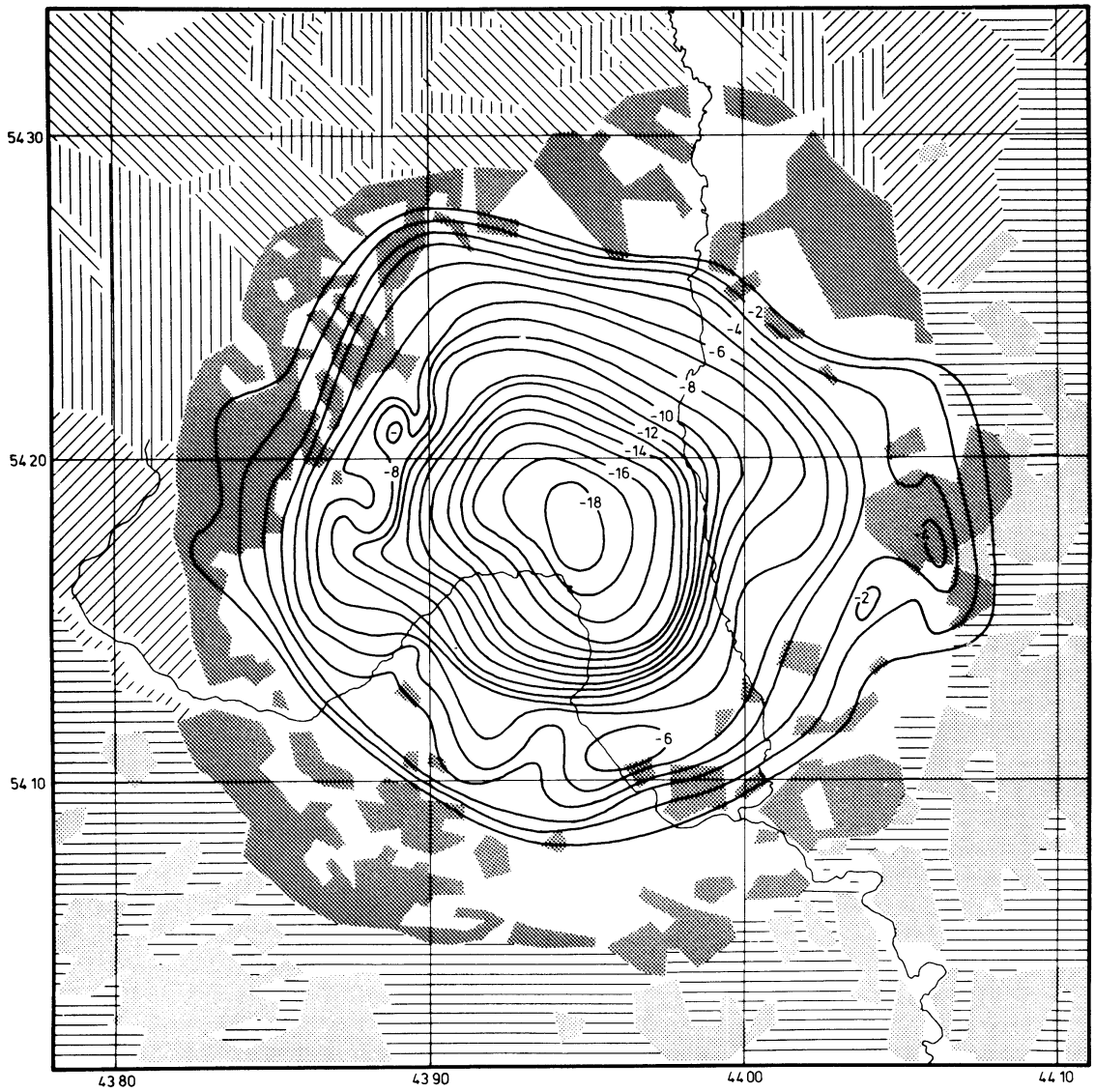


Fig. 36. Residual Bouguer gravity anomaly II after Kahle (1969) in mgal. Schematic geology according to Fig. 6.

probably taken place (Simmons *et al.*, 1975). In the basement section of the drill core Nördlingen 1973 the decrease in density and velocity is due to the presence of dike breccias and to brecciation and fracturing of basement rocks. For larger depths it is not yet possible to decide whether this is solely due to *in situ* brecciation by the shock wave or possibly also due to subsequent mass-movement during readjustment and relaxation of the crater.

The *inner ring* is a rampart like structure which encircles most of the central crater. Towards the center of the crater it forms a steep, well-defined contact to the lake sediments and the suevite (Figs. 30, 40). In contrast the exterior side of the inner ring is poorly defined. In some places the inner ring is interrupted and relatively thick lake sediments are found outside such gaps (Fig. 30). In the

1977iecp.symp..343P



Table 5. Seismic velocities and densities of pre-crater and crater rocks.

| Pre-crater rocks | Velocity (m/s) | Density (g/cm$^3$) | Crater rocks | Velocity (m/s) | Density (g/cm$^3$) |
|---|---|---|---|---|---|
| Malmian limestones | 4600–5000 | 2.52 | Pelitic lake sediments | 1700–2200 | 1.85–1.9 |
| Dogger-Malm | 2500–3000 | 2.25–2.35 | Psammitic-psephitic lake sediments | 2700–3000 | 2.15 |
| Keuper-Dogger | 2500–2800 | 2.25–2.35 | Suevite* | 3100–3400 | 2.25–2.30 |
| Basement* | 5000–6000 | 2.65–2.95 | Brecciated basement* (including dyke breccias) | 3000–6000 | 2.45–2.90 |
| | | | Inner ring | 3300–4000 | — |
| | | | Megabloc zone | 2500–4000 | — |

*See Figs. 29 and 34.

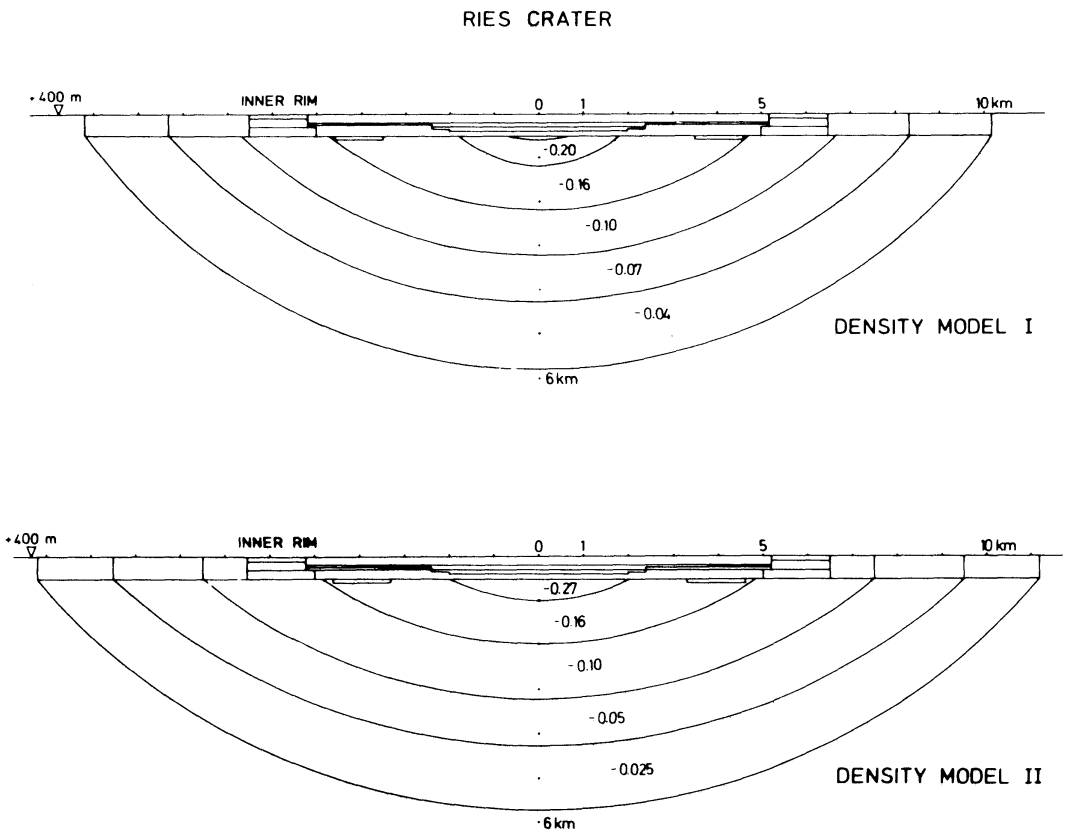


Fig. 37. Density distribution models for the Ries crater. Density differences between off-structure rocks and rocks within the crater in g/cm$^3$. Density differences within the upper 500 m not shown. No vertical exaggeration (Ernstson and Pohl, 1977).

north, the inner ring structure is apparently divided into several approximately concentric highs and troughs in a steplike arrangement. Outcrops, drillholes and seismic data show that the inner ring structure is formed in part of weakly shocked crystalline basement rocks (Fig. 32), and in part of sedimentary rocks (Fig. 20). Shallow drillholes at Nördlingen show in particular that sediments are underlying the basement rocks, indicating an inverted stratigraphy (Fig. 21).

Just outside the inner ring the *megablock zone* consists largely of ejected rock masses down to a depth of several hundred meters as indicated by the drillhole Wörnitzostheim and geophysical data. These ejecta and the lake sediments which fill several troughs outside the inner ring have replaced the pre-crater sedimentary strata in these areas. However, it is not yet proven if the pre-crater sediments have been removed by ejection or if they have subsided together with the ejecta blanket. The ring depression in the basement up to a radial distance of about 10 km (section 4.4) is considered strong evidence for subsidence, since ejection of basement rocks from outside the central crater is most unlikely. Subsidence would also explain the presence of high-velocity megablocks (probably Malmian limestones) in this zone at depths of 200–300 m

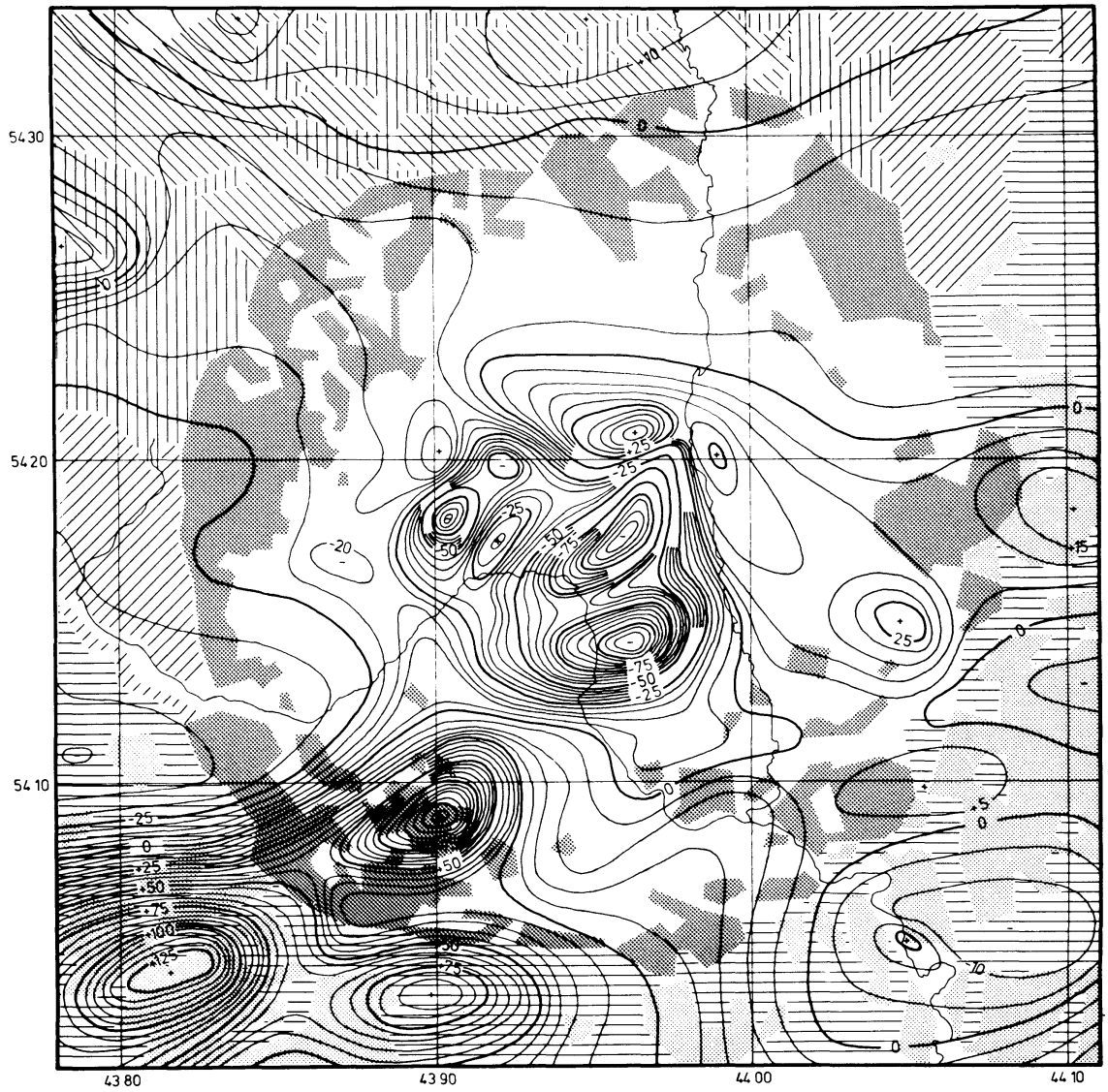


Fig. 38. Aeromagnetic map of the Ries crater area: total field anomalies in gamma. Flight height 1000 m above sea level (Bundesanstalt für Geowissenschaften und Rohstoffe, 1971). Schematic geology according to Fig. 6.

below their normal stratigraphic position. At radial distances $> 10$ km subsidence movements are confined mainly to the sedimentary cover (Gall *et al.*, 1977). The tectonic rim is defined as the outer limit of these blocks.

## 5. Cratering Model

### 5.1. *Volume estimates of excavated rocks and impact energy*

Calculations of masses and volumes of rocks which have been displaced by the impact process are subject to large uncertainties because not only are the

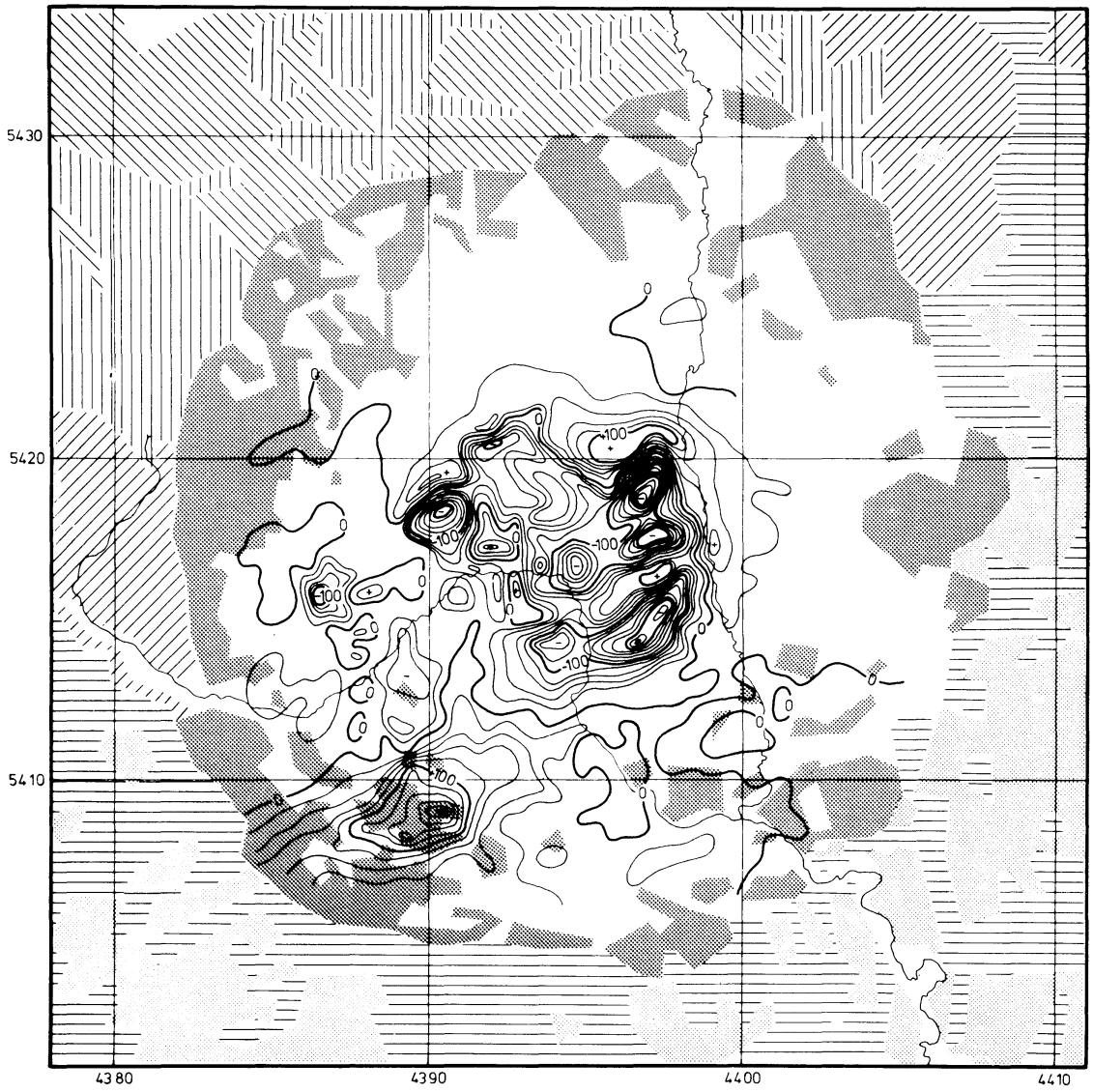


Fig. 39. Ground magnetic map of the Ries crater area; total field anomalies in gamma (Pohl and Angenheister, 1969). Schematic geology according to Fig. 6.

structure and composition of the marginal crater zone, between the inner ring and the tectonic rim, not well enough known, but also the structure and composition of the inner ring, the mass-transport by readjustment and finally the erosional processes since crater formation.

We nevertheless performed some volumetric calculations in order to constrain estimates of possible maximum and minimum values. For such calculations the following general assumptions were made: Horizontal layering of sedimentary strata, sediment thickness before the impact 600 m, pre-impact basement surface at sea-level.

5.1.1. *Estimate of the volume of excavated sediments.* To estimate a maximum value we assume that all sediments which occupied the present topographic

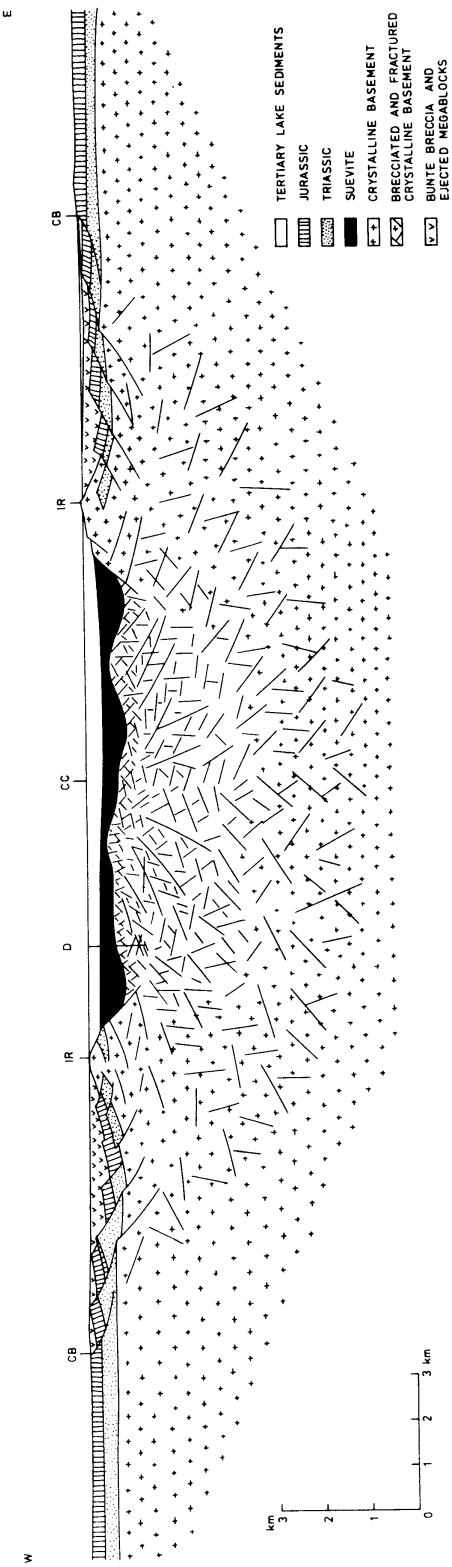


Fig. 40. Schematic cross section of the Ries crater. No vertical exaggeration; CC = crater center, IR = inner ring, CB = crater boundary (tectonic rim).

crater basin (Fig. 5) below the 600 m level were ejected (84 $km^3$). To this we add the volume of lake sediments (28 $km^3$), the volume of fallback suevite above sea level (7 $km^3$, out of a total fallback suevite volume of 13 $km^3$), and the volume of sediments replaced by basement rocks in the inner ring (5–10 $km^3$ ?) and in the megablock zone (5–10 $km^3$ ?). This gives a maximum total volume of about 129–139 $km^3$ for sedimentary rocks which could have been ejected beyond the tectonic rim (diameter ~ 25 km). It is possible to assume that half of the lake sediments (14 $km^3$) are derived from sedimentary crater deposits within the tectonic rim. We can further take into account the subsidence in the megablock zone discussed in section 4.3. A subsidence of 0.1 km only between radial distances of 6 and 10 km corresponds to a volume of c. 20 $km^3$. Thus the maximum ejected sediment volume would be decreased by about 34 $km^3$ (provided that ejected basement rocks corresponding to the subsidence volume have not all been deposited in the megablock zone). In addition, the possibility that erosion has removed a large amount of crater deposits in the megablock zone completely out of the crater, has to be considered. In conclusion we feel that the volume of sediments ejected *beyond the tectonic rim* (diameter 26 km) can hardly exceed 100 $km^3$, which is somewhat less than previous estimates (Gall *et al.*, 1975). The total volume of *excavated* sediments could be somewhat larger, because we have to take into account the volume of sedimentary deposits in the megablock zone, which may range up to 30 $km^3$ (?).

Some minimum value for the volume of excavated sediments can be estimated by projecting the central crater cavity (diameter 12 km) to 600 m above sea level. This yields about 71 $km^3$, taking the same values as above for the volumes of lake sediments, suevite and inner ring structure. However, the 71 $km^3$ would have been deposited in part in the megablock zone and in part outside the crater, so that the volume ejected beyond the tectonic boundary would be much less. This model assumes that the present topographic depression in the area of the megablock zone between the inner ring and the tectonic rim was formed exclusively by subsidence and erosion.

5.1.2. *Estimates of the volume of excavated basement rocks.* The mass deficiency (section 4.1) indicates that the presently missing volume of crystalline rocks in the basement (below −100 m) ranges between 22 and 30 $km^3$ (calculated for an original density of 2.8 $g/cm^3$). To this we add the volume of missing basement rocks between sea level and −100 m for a radial distance of 10 km

5.1.3. *Estimate of the volume of impact melt.* If we assume that all impact (excavation in the central cavity and subsidence in the megablock zone, 31 $km^3$). Thus the total volume of excavated basement rocks could range between 53 and 61 $km^3$. Part of these rocks is found in the fallback suevite (9 $km^3$, corrected for porosity) and part in the inner ring (5–10 $km^3$). This gives estimated volumes between 34 and 47 $km^3$ for basement rocks ejected beyond the inner ring. Volumes of 53 and 61 $km^3$ correspond to flat spherical cavities of a depth of 2.0 and 2.1 km and a diameter of 8.0 and 8.4 km. A subsidence of about 0.15 km between the inner ring and a radial distance of 10 km would fill up these cavities.

melt produced in the Ries event is contained in the suevite, the melt volume can be calculated from the volume of suevite and the volume fraction of melt in the suevite. According to Stöffler (1977) the volume of fallback and fallout suevite could be on the order of 8–10 $km^3$ and 0.2–0.4 $km^3$, respectively. If 75% of the original fallout suevite has been removed by erosion (rough estimate), the total primary volume of suevite ranges then from about 9 to 11 $km^3$. The melt content in the fallout suevite is 15 vol.%, in the fallback suevite 3.5–5 vol.% as measured in the drill core of Nördlingen 1973 (Stöffler *et al.*, 1977). From these figures we obtain a total volume of melt of 0.3–0.55 $km^3$. Because of the porosity of the melt particles which is on the order of 70% in the fallback suevite and 40% in the fallout suevite, the volume of the melt itself will be in the range of 0.1–0.2 $km^3$. The highest estimates of the total fallback suevite volume (Bayer. Geol. Landesamt, 1977) which are on the order of 15 $km^3$, would increase this figure to 0.2–0.6 $km^3$. Depending on the total volume of excavated rocks of the Ries estimated above (124 $km^3$ minimum, 200 $km^3$ maximum, 150 $km^3$ probable value) the melt volume in the Ries ranges between 0.27 and 0.44% of the total volume of excavated rocks for the maximum estimate of the melt volume. This is much less than melt volume estimates for Canadian craters (Grieve *et al.*, 1977) which range from 1 to 5% of the transient cavity volume which might correspond to our minimum estimate of the crater volume (124 $km^3$). The Ries impact melt volume would be appreciably higher if a coherent layer of impact melt was present in the central area of the crater.

5.1.4. *Impact energy.* A rough estimate of the impact energy can be made from the volume of displaced masses. The total excavation mass will include the mass deficit below the elevation of 400 m obtained by gravity measurements (75,000–100,000 Mt) plus the mass of the lake sediments (56,000 Mt), the mass of fallback suevite (32,000 Mt) and the mass of ejected sediments above 400 m (145,000 Mt for a radius of 10 km and a thickness of 0.2 km). This adds up to masses between 308,000 and 333,000 Mt. These are not maximum masses since fallback has only partly been taken into account. To lift a mass of 300,000 Mt up to an elevation of 5 or 10 km (max. horizontal transport 10–20 km) an energy of $1.5 \cdot 10^{26}$ erg and $3 \cdot 10^{26}$ erg respectively is needed. As only part of the impact energy is converted into kinetic energy of ejection, these figures may be multiplied by a factor of 2 to 3 in order to obtain estimates for the kinetic energy of the impacting body.

Using the scaling laws of Roddy *et al.* (1975) for Meteor Crater ($D_1 = D_2(E_1/E_2)^{1/n}$, $D$ = diameter of simple bowl-shaped crater, $E$ = impact energy), the following table for the crater diameter was calculated for impact energies of $10^{26}$ and $10^{27}$ erg and different scaling exponents $n$ ($D$ in km).

| $n$ | 3 | 3.4 | 3.5 | 3.6 | 4 |
|---|---|---|---|---|---|
| $10^{26}$ erg | 11.8 | 6.7 | 5.9 | 5.3 | 3.5 |
| $10^{27}$ erg | 25.3 | 13.1 | 11.4 | 10.1 | 6.2 |

For the more probable scaling exponents between 3.4 and 3.6 there is a rough agreement with the diameter of the central crater cavity in the Ries for an energy between $10^{26}$ and $10^{27}$ erg.

There is also a rough agreement with the diameter of a primary crater (before readjustment) calculated with the scaling equation of Gault (1974) for craters larger than 1 km which gives $D = 7.1$ km and $D = 12.6$ km for impact energies of $10^{26}$ and $10^{27}$ erg respectively.

### 5.2. *Interpretation of the subsurface structure*

We think that the subsurface structure of the crater described in the previous sections can be explained by the following cratering model. A primary cavity about 2–3 km deep is formed by the impacting body. The diameter of this transient crater probably was a few kilometers less than the diameter of the present inner ring. The rampart-like structure of the inner ring can be interpreted as the remnants of the uplifted rim of this primary crater (Angenheister and Pohl, 1974; Engelhardt, 1975) or possibly rim deposits of inverted stratigraphy. This is suggested by the inverted sequences of rocks in drillholes in the inner ring area (basement rocks overlying sedimentary rocks) and the overturned 80 m thick sediment block in the drillhole Wörnitzostheim about 2 km outside of the inner ring.

The primary cavity was filled by fallback ejecta, mainly suevite, and by readjustment movements bringing the brecciated basement up to the present elevation in the central crater. The readjustment consisted of downward and inward movements in the megablock zone producing the ring depression in the basement and inward and upward movements in the central crater giving rise to the innermost peak ring. Part of the rim of the transient crater may have collapsed into the central crater. This could explain the interruptions of the inner ring structure. Large relative horizontal movements in the central crater explain the alternating crystalline basement units of various shock stages found in the drill core Nördlingen 1973 (Fig. 21; Engelhardt and Graup, 1977; David, 1977). The upper unit (525–670 m, shock stage I, shatter cones, traces of meteoritic material, El Goresy and Chao, 1976) probably originates from a boundary region of the primary cavity, but it may have been displaced vertically and horizontally over a distance of 1–3 km. According to Stöffler (1977) the melt-poor suevitic dikes have been intruded during the formation of the primary cavity.

As a consequence of these readjustment movements the strata outside the inner ring subsided together with the outer crater deposits in the megablock zone. The amount of subsidence decreases with increasing distance from the center and terminates at the tectonic rim at a radial distance of about 12–13 km.

### 5.3. *Interpretation of the impact formations*

5.3.1. *Continuous deposits of the megablock and Vorries zone.* The outer impact formations of the Ries crater have been subdivided into a lower unit

represented by megablocks and Bunte breccia and an upper unit, the fallout suevite (section 3.2). Three major types of transport and deposition are considered to be involved in the formation of this lower unit, the bulk continuous deposits:

(1) over- and under-thrusting of megablocks by gliding and shearing
(2) ballistic transport of ejecta without major secondary mass transport upon landing of the ejecta
(3) ballistic transport of ejecta with major secondary mass transport.

Types (1) and (2) are characteristic of the megablock zone, types (2) and (3) are recognized in the "Vorries" continuous deposits.

In addition to the material transported and deposited according to (1) and (2), megablocks near the tectonic rim of the crater and probably at greater depth of the megablock zone were displaced by down-faulting and slumping of autochthonous target rocks (Figs. 20, 40). This was probably induced by subsidence of the marginal crater zone during readjustment of a transient crater cavity (see section 5.2).

We believe that the complex structure of the megablock zone is primarily the result of the radially decreasing shock wave energy. When the growing crater reached the radius of the later formed inner ring, the mode of excavation gradually transformed from a ballistic to a gliding mode of excavation (thrust faults) which is more and more restricted to the uppermost strata (Malmian) with increasing range. Consequently most of the allochthonous megablocks originate from the target area which is close to the region of the present inner ring. Many of the characteristics of the impact formations in the megablock zone continue into the Vorries continuous deposits beyond the tectonic rim of the crater. The decrease in the size of megablocks and of the abundance of blocks from the lower part of the pre-impact stratigraphy as a function of range is most likely the result of the particle velocity decreasing radially away from the point of impact in horizontal and vertical direction (e.g., Gault *et al.*, 1968; papers in this volume).

The texture of the Bunte breccia in which the megablocks are embedded, reveals a number of genetically important properties (see sections 3.2.1 and 3.3) which indicate the nature of several subsequent phases in the process of its formation: (a) *shock compression* resulting in shock metamorphism of target rocks ranging from stage II (about 350–400 kbar) to low pressure monomict brecciation (less than about 50 kbar), (b) *comminution, deformation and mixing* of fragmental rock material from all stratigraphic levels and from a broad zone of variable shock compression. This is achieved during the excavation process by which the downward and outward moving material is deflected into an upward moving flow of particulate material which shears along the slope of the growing crater cavity. It is plausible to assume that part of the deformation of the fragments and most of the Bunte breccia takes place during this process. (c) *impacting of the ejecta* on the ground and *horizontal movement* on the target surface. Certain textural and deformational effects of the Bunte breccia may be assigned to this last phase such as the formation of the polished and striated

surfaces on limestone, flow textures around large blocks and near to the base of the breccia deposits, and plastic deformation of incompetent rocks such as shale and clay (Wagner, 1964; Hüttner, 1969; Chao, 1976, 1977). The increasing incorporation of local material into Bunte breccia with increasing range is explained by the increasing impact velocity of the landing ejecta as described by the model of Oberbeck (1975). The horizontal and radial flow of the primary and secondary ejecta also explains the preferential filling of local depressions of the target surface which results in an extremely variable thickness of the continuous deposits in the Vorries (see section 3.3).

Chao (1976, 1977) has developed a different model for the emplacement of the Bunte breccia and megablocks. He suggests that they were emplaced predominantly by a roll and glide mode of transport rather than ballistically. To our opinion all observed textural and deformational features can be assigned to one of the phases (a), (b), or (c) discussed above. There is no unequivocal field evidence that excludes ballistic transport. In general, horizontal gliding requires preceding ballistic transport. Only where the particle velocities are insufficient for ballistic ejection, that is in the marginal zone of the crater, gliding may be an important primary mode of displacement.

5.3.2. *Suevite and impact melt rocks.* Some genetically important properties of suevite as well as the characteristic differences between fallout and fallback suevite have been discussed in section 3.2.3. According to these data and theoretical considerations about cratering mechanics (e.g., Gault *et al.*, 1968; and papers in this volume) the following model for the origin of suevite is proposed (see also Stöffler, 1977). Upon impact a shell of melt which surrounds the central region of vaporized rock is formed in the target by the propagating shock wave. The region of the melt zone which is nearest the free surface of the transient cavity, is first moving downward and sideward and then accelerated upward into ballistic trajectories. This gives a plausible mechanism for the mixing of melt and rock fragments of decreasing intensity of shock metamorphism. The uppermost part of the shell of melt which involved mainly sedimentary rocks, was probably ejected with very high velocity beyond the present outer margin of the continuous deposits. This had already happened before the stagnation point of the penetrating projectile was reached. The lower part of the melt zone, preferably the outer shell of it, which was mainly confined to the crystalline basement rocks had a smaller particle velocity and was ejected late in the excavation process, after the Bunte breccia was formed. This is the most probable source of melt from which particles already mixed with shocked rock debris during the downward movement were disrupted by the upward acceleration and subsequently shaped into bomb-like forms, which are characteristic of the fallout suevite. Fragment-laden melt particles and rock fragments were probably mixed with expanding vaporized target rock and deposited as a high density current. A few very large lumps of melt were ejected to the eastern crater rim forming isolated bodies of impact melt rock (see section 3.2.4). It is an open question how the discontinuous distribution of fallout suevite and the admixture of sedimentary rock fragments from the upper section of the target can be explained in the scope of this schematic model.

The source region of the melt inclusions in the fallback suevite must be a deeper part of the melt zone in which the velocity and vector of particle movement did not result in an ejection beyond the rim of the primary crater cavity. Also the innermost, hottest, and less viscous shell of the melt zone should have been incorporated into the suevite since it cannot be ejected beyond the crater due to the vertical downward movement. Thereby fused sedimentary strata (depending on the penetration depth of the projectile and extent of the zone of vaporized rock) could be mixed into the melt. This might explain the smaller size of the melt inclusions and their extreme vesiculation which could result from the high content of water in the sedimentary rocks.

The question is whether the material of the fallback suevite was actually ejected vertically to relatively large heights or whether it moved turbulently more or less like a surge in the crater. The latter seems to be required to explain the intrusive character of the lowermost suevitic breccia (below 515 m) and the "suevitic" dike at 642 m in the drill core Nördlingen 1973. On the other hand the "sorted" suevite above 331 m of this drill core speaks in favor of a late genuine fallback phase which interacted with the atmosphere. The main layer of the melt-rich suevite within the central crater might be explained by a vertical ejection and fallback mechanism rather than by ground surging (see continuous decrease of melt content with depth; Fig. 25). An earlier ground surge derived from an area at some lateral distance from the projectile could have formed the melt-poor, cold suevite intrusively. On top of it the true fallback suevite originating from the vicinity of the projectile was deposited later in time.

*Acknowledgment*—The authors are indebted to various colleagues who provided useful information and unpublished data, especially to Prof. W. v. Engelhardt, and Dr. G. Graup, Tübingen, and Dr. F. Hörz, Houston. They should like to thank Mrs. G. Grant, Miss F. Möllers, Mrs. U. Ewald, H.-D. Knöll, U. März, R. Ostertag, and W.-U. Reimold for their valuable technical assistance in the preparation of the manuscript. We thank the German Research Association (Deutsche Forschungsgemeinschaft) for its generous financial support over the past decade. We acknowledge the very helpful comments of Dr. F. Hörz, Houston, and Dr. H. C. Halls, Toronto, who reviewed the manuscript with great care.

## REFERENCES

Abadian, M.: 1972, Petrographie, Stoßwellenmetamorphone und Entstehung polymikter kristalliner Breccien im Nördlinger Ries. *Contr. Mineral. Petrol.* **35**, 245–262.

Abadian, M., Engelhardt, W. v., and Schneider, W.: 1973, Spaltenfüllungen in allochthonen Schollen des Nördlinger Ries. *Geologica Bavarica* **67**, 229–237.

Ackermann, W.: 1958, Geologisch-petrographische Untersuchungen im Ries. *Geol. Jb.* **75**, 135–182.

Ammon, L. v.: 1905, Die Scheuerfläche von Weilheim in Schwaben. Ein Beitrag zur Riesgeologie. *Geogn. Jh.* **18**, 153–176.

Angenheister, G. und Pohl, J.: 1964, The remanent magnetization of the suevite from the Ries area (Southern Germany) *Z. Geophysik*, **30**, 258–259.

Angenheister, G. and Pohl, J.: 1969, Die seismischen Messungen im Ries von 1948–1969. *Geologica Bavarica* **61**, 304–326.

Angenheister, G. and Pohl, J.: 1974, Beiträge der angewandten Geophysik zur Auswahl des Bohrpunktes der Forschungsbohrung Nördlingen 1973. *Geologica Bavarica* **72**, 59–63.

Bader, K. and Schmidt-Kaler, H.: 1977, Der Verlauf einer präriesischen Erosionsrinne im östlichen Riesvorland zwischen Treuchtlingen und Donauwörth. *Geologica Bavarica* **75**, 401–410.

Bauberger, W., Mielke, H., Schmeer, D., and Stettner, G.: 1974, Petrographische Profildarstellung der Forschungsbohrung Nördlingen 1973 (von Meter 263 an bis zur Endteufe im Maßstab 1 : 200). *Geologica Bavarica* **72**, 33–34.

Bayer. Geol. Landesamt (ed.): 1969, Das Ries. *Geologica Bavarica* **61**, 478 pp.

Bayer. Geol. Landesamt (ed.): 1974, Die Forschungsbohrung Nördlingen 1973. *Geologica Bavarica* **72**, 98 pp.

Bayer. Geol. Landesamt (ed.): 1977, Ergebnisse der Ries-Forschungsbohrung 1973: Struktur des Kraters und Entwicklung des Kratersees. *Geologica Bavarica* **75**, 470 pp.

Birzer, F.: 1969, Molasse und Ries-Schutt im westlichen Teil der Südlichen Frankenalb. *Geol. Bl. NO-Bayern* **19**, 1–28.

Blohm, E.-K., Friedrich, H., and Homilius, J.: 1977, Ein Ries-Profil nach geoelektrischen Tiefensondierungen. *Geologica Bavarica* **75**, 381–393.

Bolten, R. and Müller, D.: 1969, Das Tertiär im Nördlinger Ries und in seiner Umgebung. *Geologica Bavarica* **61**, 87–130.

Bundesanstalt für Geowissenschaften und Rohstoffe, Hannover: 1971, Aeromagnetic Map of the German Federal Republic 1 : 100 000.

Chao, E. C. T.: 1963, The petrographic and chemical characteristics of tektites. In *Tektites* (J. A. O'Keefe, ed.), p. 51–94. Univ. of Chicago Press.

Chao, E. C. T.: 1967, Impact metamorphism. In *Researchers in Geochemistry* (P. H. Abelson, ed.), **2**, p. 204–233. John Wiely and Sons, Inc., New York.

Chao, E. C. T.: 1968, Pressure and temperature histories of impact metamorphosed rocks—based on petrographic observations. In *Shock Metamorphism of Natural Materials* (B. M. French and N. M. Short, eds.), p. 135–158. Mono Book Corp. Baltimore.

Chao, E. C. T.: 1973, Geologic implications of the Apollo 14 Fra Mauro breccias and comparison with ejecta from the Ries Crater, Germany. *J. Research U.S. Geol. Survey.* **1**, 1–18.

Chao, E. C. T.: 1976, The Ries Crater, a model for the interpretation of the source areas of lunar breccia samples (abstract). In *Lunar Science VII*, p. 126–128. The Lunar Science Institute, Houston.

Chao, E. C. T.: 1977, Preliminary interpretation of the 1973 Ries drill core. *Geologica Bavarica* **75**, 421–441.

Cotta, B. v.: 1834, Geognostische Beobachtungen im Riesgau und dessen Umgebungen. *N. Jb. Miner. usw*, p. 307–318.

David, E.: 1977, Abschätzung von impaktmechanischen Daten aufgrund von Ergebnissen der Forschungsbohrung Nördlingen 1973. *Geologica Bavarica* **75**, 459–470.

Dehm, R.: 1969, Geschichte der Riesforschung. *Geologica Bavarica* **61**, 25–35.

Dehm, R., Gall, H., Höfling, R., Jung, W., and Malz, H.: 1977, Die Tier- und Pflanzenreste aus den obermiozänen Riessee-Ablagerungen in der Forschungsbohrung Nördlingen 1973. *Geologica Bavarica* **75**, 91–109.

Dence, M. R.: 1971, Impact melts. *J. Geophys. Res.* **76**, 5552–5565.

Dennis, J. G.: 1971, Ries structure, Southern Germany, a review. *J. Geophys. Res.* **76**, 5394–5406.

Dorn, P.: 1948, Ein Jahrhundert Riesgeologie, *Z. dt. geol. Ges.*, **100**, 348–365.

Dressler, B. and Graup, G.: 1974, Gesteinskundliche Untersuchungen am Suevit der Bohrung Wörnitzostheim I im Nördlinger Ries. *Der Aufschluß* **25**, 404–411.

El Goresy, A.: 1968, The opaque minerals in impactite glasses. *Shock Metamorphism of Natural Materials* (B. M. French and N. M. Short, eds.), p. 531–554. Mono Book Corp., Baltimore.

El Goresy, A. and Chao, E. C. T.: 1976, Evidence of the impacting body of the Ries crater—the discovery of Fe-Cr-Ni veinlets below the crater bottom. *Earth Planet. Sci. Lett.* **31**, 330–340.

Engelhard, L. and Hansel, J.: 1976, Ein Beitrag zur Erkundung der Struktur des Nördlinger Rieses auf Grund geoelektrischer Schlumberger-Sondierungen. *Abh. Braunschw. Wiss. Ges.* **26**, 1–19.

Engelhardt, W. v.: 1976a, Neue Beobachtungen im Nördlinger Ries. *Geol. Rundschau* **57**, 165–188.

Engelhardt, W. v.: 1976b, Chemical composition of Ries glass bombs. *Geochim. Cosmochim. Acta* **31**, 1677–1689.

Engelhardt, W. v.: 1972, Shock produced rock glasses from the Ries Crater. *Contr. Mineral. Petrol.* **36**, 265–292.
Engelhardt, W. v.: 1975, Some new results and suggestions on the origin of the Ries basin. *Fortschr. Miner.* **52**, 375–384.
Engelhardt, W. v.: 1977, personal communication.
Engelhardt, W. v., Stöffler, D., and Schneider, W.: 1969, Petrologische Untersuchungen im Ries. *Geologica Bavarica* **61**, 229–296.
Engelhardt, W. v. and Stöffler, D.: 1974, Ries meteorite crater, Germany. *Fortschr. Miner.* **52**, Beih. 1, 103–122.
Engelhardt, W. v, and Graup, G.: 1977, Stoßwellenmetamorphose im Kristallin der Forschungsbohrung Nördlingen 1973. *Geologica Bavarica* **75**, 255–271.
Ernstson, K.: 1974, The structure of the Ries crater from geoelectric depth soundings. *J. Geophys.* **40**, 639–659.
Ernstson, K. and Pohl, J.: 1974, Einige Kommentare zu den bohrlochgeophysikalischen Messungen in der Forschungsbohrung Nördlingen 1973. *Geologica Bavarica* **72**, 81–90.
Ernstson, K. and Pohl, J.: 1977, Neue Modelle zur Verteilung der Dichte und Geschwindigkeit im Ries-Krater. *Geologica Bavarica* **75**, 355–371.
Förstner, U.: 1967, Petrographische Untersuchungen des Suevit aus den Bohrungen Deiningen und Wörnitzostheim im Ries von Nördlingen. *Contr. Mineral. Petrol.* **15**, 281–307.
Gall, H.: 1969, Geologische Untersuchungen im südwestlichen Vorries. Das Gebiet des Blattes Wittislingen. Diss. Univ. München, 166 pp.
Gall, H.: 1974, Geologische Bau- und Landschaftsgeschichte des südöstlichen Vorrieses zwischen Höchstädt a.d. Donau und Donauwörth. *N. Jb. Geol. Paläont. Abh.* **145**, 1, 58–95.
Gall, H. und Müller, D.: 1975, Reutersche Blöcke—außeralpine Fremdgesteine unterschiedlicher Herkunft in jungtertiären und quartären Sedimenten Südbayerns. *Mitt. Bayer. Staatsamml. Paläont. Hist. Geol.* **15**, 207–228.
Gall, H., Müller, D., and Stöffler, D.: 1975, Verteilung, Eigenschaften und Entstehung der Auswurfsmassen des Impaktkraters Nördlinger Ries. *Geologische Rundschau*, **64**, 915–947.
Gall, H., Hollaus, E., and Trischler, J.: 1976, Obermiozäne Seesedimente und Bunte Trümmermassen der Forschungsbohrung Wörnitzostheim I im Nördlinger Ries, *Geolog. Blätter NO-Bayern.* **26**, 188–206.
Gall, H. and Müller, D.: 1977, 4. Stratigraphie. *Erläuterungen zur Geologischen Karte des Rieses 1 : 50 000.* Bayerisches Geologisches Landesamt, München, in press.
Gall, H., Müller, D., and Pohl, J.: 1977, Zum geologischen Bau der Randzone des Impaktkraters Nördlinger Ries. *N. Jb. Geol. Paläont.* **1977**, 65–94.
Gault, D. E.: 1974, Impact cratering, *A Primer in Lunar Geology*, (R. Greeley and P. Schultz, eds.). NASA TM-X-62, 359, 137–176.
Gault, D. E., Quaide, W. L. and Oberbeck, V. R.: 1968, Impact cratering mechanics and structures. In *Shock Metamorphism of Natural Materials* (French, B. M. and Short, N. M., eds.), p. 87–99, Mono Book Corp., Baltimore.
Gentner, W., Lippolt, H. J., and Schaeffer, O. A.: 1963, Argonbestimmungen an Kaliummineralien—XI. Die Kalium-Argon-Alter der Gläser des Nördlinger Rieses und der böhmischmährischen Tektite. *Geochim. Cosmochim Acta* **27**, 191–200.
Gentner, W. and Wagner, G. A.: 1969, Altersbestimmungen an Riesgläsern und Moldaviten. *Geologica Bavarica* **61**, 296–303.
Graup, G.: 1975, *Das Kristallin im Nördlinger Ries.* Diss. Univ. Tübingen, Germany.
Graup, G.: 1977, Die Petrographie der kristallen Gesteine der Forschungsbohrung Nördlingen 1973. *Geologica Bavarica* **75**, 219–229.
Grieve, R. A. F., Dence, M. R., and Robertson, P. B.: 1977, Cratering processes: as interpreted from the occurrence of impact melts. In *Impact and Explosion Cratering* (D. J. Roddy, R. O. Pepin, and R. B. Merrill, eds.), Pergamon Press, New York. This volume.
Harr, K.: 1976, Petrographische Untersuchungen an Glastuffen und Bentoniten der südwestdeutschen Molasse, Diss. Tübingen.

Hörz, F.: 1965, Untersuchungen an Riesgläsern *Beitr. Miner. Petrol.* **11**, 621–661.
Hörz, F.: 1976, Personal Communication.
Hörz, F., Gall, H., Hüttner, R., and Oberbeck, V. R.: 1975, The Ries crater and lunar basin deposits. *Proc. Lunar Sci. Conf. 7th*, p. 396–398.
Hüttner, R.: 1958, *Geologische Untersuchungen im SW-Vorries auf Blatt Neresheim und Wittislingen.* Diss. Univ. of Tübingen, Germany. 347 pp.
Hüttner, R.: 1969, Bunte Trümmermassen und Suevit. *Geologica Bavarica* **61**, 142–200.
Jung, K. and Schaaf, H.: 1967, Gravimetermessungen im Nördlinger Ries und seiner Umgebung. Abschätzung der gesamten Störungsmasse. *Z.f. Geophysik* **33**, 319–345.
Jung, K., Schaaf, H., and Kahle, H. G.: 1969, Ergebnisse gravimetrischer Messungen im Ries. *Geologica Bavarica* **61**, 337–342.
Kahle, H. G.: 1969, Abschätzung der Störungsmasse im Nördlinger Ries. *Z. Geophysik* **35**, 317–345.
Morgan, J. A.: 1976, Personal Communication.
Müller, D.: 1969, Ein neues Profil vom Mittelkeuper bis zum Unterdogger bei Harburg nahe dem Nördlinger Ries. *Mitt. Bayer. Staatssamml. Paläont. Hist. Geol.* **9**, 73–92.
Müller, D.: 1972, *Die Oligozän-Ablagerungen im Gebiet des Nördlinger Rieses.* Diss. Univ. München, Germany. 249 pp.
Oberbeck, V. R.: 1975, The role of ballistic erosion and sedimentation in lunar stratigraphy. *Rev. Geophys. Space Phys.* **13**, 337–362.
Oberheinischer Geologischer Verein (ed.): 1926, Das Problem des Rieses. *Verlag der Stadt Nördlingen*, Nördlingen, Germany. 291 pp.
O'Keefe, J. A. and Weiskirchner, W.: 1970, Die Tektite als natürliche Gläser. *Glastechnische Berichte* **43**, 199.
Pohl, J.: 1965, Die Magnetisierung der Suevite des Rieses. *N. Jb. Miner. Abh.* **H.9–11**, 268–276.
Pohl, J.: 1971, On the origin of the magnetization of impact breccias on Earth. *Z.f. Geophysik*, **37**, 549–555.
Pohl, J.: 1974, Magnetisierung der Bohrkerne in der Forschungsbohrung Nördlingen 1973. *Geologica Bavarica*, **72**, 65–74.
Pohl, J.: 1977, Paläomagnetische und gesteinsmagnetische Untersuchungen an den Kernen der Forschungsbohrung Nördlingen 1973. *Geologica Bavarica* **75**, 329–348.
Pohl, J. and Angenheister, G.: 1969, Anomalien des Erdmagnetfeldes und Magnetisierung der Gesteine im Nördlinger Ries. *Geologica Bavarica*, **61**, 327–336.
Pohl, J. and Will, M.: 1974, Vergleich der Geschwindigkeitsmessungen im Bohrloch der Forschungsbohrung Nördlingen 1973 mit seismischen Tiefensondierungen innerhalb und außerhalb des Ries. *Geologica Bavarica* **72**, 75–80.
Preuss, E.: 1964, Das Ries und die Meteoritentheorie. *Fortschr. Mineral.* **41**, 271–312.
Reich, H. and Horrix, W.: 1955, Geophysikalische Untersuchungen im Ries und Vorries und deren geologische Deutung. *Beih. Geol. Jb.* **19**, 119 pp.
Reuter, L.: 1926, Die Verbreitung jurassischer Kalkblöcke aus dem Ries im südbayerischen Diluvial-Gebiet. *Jber. u. Mitt. Oberrh. Geol. Ver. N.F.* **14**, 191–218.
Rittmann, A.: 1973, *The stable mineral assemblage of igneous rocks: a method of calculation.* Springer, Berlin–Heidelberg–New York.
Roddy, D. J., Boyce, J. M., Colton, G. W., and Dial A. L. Jr.,: 1975, Meteor crater, Arizona, rim drilling with thickness, structural uplift, diameter, depth, volume, and mass-balance calculations. *Proc. Lunar Sci. Conf. 6th*, p. 2621–2644.
Scheuenpflug, L.: 1973, Zur Problematik der Weißjuragesteine in der östlichen Iller-Lech-Platte. *Eiszeitalter und Gegenwart* **23/24**, 154–158.
Schmidt-Kaler, H.: 1969, Versuch einer Profildarstellung für das Rieszentrum vor der Kraterbildung. *Geologica Bavarica* **61**, 38–40.
Schmidt-Kaler, H., Treibs, W., and Hüttner, R.: 1970, Geologische Übersichtskarte des Rieses und seiner Umgebung 1:100 000. Exkursionsführer zur Geologischen Übersichtskarte des Rieses 1:100 000. *Bayerisches Geologisches Landesamt*, München, 68 pp.
Schneider, W.: 1971, Petrologische Untersuchungen der Bunten Breccie im Nördlinger Ries. *B. Jb. Miner. Abh.* **114**, 136–180.

Shoemaker, E. M. and Chao, E. C. T.: 1961, New evidence for the impact origin of the Ries Basin, Bavaria, Germany, *J. Geophys. Res.*, **66**, 3371–3378.

Simmons, G., Siegfried, R., and Richter, D.: 1975, Characteristics of microcracks in lunar samples. *Proc. Lunar Sci. Conf. 6th*, p. 3227–3254.

Stähle, V.: 1972, Impact glasses from the suevite of the Nördlinger Ries. *Earth Planet. Sci. Lett.* **17**, 275–293.

Stähle, V. and Ottemann, J.: 1977, Petrographische Studien am Suevit und an den Gangbreccien der Forschungsbohrung Nördlingen 1973, *Geologica Bavarica* **75**, 191–217.

Stöffler, D.: 1966, Zones of impact metamorphism in the crystalline rocks of the Nördlinger Ries crater *Contr. Miner. Petrol.* **12**, 15–24.

Stöffler, D.: 1969, Kristalline Trümmermassen. in Petrologische Untersuchungen im Ries, Engelhardt, W. v. Stöffler, D. and Schneider, W. *Geologica Bavarica*, **61**, 285–288.

Stöffler, D.: 1971a, Progressive metamorphism and Classification of Shocked and Brecciated Crystalline Rocks at Impact Craters. *J. Geophys. Res.* **76**, 5541–5551.

Stöffler, D.: 1971b, Coesite and Stishovite in Shocked Crystalline Rocks. *J. Geophys. Res.* **76**, 5474–5488.

Stöffler, D.: 1977, Research drilling, Nördlingen 1973: polymict breccias, crater basement, and cratering model of the Ries impact structure. *Geologica Bavarica*, **75**, 443–458.

Stöffler, D., Knöll, H.-D., Reimold, W.-U. and Schulien, S.: 1976, Grain size statistic, composition and provenance of fragmental particles in some Apollo 14 breccias. *Proc. Lunar Sci. Conf. 7th*, p. 1965–1985.

Stöffler, D., Ewald, U., Ostertag, R., and Reimold, W.-U.: 1977, Ries deep drilling: I. Composition and texture of polymict impact breccias. *Geologica Bavarica.* **75**, 163–189.

Wagner, G. A.: 1977, Spaltspurendatierungen an Mineralien aus kristallinen Riesgesteinen. *Geologica Bavarica*, **75**, 349–354.

Wagner, G. H.: 1964, Kleintektonische Untersuchungen im Gebiet des Nördlinger Rieses. *Geol. Jb.* **81**, 519–600.

Werner, E.: 1904, Das Ries in der Schwäbisch-fränkischen Alb. *Bl. Schwäb. Albvereins*, **16**, 153–167.